THE UNIVERSITY OF SHEFFIELD

Department of Chemical and Biological Engineering

Thesis

Development of a novel rheometer for viscoelastic fluids

Student: Elena Kuvshinova

Supervisors: Professor William Zimmerman

Dr. Julia Rees

2017

Abstract

Our understanding of the rheology of complex fluids becomes increasingly important for the study and manufacture of new materials. Extensional rheometry plays a key role in many industrial processes and is therefore central to the design of processing operations for a wide range of polymer materials, food and medicine technologies. The evolution of scientific equipment and mathematical algorithms means that it is now possible to solve complicated problems pertaining to complex fluids that are of major importance to the further development of elongational flow engineering.

In this research a new rheometer is developed and the principles of the operation are studied in order to find methodologies that enable one to make measurements of rheological properties of complex fluids in a "one step" manner. The flow field within the T-junction geometry of the device for fluids that exhibit elongational rheometry is non-homogeneous due to the stagnation point. In contrast with the operation of conventional rheometers, data processing from the prototype rheometer involves modelling of the flow field and the construction of the mapping algorithm to connect data obtained from the device with the underlying elastic constitutive parameters of the fluid using inverse approach.

Contents

List of Tables

List of figures

Nomenclature

τ	Stress tensor
$\boldsymbol{D}$	Rate of deformation tensor
$\sigma(t)$	Shear stress
$\dot{\gamma}(t)$	Shear rate
η_0	Constant shear viscosity
$\eta_s(\dot{\gamma})$	Viscosity, which depends on shear rate
De	Deborah number
λ	Relaxation time
T_0	Time of observation
p	Pressure
N_1	First normal stress difference
N_2	Second normal stress difference
$\dot{\varepsilon}$	Rate of elongation
t	Time
η_e	Extensional viscosity
L	A typical length scale associated with the flow
Tr	Trouton ratio
M_w	Molecular weight
C	Capacitance

σ_E	Extension stress
v	Velocity
J	Jacobian
u	Velocity vector
ρ	Density
$\boldsymbol{I}$	Identity matrix
$\boldsymbol{T}$	Polymeric contribution for the extra stress tensor
C_p	Heat capacity
k	Thermal conductivity
q	Heat source
P_{tot}	Heat source power
Vol	Total volume of the heat sources
$\boldsymbol{n}$	Normal vector
h	Heat transfer coefficient
T_{ext}	External temperature
H	Length of a pressure head
t_{dif}	Displacement between two similar patterns of signals
R_{fg}	Correlation coefficient.
Wi	Weissenberg number

Chapter 1: General project description

1.1. Introduction

The development of industrial processes poses new tasks for engineering processes and for the monitoring and control of resulting products. Rheology is the science that is concerned with fluid flow and deformation. It plays an important role in processing, controlling and handling in food, pharmaceutical, cosmetic, metallurgical, chemical and other industrial branches. Also, rheological principles are widely in use for the study of biomedical, geological, chemical and structural problems. Whilst for Newtonian fluids the basic principles are well established, for complex fluids there are still many unsolved issues. Researchers dealing with rheometry of viscoelastic fluids point out that there is still a knowledge gap between experiments and an appropriate theory which could be used for prediction.

Complete understanding of the behaviour of complex fluids is difficult due to the existence of both shear and elastic effects in all processes when viscoelastic fluids are subjected to deformation. Special idealized experimental techniques are necessary for dividing these two phenomena. It is not always possible to realise this in conditions close enough to real industrial environments. Another item on the wishlist of rheologists is the ability to obtain direct measurements of constitutive parameters of fluids. This cannot always be realised. Often parameters of interest need to be derived from other physical values.

Conventional rheometers for both Newtonian and complex fluids normally provide one set of constitutive parameters for each experiment. Thus in order to work an entire rheometric curve for a liquid, one has to carry out a lot of experiments, which is impractical in real industrial conditions. Additionally, many rheometrical techniques use optical or visualisation principles to obtain measurements. The equipment required is typically bulky, expensive and excludes opaque liquids from consideration.

The development of computer technology and numerical tools makes now possible the simulation of complex processes of fluid dynamics, but this requires the availability of CFD models that are sophisticated enough to describe real viscoelastic flows. Hitherto researchers have had to work with idealised models, thus verification of models by direct comparison of theoretical predictions with experimental data presents certain difficulties.

All of the issues noted above indicate that it is desirable to develop a system that comprises a physical rheometer together with an adequate CFD model to enable in-situ process information collection. For this task it is necessary to build a device that generates a range of viscoelastic responses within a single experiment. This device must be capable of producing accurate rheological data for viscoelastic fluids that arise in industrial applications, work with opaque liquids and liquids with high viscosity (such as gels, pastes and emulsions). Such an instrument would be of major importance for industrial process optimisation, design, equipment operation and control. In many cases this could result in a major reduction in production costs.

The target of this study is the development of a stagnation-point rheometer that is able to generate an elastic response in a single experiment. A numerical algorithm will be developed for the so-called "inverse problem" that permits the derivation of constitutive parameters of complex fluids from an information rich data set of measurable flow parameters. The rheometer is designed with the view that it will be suitable for use in industrial processes for a broad range of fluids.

1.2. Research objectives

The research is mainly focused on the development of a rheometer to be used in different areas from science to industry for the characterisation of complex fluids. Conventional rheometers widely used for these purposes usually provide constitutive parameters of fluids for a single flow rate. This means that several experiments must be performed in order to obtain the viscosity constitutive equation. Additionally, many methods involve different visualisation techniques, which are unsuitable for the characterisation of opaque substances. The specific T-shaped channel used in this study allows us to generate a large range of extensional rates in the vicinity of the stagnation point which is situated in the center of the back wall of the channel.

The hypothesis of the research is as follows: pressure-driven flow within a T-shaped channel generates a non-homogeneous extensional flow field. This allows us to obtain information relating to the constitutive parameters of viscoelastic liquids from a single experiment using the mathematical technique known as an "inverse method".

This can be achieved by:

1. Developing the procedure for determining the extensional component of viscoelastic flows.

2. Defining the constitutive parameters which might be applied to model viscous and viscoelastic flows for non-Newtonian fluids.

3. Mapping of the measured physical parameters of a flow using an inverse method to find the constitutive parameters corresponding to the extensional property of a fluid.

1.3. Methodology

To achieve these general objectives the following procedure was adopted:

1. Build a system capable of generating extensional flows. The device contained an embedded set of sensors within the channel walls to measure physical parameters caused by the flow dynamics. Design of the device benefitted from a computational model of the underlying physical processes thus making it possible to perform temperature and parametric control of an experiment.

2. An inverse model was created for defining the characteristic parameters of a fluid measured by the system. This involved:

- solution of the forward problem. This included solving the relevant system of partial differential equations using finite element methods to model viscoelastic flows.

- validating the model by comparing it with experimental rheological data obtained from known test fluids from conventional rheometers.

- creating an algorithm for the inverse procedure. This involved selection of the measured parameters, checking invertability, uniqueness and sensitivity of the inverse functions.

3. Verification of the procedure developed to determine the constitutive parameters of viscoelastic fluids using the T-junction rheometer and mathematical inverse model for different types of liquids.

1.4. Scope of the study

The research consists of two parts. The first section focuses on the investigation of elongational properties of fluids and methods for their measurements based on the stagnation point phenomena. Polyacrylamide based fluids are used as the test liquids. Their shear and elastic characteristics are determined for use as the input parameters for the second part of the study, which is concentrated on solving forward and inverse problems. The forward problem involves the use of finite element modelling for viscoelastic liquids. The associated inverse problem involves the development of a mathematical algorithm to derive the relevant mapping from the measured statistical quantities to the constitutive parameters.

1.5. General benefits of the research

The project resulted in the construction of a new T-shaped rheometer (T-ometer) whose operation was tested over a range of parameters. Application of the device will permit the measurement of constitutive parameters of viscoelastic fluids from a single experimental run. This device is being developed with the aim of making it suitable for on-line control systems applicable for a wide range of industrial processes, including the manufacture of opaque fluids with high densities and viscosities. This is an ambitious, but hopefully realistic goal.

Chapter 2: Literature review

2.1. Influence of extensional properties of fluids on flow dynamics

Demand for the real time control for manufacturing processes of food, pharmaceutical, chemical and cosmetic industries is growing at an increasing pace. An important feature of this task is the rheological characterisation of precursors and end products. The requirements of such technologies combine automatisation, real time monitoring and high sanitary standards. New technologies often have to operate with complex fluids, which can simultaneously exhibit both viscous and elastic effects. Whilst there are reliable and broadly used techniques for dealing with shear flows, there is still a gap in the adaptation of conventional extensional rheometers for on-line or in-line applications.

The ability to perform real time measurements and control of rheological parameters of fluids in industrial processes has been a significant goal of the last few decades. Increasing pressure to reduce time- to- market and costs of production has motivated the development of new instruments that are reliable and easy to use methods for rheological investigations of chemical and natural substances. The market share of phytochemicals in the US alone was estimated in total to be US$31 billion in 2000 (Harjo, Wibowo and Ng, 2004). Devices and procedures are well developed and widely used for the shear characterisation of non-Newtonian fluids. However, measurements of extensional viscosity are still challenging. There are many physical and technological restrictions that pose limitations on applied techniques. In addition, in order to address the feasibility of measurement principles for extensional rheology, other requirements, such as those specific for food, medical or cosmetic processing: sanitary, tactile properties, digestive characteristics, exist.

The importance of knowledge about the extensional viscosity of polymers can hardly be overestimated. It provides both understanding of fluid behaviour on a molecular level as well as guidance for processing development and optimisation. Polymer melts and solutions with coiled or branched large molecules exhibit predominantly extensional flow in many industrial processes, such as film blowing, fibre spinning, and injection molding (Zatloukal and Musil, 2009). Knowledge and investigation of extensional viscosity is particularly important in the polymer industry. Many testing platforms were developed that are now widely used for the uniaxial characterisation of polymer melts: tensile rheometer, elongation rheometer, filament stretching rheometer. Usually an initial sample with known geometry is the subject of a

deformation with a defined mechanical motion that causes a strain. Measurement of this strain enabled the extensional viscosity to be defined (Andrade, Skurtys and Osorio, 2013). For polymer solutions with coiled or branched molecular structures, a coil-stretched phenomenon is described, which characterises a sudden transition from a tangled or coiled state to a stretched state in an extensional flow field (de Gennes, 1974).

A significant class of rheological problems is connected with the production of food and cosmetics. Control of the rheological characteristics is very important, not only for processing, but also for consumer perception and handling. Components of chocolate, such as chocolate fat, cocoa particle size and surfactant, in different concentrations can change the yield stress and viscosity of the chocolate melt, as well as gustatory properties of the product (Ardakani, Mitsoulis and Hatzikiriakos, 2011). The main compound of wheat dough - glutenin proteins - affect the viscoelastic properties and machinability of bread making (Hernández-Estrada *et al.*, 2014)(Arabo, 2011). A carbonated dairy product called "kefir" is made by the fermentation of a special bacterial culture which possesses a dynamic flora. This means that uniform textural characteristics of the product cannot be guaranteed, which can affect a consumer's acceptance of the product. Thus the ability to control the viscoelastic properties of kefir is desirable (Glibowski and Kowalska, 2012). Vegetable oils are very important in the food industry. They are a mixture of several triglycerides, and the particular combination of these triglycerides defines the viscosity of a vegetable oil (Sadat and Khan, 2007). The process of aggregation and long term product quality are of great significance for colloid suspensions. In turbulent flows, which often arise in reactors for suspensions, the unsteady flow field creates both shear and extensional phenomena (Anne-Archard *et al.*, 2013). Another type of fluid, which prevails in the food industry is bubbly liquids where the bubble volume fraction is typically below 50%. The presence of the bubble phase changes the rheological properties of the initial liquid towards shear thinning and viscoelastic. In food processing bubbly liquids experience both shear and extensional impact, so investigations into the behaviour of such liquids is important for the design and processing of new food products (Torres-Moreno *et al.*, 2015). The investigation of extensional properties of emulsion systems still poses a challenging problem. Emulsions occur frequently in the food and pharmaceutical industries, such as in shampoos, medicines and bitumen. Data obtained from current monitoring systems are still insufficient, and this raises considerable problems in final product testing and process design (Różańska *et al.*, 2013). An interesting phenomenon manifests itself during investigations of the influence of drop size on the

dispersed phase viscosity: similar to the case of polymer fluids, there is a region of stagnation where viscous droplets in the emulsion behave like coiled molecules they start to stretch, thus exhibiting features of extensional flow (Hall *et al.*, 2011).

These are just a few examples of importance that arise in the production of consumer goods as a practical matter of rheology.

Conventional rheometers are mainly used in the endpoint test of the quality of the product and require a high level of manual intervention, which leads to disposal of the product at about 5% below spec (Rees, 2014).

In many chemical manufacturing processes there is a desire to substitute oil derivatives by more sustainable resources which have less stable and more predictable qualities. Therefore, the availability of in-line and on-line rheological tests in the important stages of manufacturing processes are of the great interest.

According to the classification given in (Bird *et al.*, 1989), flows could be divided into two types: shear and shear-space free flows. In many cases materials exhibit properties of both elastic and viscous fluids. Pure elasticity, as well as pure viscosity, are idealisations achieved at some limiting conditions. In industrial processes viscoelastisity can manifest phenomena such as die swell of the stretching of polymer molecular chains that can lead to "neck" regions.

These types of materials usually exhibit viscous properties under conditions of constant shear when they are in an equilibrium configuration. When the shear conditions change (e.g. the flow changes its direction or the channel cross-section changes) then elastic effects can appear. Thus these phenomena could significantly affect industrial processes such as extrusion, moulding, film blowing and spinning (Hernández-Estrada *et al.*, 2014)

2.2. Rheology of complex fluids

The scientific term "rheology" was proposed by E. Bingham in 1920. It means the study of flow and deformation (Soulages *et al.*, 2009) especially in applications of non-Newtonian materials. One of the most important parts of rheological investigations concerns the behaviour of substances in the transient regime between solid and fluid. In other words,

rheology tries to define a relationship between the stress acting on a given material, resulting deformation and/or flow that takes place. As a discipline rheology overlaps continuum mechanics, material science and applied mechanics (Tanner, 2009).

The development of science and industry poses new challenges for scientific methods and experimentation apparatus. Extensional fluid occurs during industrial processes that involve any kind of flow of substances possessing elastic properties. Production of foods, cosmetics, pharmaceuticals, paints, polymers, alloys and many other goods, as well as biomedical analysis, all require rheometry as a means of measurement and process regulation. Theoretically and empirically, all varieties of the above mentioned fluid characteristics of continuum and applied dynamics can be narrowed down to the study of fundamental relations, known as constitutive relations. Basic concepts of stress (force per area) and strain (deformation per length) are key to all rheological evaluations. Stress is a measurement of force per unit of surface area and is expressed in units of Pascals (Pa). One of the fundamental parameters, which characterizes flow behaviour of liquid and semi-liquid fluids, is viscosity, which is an intrinsic parameter and a measure of a fluid's resistance to motion (flow) when a shearing stress is applied (Tabilo-Munizaga and Barbosa-Cánovas, 2005). For Newtonian fluids this parameter is constant under any conditions, but for non-Newtonian or complex fluids the dependence of deformation on the applied stress is more complicated. As knowledge of physical properties of a liquid plays an important role in modern process control, there is an increasing demand for robust and reasonably priced controlling devices.

The viscosity of Newtonian fluids exhibits a linear character, depending only on environmental conditions such as pressure and temperature, while for non-Newtonian fluids the relationship between shear stress and shear rate (or stress and rate of strain for elongation flows) is non-linear. For complex fluids there is a lot of factors, which might have an effect on the viscosity. In addition to the factors mentioned above, these can include time and kinematic history of a flow, flow geometry, storage conditions (exposure to light or mechanical degradation). Usually, Newtonian behaviour is inherent to low molecular weight liquids or even to polymers at very low shear rates (rates of deformation). Complex fluids in general could be defined as those for which "the extra-stress tensor cannot be expressed as a linear, isotropic function of the component of the velocity gradient" (Owens and Phillips, 2005). The viscosities of complex fluids are defined by a number of parameters via constitutive equations. It was noted that in rheology the flow of a fluid can be interpreted precisely if the exact values of the parameters of the materials are obtained. It involves a

curve-fitting technique, which presumes the choice of a specified model (Syed Mustapha *et al.*, 1999). The most common quantitative models that describe the behaviour of viscous and viscoelastic fluids, are the Newtonian, Bingham, Carreau, Power Law, Herchel-Bulkley, Oldroyd-B and dumbbell models (Macosko, 1993), (Chhabra and Richardson, 2008).

2.2.1. Non-Newtonian fluids

Rheometry is based on an approach that is developed from the theory of the general viscous fluid. Proposing that stress depends only on the rate of deformation we can write (Macosko, 1993):

$$\tau = f(2D), \tag{2.1}$$

where τ - stress tensor, D - rate of deformation tensor.

For Newtonian fluids the functional relationship or the constitutive equation is

$$\sigma(t) = \eta_0 \dot{\gamma}(t), \tag{2.2}$$

where $\sigma(t)$ - shear stress, $\dot{\gamma}(t)$ - shear rate, η_0- constant shear viscosity.

Whilst for Newtonian fluids the stress at a point is linearly proportional to the strain rate, i.e. the shear viscosity is constant, there is a class of fluids, which are characterised by a non-linear relationship between the applied stress and the rate of deformation. For these fluids the constitutive equation can be defined as

$$\sigma(t) = \eta_s(\dot{\gamma})\, \dot{\gamma}(t), \tag{2.3}$$

where $\eta_s(\dot{\gamma})$ - viscosity, which depends on shear rate.

These fluids are commonly defined as non-Newtonian or complex fluids. The latter name was given to these types of liquids due to their ability to exhibit complex flow, combining both shear and elastic components. The nature of non-Newtonian behaviour could be different:

- materials that are not pure (suspensions, emulsions) are prone to form agglomerates and anisotropic structures;

- liquids with large coiled or branched molecules (polymers, gels), which are stretched under applied stress;

- liquids with special intermolecular forces (ionic liquids, magnetic liquids).

Complex fluids can be grouped based on principles of their dependence or independence on time and on whether they exhibit elastic properties (Chhabra and Richardson, 2008):

1. The shear rate depends only on the shear stress - purely viscous fluids.

2. The shear rate depends additionally upon the duration of shearing and the kinematic history - time-dependent fluids.

3. Fluids exhibiting both viscous and elastic characteristics - viscoelastic fluids.

Boger, 1996, classified complex fluids as inelastic and viscoelastic, and a particular fluid classification was defined by Deborah number (*De*), which is the ratio of a characteristic relaxation time associated with the material to a characteristic time of the deformation process or time of an experiment (Boger, 1996):

$$De = \frac{\lambda}{T_0}, \tag{2.4}$$

where λ - relaxation time, T_0 - time of observation.

According to the definition, *De* can be used to determine which are dominant in a flow processes: high *De* indicates elastic effects dominate, whilst low *De* shows that the flow regime is close to Newtonian.

Figure 1 presents the classification of complex fluids by Boger, who pointed out that the viscosity of complex fluids could be constant, dependent on shear rate, time or thermal history, and could possess a yield stress. The author emphasised that constant viscosity did not categorically mean Newtonian fluid behaviour, because some viscoelastic fluids could exhibit constant viscosity and high elasticity, for example Boger fluids, which will be discussed in the section 2.5.

A central objective of rheological fluid investigations is to determine the relationship between the stress acting on a fluid and its response or strain. Measurement of shear stress in a wide range of shear rates of a flow allows one to define and predict fluid behaviour. Curves fitted to experimental data of this relationship are called "Master curves" or rheograms, and demonstrate the main types of viscoelastic fluid response (fig. 2).

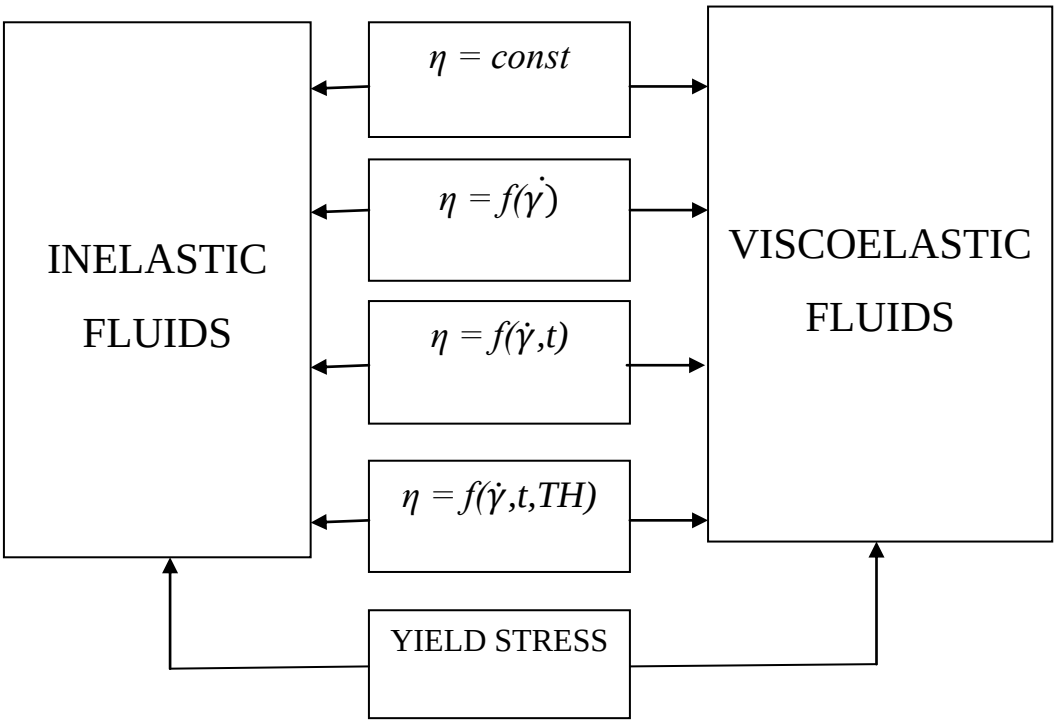

Figure 1. Classification of rheological complex fluids, *TH* - thermal history (Boger, 1996).

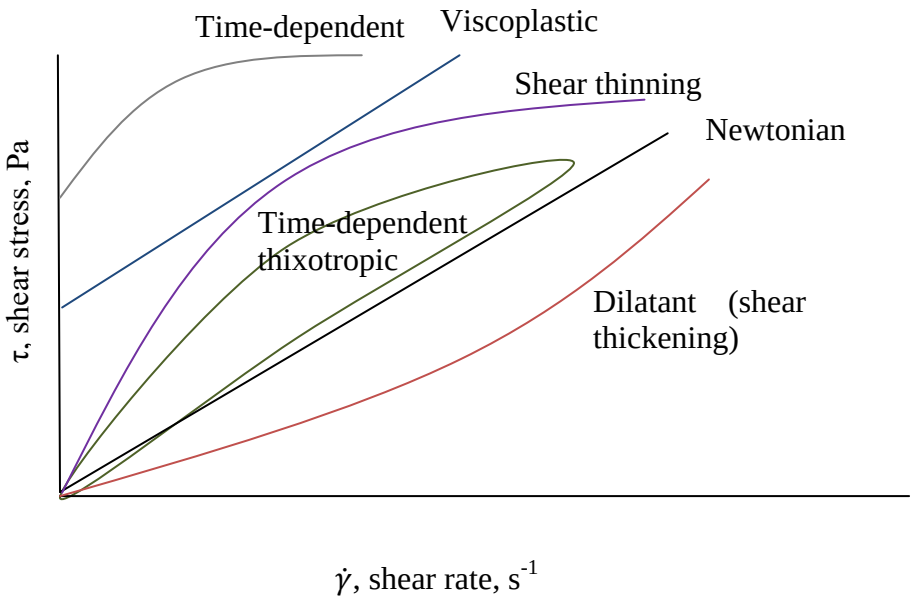

Figure 2. Rheograms of non-Newtonian fluids.

There are a number of constitutive equations that could be chosen to model a particular liquid behaviour to a reasonable degree of accuracy. Usually they involve a definition of two or more curve-fitting parameters such as the fluid consistency coefficient, or the flow behaviour

index in the case of the power-law model. For Carreau liquids, where viscosity values are limited, the relevant parameters are the flow behaviour index, zero shear viscosity and the relaxation time. Models assuming using three and more parameters describe more complicated viscoelastic effects. In this regard one of the most sought and studied problem concerning complex fluids is the investigation of the elasticity of liquids, which is not a straightforward process.

2.2.2. Extensional viscosity

Viscoelastic fluids are an important branch of non-Newtonian fluids. They exhibit a combination of liquid and solid characteristics. These fluids include the solutions or melts of high molecular weight polymers and aqueous solutions of some surfactants. To some degree, elastic behaviour can be explained by the stretching of the topological molecular microstructure. The branched, or linear but coiled, molecules of polymers can form long-chains or a microstructures network depending on the concentration or temperature (Li *et al.*, 2012).

In many cases materials can exhibit properties of both elastic and viscous fluids. Pure elasticity as well as pure viscosity can be exhibited realized at some limiting conditions. In industrial processes viscoelastisity can manifest as die swell, stretching of polymer molecular chains that can lead to "neck" region, as well as other interesting phenomena. Nowadays, the study of elongation characteristics, in addition to the shear properties of materials, is important for manufacturers. Many processes such as spinning, the melting of polymers and metals, pouring, film blowing, pumping and extrusion involve extensional flows. In many industrial and everyday household processes such as food consumption, dental hygiene and painting, a flow in converging or diverging regions of dies and in moulds could have large extensional components. Elongation phenomena become very important when working with polymers as extensional flow affects the orientation of polymer molecules and thus defines the properties of the final product. Extensional viscosity as a material function has to be taken into account for process modelling and design, process and quality control, as well as "on-shelf life" storage of products and food, medicine and cosmetics, sensory perception (sipping, spreading, swallowing etc.).

Viscoelastic materials usually exhibit viscous properties under conditions of constant shear when they are in an equilibrium configuration. When the shear conditions change (flow

changes its direction or the channel cross-section changes) then elastic effects can appear. Thus these phenomena could significantly affect industrial processes such as extrusion, moulding, film blowing, spinning and others (Brydson, 1981).

The specific characteristics of an extensional flow can be found in numerous sources starting from textbooks (Chhabra and Richardson, 2008, Macosko, 1993) to articles that address the problem. Comparing a shear flow with an extensional one, it could be noted that the main difference is that in the former the particles within the flowing fluid move in the same direction while in the latter particles can move towards each other (compressing) or away from each other (stretching).

Let us now consider a Newtonian fluid with components of the Cauchy stress tensor **σ,** constant shear flow ($\dot{\gamma}$) and constant pressure *p*:

$$\sigma_{xx}= \sigma_{yy}= \sigma_{zz}= -p, \tag{2.5}$$

$$\sigma_{xy}= \sigma_{yx}= \sigma=\eta_0\dot{\gamma}, \tag{2.6}$$

$$\sigma_{xz}= \sigma_{yz}=0. \tag{2.7}$$

For non-Newtonian and viscoelastic fluids in particular, the components of the tensor are:

$$\sigma_{xy}= \sigma_{yx}= \sigma=\eta_s(\dot{\gamma})\dot{\gamma}, \tag{2.8}$$

$$\sigma_{xx} - \sigma_{yy}=N_1(\dot{\gamma}), \tag{2.9}$$

$$\sigma_{yy} - \sigma_{zz}=N_2(\dot{\gamma}), \tag{2.10}$$

$$\sigma_{xz}= \sigma_{yz}=0, \tag{2.11}$$

where N_1 and N_2 - are the first and second normal stress differences, which together with $\eta_s(\dot{\gamma})$ are called "viscometric functions" (Owens and Phillips, 2005).

If a liquid extends homogeneously then the rate of elongation ($\dot{\varepsilon}$) is independent of the geometry, but is dependent on the time (*t*). Shear components are equal to zero, so for incompressible liquids, we see from the Cauchy tensor (2.8 - 2.11) that the stress components are proportional to the elongation rate:

$$\sigma_{xx} - \sigma_{yy}=\eta_e(\dot{\varepsilon})\ \dot{\varepsilon}, \tag{2.12}$$

where η_e - extensional viscosity, $\dot{\varepsilon}$ - rate of strain.

Formally extensional (tensile, elongational) viscosity could be defined as a measure of the resistance of a material to an applied extension. The rate of deformation tensor for a uniaxial purely extensional flow can be represented as follows (Morrison, 2001):

$$\sigma = \dot{\varepsilon} \begin{pmatrix} 1 & 0 & 0 \\ 0 & -\frac{1}{2} & 0 \\ 0 & 0 & -\frac{1}{2} \end{pmatrix}, \quad (2.13)$$

where σ - rate of strain tensor.

According to the Official Nomenclature for Material Functions of the Society of Rheology (Dealy, 1984), extensional viscosity is calculated as

$$\eta_e = \frac{\sigma_e}{\dot{\varepsilon}}, \quad (2.14)$$

where σ_e - net tensile stress and is given by:

$$\sigma_e = \sigma_{11} - \sigma_{22} = \sigma_{11} - \sigma_{33}. \quad (2.15)$$

Also

$$\dot{\varepsilon} = \frac{1}{L}\frac{dL}{dt}, \quad (2.16)$$

where L – a typical length scale associated with the flow.

The question of whether different reaction rates of a fluid occur on shearing or stretching deformations was first posed by Trouton (Petrie, 2006) towards the beginning of the 20th century. He carried out a series of experiments on different liquids and found that in general the extensional viscosity is three times higher than the shear viscosity. Later this ratio was named as the Trouton ratio:

$$Tr = \frac{\eta_e}{\eta_s}, \quad (2.17),$$

where η_e - extensional viscosity, η_s - shear viscosity, Tr - Trouton ratio.

However, it was shown in later experiments that the Trouton ratio is materially dependent and Tr=3 only occurs for Newtonian or purely viscous fluids. For other types of fluids it has

the same value for very small rates of strain but can be significantly larger at higher rates because of the extensional viscosity hardening effect, which is a common place. Chan et al. emphasized that a higher stress is needed to create an extensional flow at the same rate of strain deformation (Chan *et al.*, 2007). In accordance with this property, shear flows are called "weak" and extensional flows are called "strong" flows (Barnes and Roberts, 1992). Many authors have reported broad variability of Trouton ratio values for different types of elongational flow, for example, 10^4 (Jackson, Walters and Williams, 1984), 4 (Williams and Williams, 1985), 28 (Odell and Carrington, 2006), 150 (Rothstein and McKinley, 2001). It was pointed out that this variation of Trouton ratio depended on shear rate and flow conditions.

Despite progress in the development of experimental techniques and in theoretical modelling for shear flows, the area of extensional flows has still not been systematically investigated. Petrie, 2006, considered extensional viscosity to be a material property defined for steady, spatially uniform flows, however in reality, flows are neither steady nor spatially uniform. This author also suggested the use of the definition "transient extensional viscosity" to emphasize this phenomena.

2.3. Extensional flow measurements

As viscoelastic flows exhibit both viscous and elastic properties, the main difficulty in defining the extensional viscosity is to eliminate the influence of shear motion. In addition to this serious limitation, the range of data, that can be achieved experimentally, can be further complicated by factors including end effects, temperature sensitivity, and non-constant conditions relating to sample preparation (Maia *et al.*, 1999). Another aspect of the problem is that different experimental approaches include different kinetics - stretching, pressure drops, elongations etc. Gravity, surface tension effects and channel wall properties can also lead to significantly different results. Also, there is no general data base of extensional viscosity properties for different materials as each measurement technique operates with its own data set.

- Binding et al. Spinline rheometer;
- Boger & Binnington Contraction flow;
- Ferguson & Hudson Spinline rheometer;

- James et al. Converging flow rheometer;
- Jones et al. Pendant drop (filament stretching);
- Laun & Hingmann Opposed jets;
- Matta & Tytus Falling weight (filament stretching);
- Nguyen et al. Filament stretching;
- Oliver Horizontal jet (spinning);
- Schweizer et al. Opposed jets (stagnation flow).

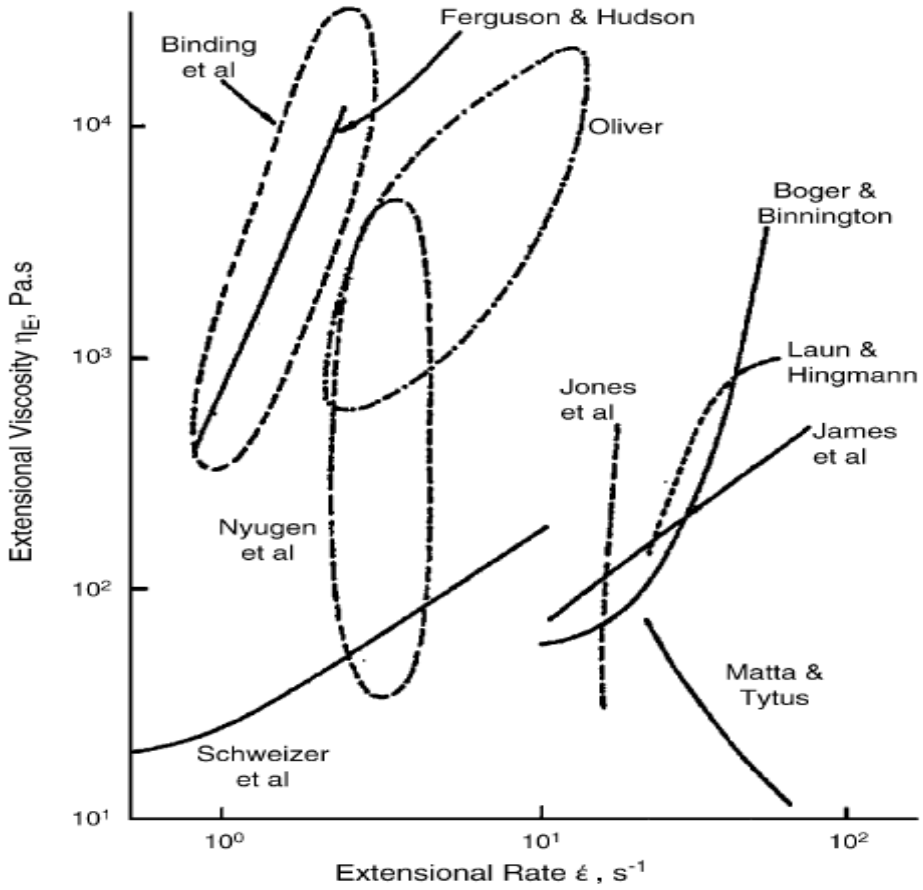

Figure 3. Results for "M1" steady state elongational viscosity measurements from the use of several different rheometric techniques (Petrie, 2006), where M1 is a solution of polyisobutylene in a base solvent of polybutene and kerosene.

As it has been discussed above, one of the problems concerning elongation experiments is the difficulty of the calibration process. There are no reference materials that can be used. Petrie,

2006 cited an example of the "M1 project, in which extensional viscosity measurements, obtained by different techniques, were compared (fig. 3). The author explained that the use of different measurement techniques had arised due to different flow histories and conditions.

For the moment, it is generally agreed that for a test liquid of interest, the extensional viscosity at very low shear rates could be investigated with use of a specific method as suggested in the following list. Experimental approaches corresponding to each group in fig.4 are as follows (Petrie, 2006):

It could be concluded from the information presented in fig. 3 that higher extensional rates are achievable using rheometers, such as contraction flow, converging flow and opposed jets. These rheometers cannot operate with samples constrained within a fixed volume.

Over the last twenty years, experimental techniques for elongation flow investigation have made considerable progress. The main developmental trends involve eliminating the influence of shear that can arise due to the influence of the confining walls, and identifying the role of strain in non-homogeneous flows. All existing methods are classified in accordance with the approaches used for generating regions of elongation within the flow regime. The investigational method has to be chosen in accordance with the material properties and the aims of the experiments.

The basic experimental arrangements have been widely described in the literature. Technically, all methods for measuring extensional viscosity could be divided into those based on "flow-through" principles and those based on "stagnation point" principles. The first group includes contraction and convergent flows, spinning, and flows incorporating stretching or compression. Stagnation flow rheometers include four-mill, opposed nozzles, cross-section and T-shaped geometries (fig. 4).

Choice of a particular approach for making extensional viscosity measurements is to a great degree defined by fluid properties (fig. 5). Stretching (uniaxial or planar) or compression is achieved by applying a force to one side of the sample with the aim of creating a linear deformation towards other side. These sets of methods allow us to obtain a pure elastic deformation without involving any shear components under the background condition of homogeneous flow. This condition restricts the properties of the sample types that are suitable for investigation using these techniques to those liquids that are able to maintain the

shape of their volume, so this class of rheometers is only suitable for fluids with high viscosities $\eta \geq 10^3$ Pa·s (gels, polymer melts and so on).

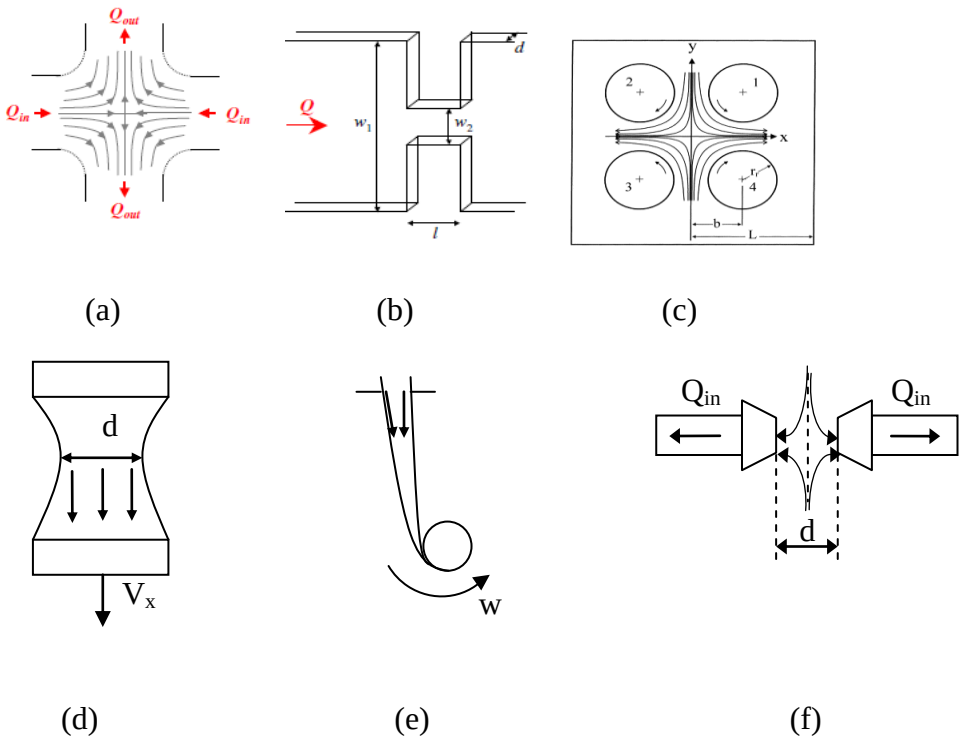

Figure 4. Types of extensional rheometers: (a) - cross-slot, (b) - contraction flow (Pipe and McKinley, 2009), (c) - four rolled mill (Tretheway and Leal, 2001), (d)- stretching, (e) - fibre spinning, (f) - opposed nozzles.

For liquids with lower viscosities a fibre spinning method can be used. This methodology is applicable for samples which tend to flow if they are not constricted in a confined volume and for which it is impossible to separate part of the sample and apply a force to it. To perform the measurement, a sample continuously extrudes from a tube and is stretched by a rotating wheel. This technique provides data on the transient uniaxial extensional viscosity. The extensional rate is determined from measurements of the fibre diameter and flow rate. Some negative aspects are typically associated with this method: shear effect in the feed die, effects of gravity and surface tension, and uncertainty in the diameter of the fiber. This method can be used for polymer solutions and suspensions with low viscosity ($\eta \geq 1$ Pa·s), particularly for simulations of the spinning process involving orientated polymer molecules.

Stagnation flow conditions can be achieved by two colliding streams of liquids. Depending on the geometry of the setup, stagnation flows can be axisymmetric or planar. These flows are not homogeneous because in the central part of the flow the strain is much higher on the boundary than it is on adjacent layers. If high strain exists it is possible to achieve a steady state. Such rheometers include opposed jets, four roll mills and cross slot devices.

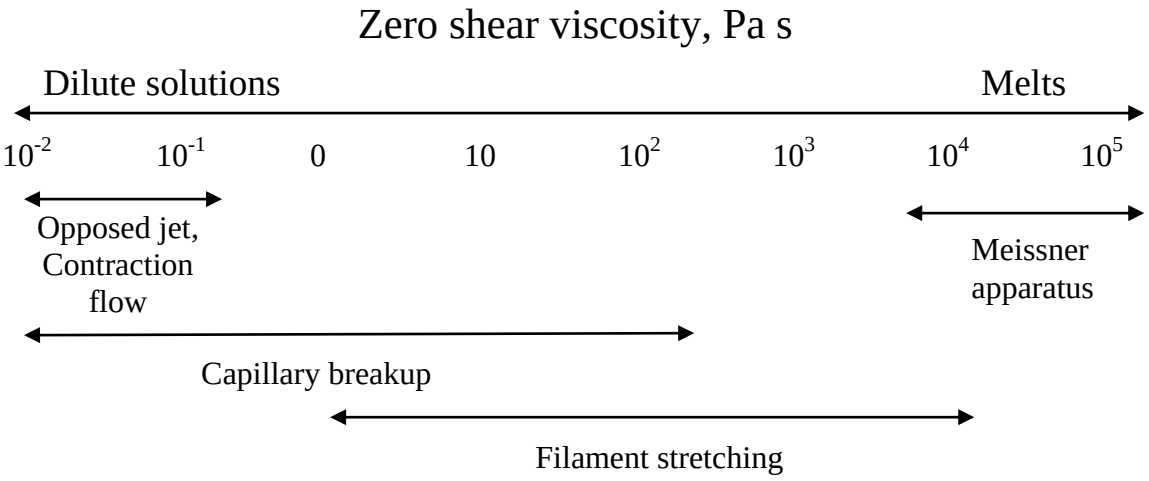

Figure 5. Applicability of different techniques of measuring of extensional viscosity depending on shear viscosity of a fluid

(http://www.mate.tue.nl/~peters/4K400/Rheol_Chap07.pdf)

Converging flow and contraction rheometers are based on pressure drop principles. Another class of these devices involves entrance pressure drop conditions. The later configuration can be achieved using a conventional capillary rheometer and can allow obtaining data corresponding to steady-state extensional viscosities. These devices have been used for decades to investigate the extensional properties of liquids by relating the measured pressure drop across the contraction region to the imposed flow rate. These flows are mixed kinematic types and typically contain shear and elongational components (Pipe and McKinley, 2009).

Corresponding to each of the rheometric configurations described above, there exists an underlying principle "One experiment - one point of viscosity data". Such time consuming

measurement methodologies are not applicable for the development of "on-line" fast response rheometers. Novel, information-rich automated approaches for measurement of rheological properties of liquid materials should ideally be carried out with the application of rheometers that possess channel geometries that are capable of supporting the existence, simultaneously, of a range of strain rates within a single experiment to cover the needs of modern industry.

That is why, for the above purposes, a stagnation point rheometer with a T-junction geometry was chosen. Provided that stretching of fluid elements occurs along the back wall of the channel, the range of elongations can be observed in a single experiment. This setup can be used for the investigation of fluid elastic properties. As a consequence of the no-slip boundary condition and continuity, the local velocity vector and all velocity gradients are zero. Thus a non-homogeneous axisymmetric extensional flow is generated at the stagnation point, which is situated at the geometrical centre of the back wall. These conditions can promote purely elastic flow phenomena (Soulages *et al.*, 2009). In addition, a set of different sensors could be incorporated into the channel walls that could measure the pressure and velocity fields of an extensional flow.

2.4. Real time extensional rheometers

Real time monitoring devices should include the following properties: regular renewal of the sample, a response time that is adequate for the processing time and a self-cleaning design. The principles of real time monitoring and control of viscoelastic flows can involve on-line, or in-line installation. On-line rheometers could be flow-through and immersed depending on their construction (Cullen *et al.*, 2001). Padmanabhan, 1995 suggested classification of real time monitoring systems, including on-line, in-line and on-line recycled type (fig. 6). The first real time rheometers, that were developed, were based on the traditional principles of conventional off-line rheometers, using rotational, oscillatory or tube flow. Fluid response (usually fluid velocity), could be measured via applied stress (pressure, torque). Shear rate and shear stress could then be derived and consequently fluid viscosity could be defined.

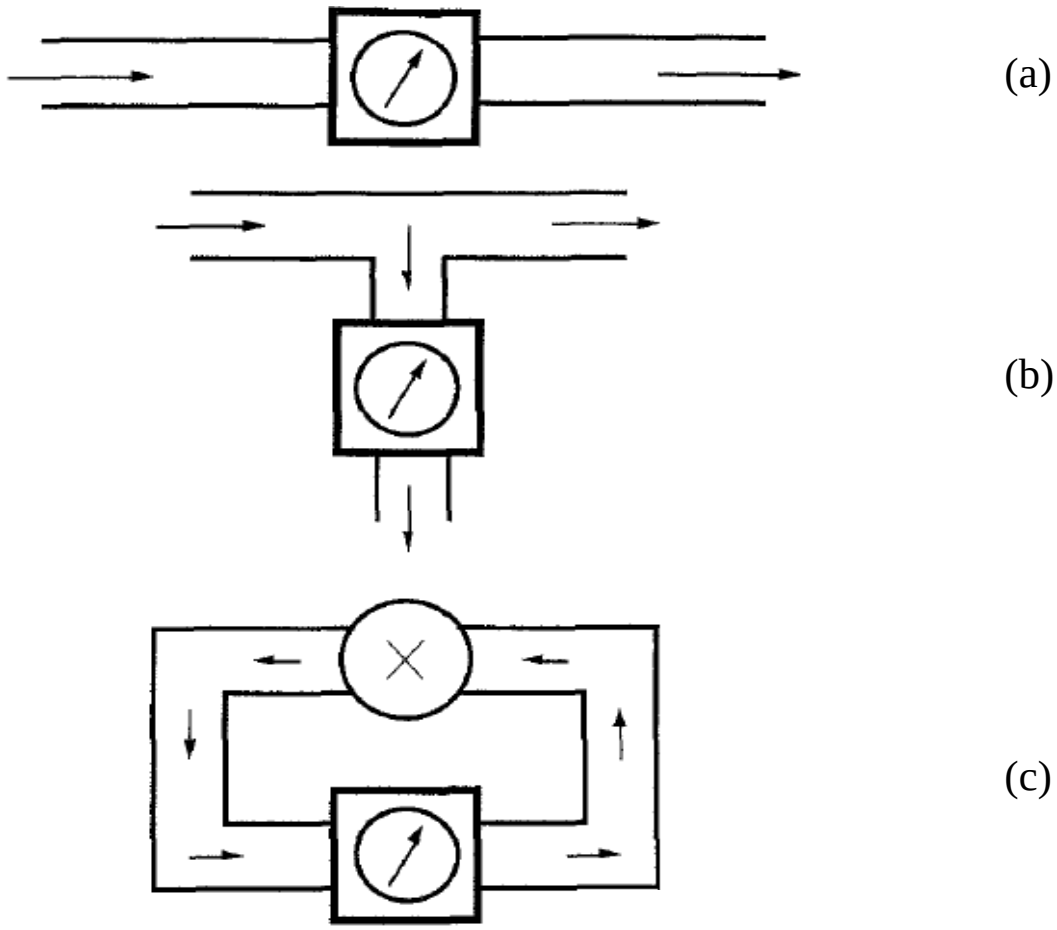

Figure 6. Diagrams of real time processing rheometers: (a) - in-line; (b) - on-line or by-pass; (c) - recycled on-line (Padmanabhan and Bhattacharya, 1993).

Most techniques that involve extensional viscosity measurements can be grouped into the following categories: rotational methods, converging flow methods and stretched methods (Wang and Huang, 2013).

Several types of extensional rheometers have been developed on the basis of the above mentioned techniques and are used for the characterisation of viscoelastic fluids (Tabilo-Munizaga and Barbosa-Cánovas, 2005). All of them have a specific range of liquids that they could be used for. There is a limited number of physical principles upon which measurements can be based. These include uniaxial stretching of a sample with a clamped end (Meissner apparatus); stagnation point flow (four roll mill or cross-slot channel, opposed jets, porous flow); capillary break up; converged channel and orifice die (filament stretching). The choice to use a particular type of rheometer is influenced by an intrinsic property of a fluid, namely the viscosity which can range from very high, e.g. 10^5 Pa·s polymer melts down to 10^{-3} Pa·s

for very diluted solutions. Additionally, the choice of measuring technique is determined by flow conditions, such as extensional rates and strains and flow stability. Another aspect of the problem is that different experimental approaches involve different kinetics - stretching, pressure drops, elongations, etc. Gravity, surface tension effects and channel wall properties can all lead to significantly different results.

The measurement of extensional viscosity for low viscosity fluids (up to 1 Pa·s) is still a sophisticated process (Odell and Carrington, 2006). Such fluids cannot maintain their shape or support a thread. In addition, due to the shearing effect caused by near solid boundaries, all walled flows (contraction/expansion, cross-slot) are not shear-free.

The problems, associated with conventional extensional rheometers include their bulky size, high price and time demanding procedures. This means that their use in process time scales or even on-line/in-line regimes is questionable (Fischer and Windhab, 2011). The common procedure of off-line or end line rheological testing consists of using a series of probes with given shear rates for a constant stress applied over time. The cycle is repeated for different stress levels using new samples with identical characteristics (size and geometry) (Coussot, 2014). This procedure usually involves manual intervention and takes time.

2.4.1. Pressure drop extensional rheometers

A pressure drop technique for extensional viscosity measurements is used in many types of rheometers. Combining pressure sensors with an orifice die enables one to minimize undesirable manifestations of a very narrow downstream channel in the die: wall slip, die swallow, dependence of viscosity on high extensional strain rates and pressure. Using a pressure drop technique in an orifice die provides more precise and reliable data and potentially could be used for real-time monitoring of industrial processes (Zatloukal and Musil, 2009).

In-line slit and tube rheometers, the latter with installed pressure transducers, permitted (Padmanabhan and Bhattacharya, 1993) to measure planar and uniaxial extensional viscosities for polymer melts. A pressure drop method used in conjunction with an abrupt channel contraction was used to calculate extensional viscosity by three different methods. Two of them showed good agreement in trends, but indicated deviation in magnitude. The third approach gave different values for either trend or magnitude.

Combination of birefringence and pressure drop monitoring in a slit die permits an inline monitoring of extensional flow (fig. 7). A new rheo-optic system has been developed that obtains information from fluids in channels of different sizes. Three flush mounted transducers measured wall-acting normal stresses, giving information about the pressure drop along the slit die. Optical probes in the channel provided data about birefringence. The construction developed has been recommended for monitoring extrusion processes, though significant differences with data obtained by off line rheometers has been found (Silva, Santos and Canevarolo, 2015).

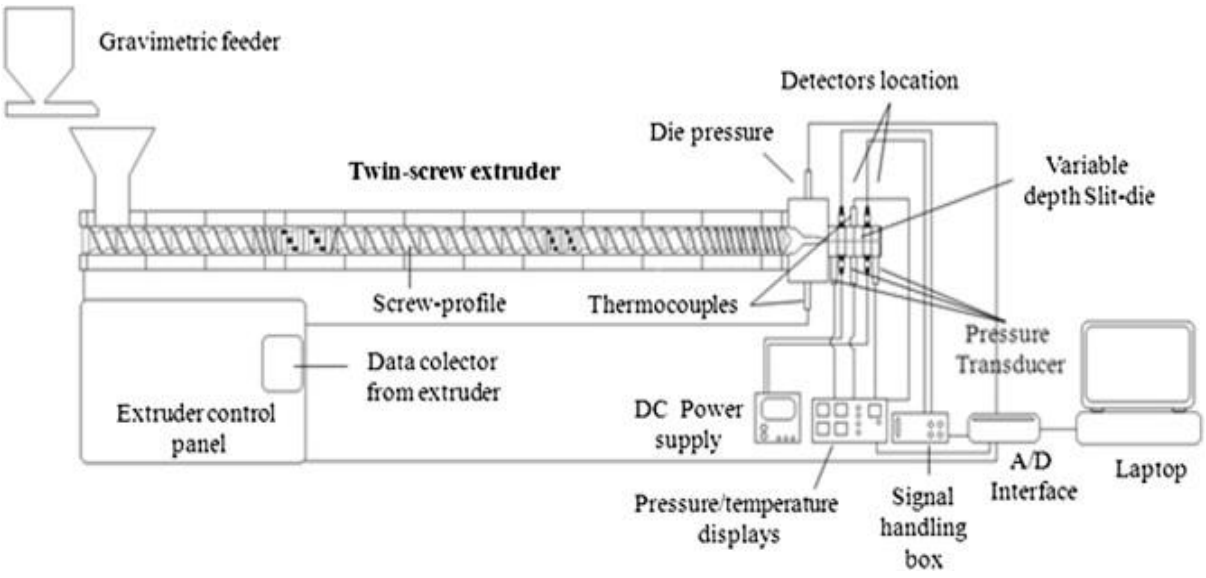

Figure 7**.** Schematic diagram of the experimental apparatus to inline monitor the pressure drop and birefringence of the polymer flow during extrusion (Silva, Santos and Canevarolo, 2015).

An in-line rheometer for making viscosity measurements of polymeric starch materials was described by (Xie, Halley and Avérous, 2012). A two channelled slit die was incorporated at the exit of the extruder. The construction of the device permitted measurements to be made of the pressure gradient along the channel due to variations in the shear rate. Data obtained were used to derive constitutive parameters of power law starch melts. The authors pointed out the influence of elastic properties of starch polymers on processing conditions and on end

product properties. However, their device did not provide extensional viscosity measurements. The same results were obtained by (Martin, Averous and Della Valle, 2003): their slit and cylindrical die in-line viscometers demonstrated high efficiency in the rheological characterisation of plasticized wheat starch across a broad range of shear rates (1 - 1000 s^{-1}). The device installed at the end of the extrusion line measured power law parameters of shear viscosity for viscoelastic polymers, but again it was not possible to obtain data on the elastic properties of the fluid.

However, extensional viscosities measured by orifice die are dependent on extrusion velocities, which can affect the results of tests. Steady state experiments enable more uniform data to be obtained (Wang and Huang, 2013). The use of fibre spinning tests for determining polymer extensional viscosities is widespread due to its simplicity, reproducibility and closeness to real industrial conditions (Muke *et al.*, 2001).

2.4.2. On-line rheometers based on stretched methods

Capillary rheometers can be used for online monitoring of food and polymer processing and provide quick fluctuation samples in a closed loop, enabling the extensional characteristics of fluids of interest to be defined (S. Smith, M. N. H. Irving and B. Simpson, 1970).

Another rheo-optic system involves filament stretching apparatus and a laser micrometer. Data obtained were related to transient extensional rheology. Real time monitoring assumes comparison of the measured diameter of a filament with an ideal one, defined by modelling of the process. The resulting error is used to adjust the rate of stretching in equally spaced time intervals (Anna, Rogers and McKinley, 1999). Common shortcomings of all optical systems, used for the determination of flow parameters, arise from the physical basis of optical investigation principles: firstly, opaque matter could not be a subject for the research and, secondly, data are measured only for part of the flow field, which is in the focus of the optical devices.

2.4.3. Stagnation point real time rheometers

The creation of a master curve usually requires the implementation of consecutive tests with different shear or flow rate conditions. Sometimes pre-shearing of the sample is needed, which affects response time. In contrast, stagnation point flows generate planar or uniaxial extensions and provide high strain rates and non-homogeneous flow regimes. Pressure drop techniques applied to cross slot channels or opposed jet devices enables extensional viscosity measurements to be obtained (Muke *et al.*, 2001), (Eastman, Goodwin and Howe, 2000). The

problem associated with this type of measurement is the difference in residence time between the region in the vicinity of a stagnation point and points downstream from the centre. The strain rate along the flow ranges from infinity at the stagnation point to very low values in the channel exit, thus stagnation point methods create non-homogeneous extensional flows. A further problem associated with these flows is that they are not purely elastic owing to shear effects occurring in jets and near channel walls. Additionally, the stagnation point in an opposed jet device is not stable due to elastic instabilities, thus optical control is required during the tests (Longo *et al.*, 2013). An extensional flow oscillatory rheometer has been proposed for extensional viscosity tests. Combining oscillatory flow with a stagnation point geometry enables one to separate a shear component from an extensional component. A microrheometer was developed along these lines for testing viscoelastic fluids with low viscosity (fig. 8) (Odell and Carrington, 2006).

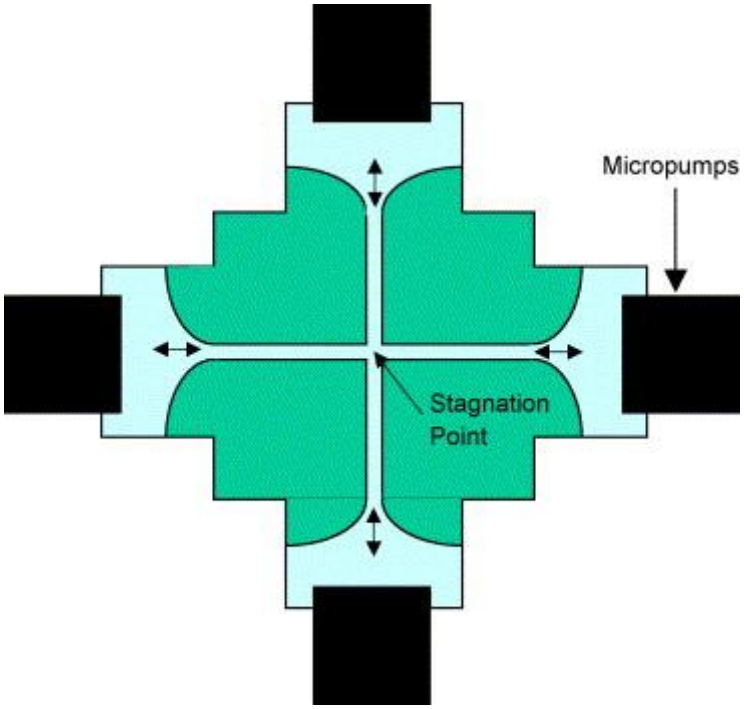

Figure 8. Schematic diagram of the cross-slots flow cell of the extensional flow oscillatory rheometer (Odell and Carrington, 2006).

A T-junction rheometer based on the application of mathematical modelling of the flow of a viscoelastic fluid that enables one to obtain the velocity or pressure field in single test could potentially be used as an in-line device for a wide range of liquids. Mapping of physical characteristics of the flow to the constitutive parameters of fluids using inverse method makes it possible to monitor various industrial processes (Rees, 2014).

2.4.4. Non-conventional real time rheometers

An unusual construction for a rheometer involving the measurement of gravity currents was developed by (Longo *et al.*, 2013), for testing flows with very low shear rates. Viscous spreading of non-Newtonian fluids over horizontal or inclined surfaces was taken as the basis of the method. A low error level was associated with this method which was found to work with just a small amount of test liquid. Another technique for making extensional viscosity measurements in creeping flows is a hot wire implementation, which involves analyzing natural convection as a viscous characteristic of the fluid (Miyawaki *et al.*, 1996).

A Couette geometry was used to analyze shear properties of a concentrated suspension of nanoparticles silica on-line (Anne-Archard *et al.*, 2013). The production of nanoparticles is a complicated process, which is very sensitive to physico-chemical and hydrodynamic conditions. Thus the on-line control of the stability of a system is of great interest. Four roll mill and Couette cells were used to investigate the influence of shear, turbulent and extensional flows on aggregation processes in silica suspensions. Analysis of the data obtained showed that pure extensional flow resulted in larger aggregations than for shear Couette flow, thus a lower shear thinning viscosity of the suspension occurred under elongational stress.

Non-invasive in-line measurement methods include wave-based approaches, such as resonators and ultrasonic-Doppler devices. These have been used to characterize fat suspensions, salad dressings, tomato ketchup, chocolate and cheese (Fischer and Windhab, 2011), (Birkhofer *et al.*, 2008), (Berta *et al.*, 2016). Ultrasound velocity profiles and pressure drops were measured in an in-line pipe section for a number of opaque liquids such as fat, chocolate and shampoo. Simultaneous measurements of pressure drop and velocity profile of the flow enabled the calculate shear thinning power law viscosity of the liquids of interest to be calculated. The results of the investigation were in good agreement with data obtained from off-line conventional rheometers. A disadvantage of the Doppler ultrasound method is that there could be sensitivity to noise associated with the manufacturing process.

As non-invasive tomographic techniques become more accessible, they are starting to be applied in chemical processing. They permit the velocity profile to be obtained from a single test and work with opaque substances (Arola *et al.*, 1997). The viscosity of mineral slurries, which are non-Newtonian liquids, has been measured on-line using a vibrating sphere and a rotational viscometer. The key point of this technique is that different components of the viscometer are used to analyze different ranges of shear rates (the vibrating sphere operates at higher shear rates than a rotational viscometer) (Kawatra and Bakshi, 1996).

The real time monitoring and control of extensional parameters of viscoelastic fluids in chemical, pharmaceutical and food industries aims to improve the quality of goods manufactured and to decrease the level of costs associated with wastage. Adaptation of traditional techniques and the development of novel methods for real time applications are being undertaken in response to demands from the industrial sector.

All of the techniques discussed have limitations of application depending on the materials to be analyzed, the processing method, the physics of the flow and the manufacturing parameters. These conditions should be taken into account when choosing a particular method for monitoring and control of the extensional characteristics of a product.

One of the potential solutions of this problem could be a combination of traditional sensor technologies in one device (pressure drop and velocity measurement) or to switch from one method of measurement to another (e.g.to consider the stagnation point instead of using optical and torque measurements that are associated with the pressure drop technique).

2.5. Boger fluids or elastic fluids with constant viscosity

The problem of understanding the rheological behavior of viscoelastic fluids is far from being solved, though significant work has been done to close the gap between theoretical predictions and experimental results. Mathematical descriptions of constitutive models of non-Newtonian fluids need to take into account the nonlinear shear viscosity, which depends on the shear rate of the flow. This viscosity could be characterised by flow conditions, fluid nature, kinematic pre-history of the flow, molecular chains and other factors. Scientific investigation proceeds in several directions, including complex approaches in modelling and experimental techniques. Experimental investigations could be focused on the development

of flow conditions, which could involve the forcing of pure elastic flow, and those that deal with liquids with specific properties, that permit one studies of viscous and elastic processes to be made separately.

A class of fluid was proposed by D.V. Boger in 1977 was called "a highly elastic constant viscosity fluid" (Boger, 1977). Such liquids are characterised by constant or almost constant shear viscosity and exhibit a significant elastic component. In this pioneering article the author tested rheological properties of a Newtonian liquid (maltose syrup and water) and a new complex fluid (maltose syrup and water with the addition of 0.08% of polyacrylamide) on a Weissenberg rheogoniometer and capillary rheometer. The author reported that both liquids had constant viscosity, but the polymer solution was characterised by high elasticity, exhibiting non-linear normal stress. The main conclusion of the research was the definition of a specific class of liquids that consist of a viscous Newtonian solution with a small amount of added polymer, which exhibited high viscosity and high elasticity.

The class of liquids that exhibit constant viscosity over a reasonable shear rate range and extensive elasticity are now known as Boger fluids. A number of such liquids exist, with different compositions and properties. They are widely used for the investigation of extensional properties of matter. A brief review of studies devoted to Boger fluids, is presented in Table 1. The main principle for defining a Boger fluid is the presence of a trace amount of a high molecular weight polymer with a coiled or branched molecular chain, which elongates when subjected to deformation. This provides the elastic properties of the fluid. The quantity of high molecular weight polymer should be sufficient to eliminate shear thinning and viscous effects. In many cases, the investigation of extensional properties comprises a comparison of experimental data obtained from a Boger fluid with those obtained from a Newtonian fluid of the same viscosity.
Different aspects of the nature of elasticity have been studied with Boger fluids. A significant amount of research on Boger fluids has taken place since their introduction.

The first Boger fluid consisted of a viscous Newtonian solvent and polyacrylamide of high molecular weight. This polymer is prone to mechanical degradation, so all manipulations concerning the preparation of the solution or flow feeding had to be done with precautions. Additionally, it was reported that “ready-to-use” polyacrylamide Boger fluids could be contaminated with bacteria, therefore some researchers recommended adding a small amount

of Kathon (Alves, Oliveira and Pinho, 2004). Shear thinning behavior of the fluid can be minimized by addition of one or two percent of NaCl (Magda *et al.*, 1991).

Polyacrylamide Boger fluids have been the focus of research for investigations on elastic properties. The nature of the liquid permitted studies of various aspects of viscoelastic flow to be made. The contribution of different molecular effects of long chained polymers has been investigated with regard to pressure drop scaling for complex flows for different flow rate regimes (Cartalos and Piau, 1992). Corroboration of extensional properties of low viscosity Boger fluids with different concentrations has been made from flow pattern visualisation, measuring vortex length of the contraction flow (Campo-Deaño *et al.*, 2011), (Soulages *et al.*, 2009), (Alves, Oliveira and Pinho, 2004), extensional viscosity measurement and model validation (Jackson, Walters and Williams, 1984), (Berg, Kröger and Rath, 1994), (Williams and Williams, 1985) and excess pressure drop measurements for Boger fluids compared to Newtonian ones (Pérez-Camacho *et al.*, 2015). This fluid is a bench mark for research methods and modelling validation.

Consequently the second type of Boger fluid developed comprised a mixture of high molecular weight polyisobutilene with polybutene (PB/PIB). The former cannot be dissolved in polybutene directly, so it had to be mixed with a light solvent first. A number of such solvents exists, together with several methods for creating solution, including stirring and evaporation of undesirable additives.

This Boger fluid has been used to measure the second normal stress differences in order to compare the pressure field between a polyisobutilene Boger fluid and a standard polymer solution (Magda *et al.*, 1991) in order to study the impact of rheological behaviour on dynamic wetting (Wei *et al.*, 2007) or spreading on a horizontal surface (Han and Kim, 2013), the impact of viscoelastic properties of Boger fluids on Newtonian drops suspended in a fluid (Tretheway and Leal, 2001), Trouton ratio measurements (van Nieuwkoop and Muller von Czernicki, 1996) and conducting purely extensional experiments (Gupta, Puszynski and Sridhar, 1986).

Investigations of the behaviour of Boger fluids have made a substantive contribution to the theoretical understanding of viscoelastic effects of fluids. (Mackay and Boger, 1993) tested polyisobutilene in an isobutene Boger fluid in shear and oscillatory flows. They found that the closest description of the extensional behaviour was a Hookean dumbbell model, because the solvent possessed slight elasticity. Other works illustrated the applicability of the

dumbbell model, which is limited by moderate shear rates (Prilutski *et al.*, 1983). Further investigations of this problem demonstrated that the finitely extensible nonlinear elastic model predicted viscoelastic flow parameters for high strain rates with a high level of validity (Verhoef, Van Den Brule and Hulsen, 1999).

A recent commonly used type of Boger fluid is polystyrene in an organic solvent, and it is characterised by its low viscosity. Again as a liquid with comparably low viscosity, this fluid was used in flows through a stagnation point oscillation rheometer for extensional viscosity measurements (Odell and Carrington, 2006), bench mark flow past a sphere to determine how the fluid elasticity affects the drag coefficient (Solomon and Muller, 1996), investigation of the influence of the Deborah number and channel geometry on the pressure field and the vortex size of contraction and micro contraction flows (Rothstein and McKinley, 1999), (Rothstein and McKinley, 2001), (Sankaran *et al.*, 2013), dynamic wetting (Wei *et al.*, 2007), birefringence and pressure and flow field measurements for planar contraction (Haward *et al.*, 2010), birefringence model validation (Li *et al.*, 2000) and many others.

The most popular method of preparation was suggested by (Odell and Carrington, 2006) and involved forming a solution of polystyrene in dichlormethane, then adding the mixture to dioctyl phthalate and finally evaporation by dry N_2. Another procedure proscribed direct solution of high molecular weight polystyrene in low molecular weight polystyrene and rolling the solution for 3-4 months (Wei *et al.*, 2007).

Analysis of the above sources enables defining basic principles for making an appropriate test Boger fluid. Polyacrylamide and polystyrene fluids possess low viscosity, which is an essential requirement for flow through experiments, whilst polyisobutilene fluid was mainly used in experiments where the sample could maintain its shape outside of a confining volume due to its relatively high viscosity. This means that the shear rate range is rather narrow and one could encounter problems in pushing the liquid through a channel.

On the other hand, when choosing between polyacrylamide and polystyrene fluids, the priority should be given to the former because of the clear simplicity of its preparation process. Further, polyacrylamide is soluble in water and is an ionic polymer. This property could be important in capacitance experiments (Ma *et al.*, 2015). Thus, a polyacrylamide based Boger fluids is used below in this thesis.

2.6. Fluid flow pressure measurement

To date, only a limited number of experimental studies have investigated the dependence of the macroscopic parameters of a flow on the constitutive parameters of viscoelastic fluids. The visualisation techniques including particle image velocimetry and birefringence were, and still are, the main methods of quantitative assessment of flow behaviour. These methods are restricted by the optical properties of the liquids and apparatus, and give flow statistics only in the area of observation. Furthermore, these measurements are carried out in one plane of the flow, giving a 2D mapping of the flow field. Direct stress assessments by pressure measurements are another option which could provide reliable and complex data for extensional viscosity determination.

In order to identify constitutive parameters for viscoelastic liquids from a single experiment by means of solving an "inverse problem", it is important to install a sufficient number of sensors to obtain measurements of flow fields that can be mapped to the underlying constitutive parameters. Numerical simulations (presented in Chapter four) have shown that the most information rich region, where a range of extensional rates is observed, is the vicinity of the stagnation point on the symmetry line near the back wall of the T-junction channel. This information rises questions about means which of flow measurements would permit one to solve an inverse problem. Velocity field determination by capacitance sensors is discussed in the section 2.7. The need to obtain pressure data along the channel is of great importance.

Pressure drops across a T-shaped microchannel with a rectangular cross-section for single and two-phase flows were studied by (Yue, Chen and Yuan, 2004). The authors used pressure transducers to obtain the pressure drop data of an N_2-water two phase flow system in T-shaped micromixer for the purpose of comparison with data obtained with those predicted by flow pattern-independent models. Two short limbs of the channel were used as inlets and the long channel served as the mixing part of the device. Two pressure transducers were installed along the outlet limb of the channel. The pressure drop was measured for single phase and two phase flows with controlled flow rate imposed. The main conclusion deduced from the results of the experiments was that while empirical data for single phase flow obeys the standard theory, in the case of two phase flow, the models used did not predict the pressure drop for the micromixer, so further research is needed to close the gap between theoretical predictions and experimental measurements.

Table 1. Boger fluids and relevant investigations

Composition		Shear zero viscosity	Methods and research objectives	Authors
Polymer	Solvent			
Polyacrylamide M_w*= 5.6×10^6 $18*10^6$ Concentration: 20-500 ppm 50 - 400 ppm 0.1% 0.2%	Glucose syrup, NaCl Water Maltose syrup and water Corn syrup Glycerin and water	1 Pa s 1000 pois 0.5 -70 Pa s 50 P (pois) 13 Pa s 0.5 Pa s	Pressure drop scaling in different flow regimes, showed dependence of elongation viscosity on flow rate	(Cartalos and Piau, 1992)
			Contraction-abrupt geometry, deriving degree of elasticity from vortex length	(Campo-Deaño *et al.*, 2011)
			Trouton ratio measurement and Oldroyd-B model validation Steady state flow exhibited higher elasticity than did oscillatory flow	(Jackson, Walters and Williams, 1984)
			Extensional viscosity measurement by stretching liquid bridges in microgravity	(Berg, Kröger and Rath, 1994)
			Stagnation point cross slot lubricated channel, extensional viscosity measurement	(Williams and Williams, 1985)
			Contraction axisymmetic flow, pressure drop measurement and kinematics of flow	(Pérez-Camacho *et al.*, 2015)
			Square contraction flow, study of viscoelastic fluid behavior depending on flow regime (contraction ratio, Deborah number)	(Soulages *et al.*, 2009)

ppm			Square-square contraction, investigation of influence of temperature, fluid composition and flow rate on flow pattern	(Alves, Oliveira and Pinho, 2004)
Polyisobutylene $M_w=1.3\times10^6$ g mol^{-1} 1.7 - 2.1 4.2-5 Concentration 0.1% 0.05% 1000 ppm	Polybutene and 2-Chloropropane; Polybutene; Polybutene and tetradecane; Polybutene and toluene	23.7 Pa s About 300 P 2.4 Pa s 365 poise 35 Pa s 20 Pa s 13 Pa s	Free surface rod-climbing and cone-and-plate shearing flow, Boger fluids had smaller second normal stress difference than standard polymer solution	(Magda *et al.*, 1991)
			Investigation of influence of elasticity of a fluid on its dynamic wetting	(Wei *et al.*, 2007)
			Oldroyd-B model described steady-state flow very well, while for oscillatory flow better results were obtained with Hookean dumbbell model because of elasticity of the solvent	(Mackay and Boger, 1993)
			Experimental verification of dumbbell model and finding limits for the model	(Prilutski *et al.*, 1983)
			Filament stretching, extensional viscosity at high strains was predicted by finitely extensible nonlinear elastic model	(Verhoef, Van Den Brule and Hulsen, 1999)
			Conventional rheometers, time-dependent transition study	(McKinley *et al.*, 2007)
			Impact of elasticity on spreading of fluid on horizontal	(Han and Kim, 2013)

			surface	
			Four roll mill, growth of viscoelastic effects in Boger fluid increased deformation of suspended Newtonian drops	(Tretheway and Leal, 2001)
			Droplet stretching rheometer, Trouton ratio measurement	(Van Nieuwkoop and Muller Von Czernicki, 1996)
			Fibre spinning, measurements of stress and velocity of the flow in an extensional deformation	(Gupta, Puszynski and Sridhar, 1986)
Polystyrene $M_w=8.5\times10^6$ g mol^{-1} 2×10^7 2.25×10^6 Concentration = 100 ppm 0.16% c=0.24 (0.025%)	Dioctyl phthalate; Tricresyl phosphate; Oligomeric styrene; Low molecular weight polystyrene; Polyethylene oxide and polyethylene glycol	1-31 mPa s 2 - 2.3 Pa s 22.8 Pa s (high concentration) About 500 P 12 Pa s 0.66 Pa s	Stagnation point oscillatory rheometer, extensional viscosity measurement	(Odell and Carrington, 2006)
			Flow past a sphere, investigation of impact of fluid's elasticity and molecular structure on drag coefficient	(Solomon and Muller, 1996)
			Axisymmetric contraction flow, investigation of extra pressure drop and vortex size depending on Deborah number	(Rothstein and McKinley, 2001)
			Dynamic wetting investigation depending on extensional characteristics of Boger fluids	(Wei *et al.*, 2007)
			Axisymmetric contraction flow, influence of channel geometry on vortex growth	(Rothstein and McKinley, 2001)
			Planar contraction flow, birefringence, pressure drop and flow field measurements	(Haward *et al.*, 2010)

0.003% and 0.02%			Micro contraction flow, investigation of flow field of pre-deformed fluid	(Sankaran *et al.*, 2013)
			Axisymmetric stagnation flow, investigation of potential of by finitely extensible nonlinear elastic model to predict flow birefringence	(Li *et al.*, 2000)

* - Molecular weight

Williams and Williams, (1985) tried to solve the problem of the existence of both shear and extensional effects in a cross slot shear driven flow with a stagnation point. Lubrication provided slip wall boundary conditions by reducing friction between the test liquid and the walls of the channel, thus pure elongational flow was generated in the center of the cross slot geometry. Pressure was measured by 5 transducers flush mounted in the walls of the nozzles. Data were recorded for Newtonian and Boger fluids and results were compared to determine differences in the behaviour of the test fluids. Pressure sensors were installed at the entrance of the inlet flow. Experiments were carried out with Newtonian (maltose syrup and water mixture) and Boger (maltose syrup, water and 0.1% of polyacrylamide) fluids at different flow rates. The apparatus demonstrated good agreement of results with theory for low flow rates, although the authors pointed out that further instrument modification should be made to increase the flow rate range.

A converging channel rheometer was used to examine the rheological behaviour of polymer solutions (James, Chandler and Armour, 1990). The test channel geometry and experimental regimes (high Reynolds number) were developed in such a way that they provided a constant rate of extension in the middle of the flow. Pressure drop was measured at several points of the channel by flush- mounted pressure transducers so as not to interfere with the flow. The technique used permitted extensional viscosity to be defined as a function of strain. The method had certain limits of application, for example, only a narrow range of liquids could be tested, or to only high flow rates, so the equipment should be improved to eliminate these disadvantages.

The rheological properties of polymer melts have been determined in contraction flows (Zatloukal *et al.*, 2002). The authors investigated the problem of extensional viscosity measurement manifested in many manufacturing processes dealing with polymers. The pressure drop of flow through an abrupt axisymmetric contraction was determined and then viscoelastic parameters of tested melts were derived based on the entrance pressure drop and shear rate. The measurements were obtained using pressure transducers for five low density polyethylene melts at low shear rates. Transducers with a high resolution across the lowest pressure ranges were installed to ensure accuracy of measurement. Results obtained led to the conclusion that rheological properties of polymer melts affected the entrance pressure drop, suggesting that this method could be used for the determination of extensional viscosity of viscoelastic fluids.

The pressure drop method was used to validate a new optimized cross-slot flow micro-geometry with birefringence, bulk pressure drop and PIV techniques (Haward S. J. Alves M. A., McKinley G. H., 2012). Low viscosity polyethylene oxide solution with almost constant viscosity was tested both in shear and elongation flows across a wide range of shear rates. The pressure drop attributed to the extensional viscosity was determined from the difference in the total pressure drop arising in a cross-slot shear-extensional flow and that occurring across a sheared steady flow with a single inlet and a single outlet. An excess pressure drop manifested in the cross-slot stagnation point flow variation, which was attributed to additional pressure dissipation due to elongation phenomenon of the flow.

Use of the excessive pressure drop as a method for making extensional viscosity measurements of viscoelastic fluids of low viscosity has been investigated (Odell and Carrington, 2006a). In the cross-slot device, differential pressure transducers were located in the limbs (i.e. inlet and outlet channels) of the apparatus. Shear viscosity was measured by forming an oscillating flow in a single pair of limbs (one inlet - one outlet), avoiding the creation of a stagnation point flow. By combining pure elongational planar flow with oscillatory flow, the authors managed to define separately the shear and extensional viscosities, as well as the Trouton ratio, for two polymer solutions.

Direct viscosity assessment of a gas/oil mixture has been performed using a novel sensor based on different pressure measurement principles (Rondon, Barrufet and Falcone, 2012). A special device was developed which provided laminar flow through a conical element of a sensor with a narrow radial gap. Pressure was measured at the inlet and outlet of the probe. Geometrical parameters of the device were selected in such way that the viscosity of a test fluid could be calculated from a single experiment based on pressure drop and a controlled constant flow rate. Analogue transducers were used to measure inlet, outlet and differential pressures of the flow. The sensor showed good agreement between experimental data for several Newtonian and power-law liquids across a wide range of temperatures and independent shear tests of the liquids made using a conventional rheometer. This viscosity measurement device could potentially be used to control drilling of oil wells.

A comparison study between different techniques for making flow parameter measurements was implemented by (Jerry K. Keska and Williams, 1999). In their research, the authors investigated vertical adiabatic air/water flow using capacitive and resistive methods alongside with static pressure and optical methods. Static pressure was measured using a gauge pressure sensor, which detected pressure fluctuations of the system due to changes in the physical

condition of the flow in the test chamber. Flow regimes were determined by time, amplitude and frequency of the air/water system. The results of this study led to the conclusion that electromagnetic methods showed high sensitivity and accuracy in two phase flow pattern discrimination over a broad range of flow conditions, whilst the static pressure measurement method was influenced by the intensity of the domain fluctuation. To put it another way, capacitance sensors work well with pulsating flows in changing conditions, whereas pressure method could be used for the investigation of steady state laminar flows.

Measurements of the pressure conditions in a flow are of great importance in investigation of the efficiency of energy systems. Super critical flows take place within heat exchange elements of power plants. Flows under high pressure and boiling temperatures with forced convection in inclined tubes simulate real processes occurring in power generation equipment. (Taklifi *et al.*, 2016), studied heat transfer and pressure drop gradients of sub-critical and supercritical water flows. The experiments were carried out in various operating conditions of pressure, heat and mass fluxes. Inlet and outlet pressures were measured with pressure transmitters. The results of the experiments demonstrated that the pressure drop of the flow increased with the augmentation of the mass flux. It was found that the length of the testing tube is significant for flow pattern recognition based on pressure drop.

Mining, transportation and storage of viscous oil raises the problem of development, handling and control of these processes. One of the most widely used method nowadays is the mixing of oil with hot water. Investigation of two phase flows with a high water fraction often includes flow pattern mapping. Pressure drop determination remains a non-trivial question, which is complicated by the heating processes that make the mixture less viscous. The pressure drop of a two phase flow in a horizontal pipe under different experimental conditions, measured by a differential pressure transmitter, showed that the pressure flow field is sensitive to temperature, water fraction and flow velocity (Jing *et al.*, 2016).

In order to develop a lab-on-chip system for rheological tests (McKinley *et al.*, 2007), investigated the flow of polymer solutions in converging/diverging geometries. Kinematics of pressure driven Poisseuille flow in micro-scale contraction-expansion and hyperbolic channels was studied using PIV and pressure drop measurement methods. A solid-state differential pressure transducer was used to obtain data across the channel. The authors drew two conclusions from their study: firstly, flow patterns such as corner vortices depend only on viscoelastic fluid properties and the channel geometry, but not on the flow conditions;

secondly, by deriving the excess pressure drop from measurements and modeling, the extensional viscosity could be estimated for the test fluid. Thus this devise could be considered as a suitable platform for the rheological study of low viscosity polymer solutions at low Reynolds number.

Pressure measurements in contraction flows made to determine extensional viscosity in another research work. Excess pressure loss was identified as a result of elongational flow in an axisymmetric, planar geometry. An array of flush mounted strain-gauge type pressure transducers was used to detect the pressure drop along the channel (Binding and Walters, 1988).

(Joyce and Soliman, 2016) investigated pressure losses in oscillatory two phase flow through T-shaped pipes. It was found that an air-water mixture at fixed pressure and constant temperature could generate different flow patterns depending on the mass fraction gas and liquid. Flow regimes were visually controlled at the inlet and outlets of the pipe section. 43 pressure taps with connected pressure transducers were installed in the bottom of the pipe. An energy-based separated flow model was developed, which predicted pressure loss along the T-shaped pipe configuration. 80 experiments were carried out. Data obtained demonstrated large deviations from predictions, and empirical coefficients were changed to match theoretical estimations. However, the setup and model showed good agreement in the case of single phase gas flow. As a result the pressure loss measurements could be used for two phase flow characterisation in T-shaped flow channels.

A new approach aimed at increasing the efficiency of heat exchangers was examined by (Adachi *et al.*, 2009). They suggested that forming periodic grooves between parallel plates would transform a steady state flow into a three dimensional oscillatory flow, which would enhance fluid mixing and heat transfer. As a consequence of flow kinematic variation additional pressure dissipation would occur. This process could be analysed by pressure drop measurements. Static pressure difference was measured using 3 micro-differential pressure transducers in the flow under a controlled flow rate. Experiments had shown that the pressure drop in the channel with periodic grooves depended on the Reynolds number increasing up to critical values, which was determined experimentally.

Another work devoted to investigation related to heat exchangers was made by (Hsu *et al.*, 2015). The frictional pressure drop was studied for pressure driven single phase /two phase flows in a pipe with a 90^0 bend. The experiments were conducted across a wide range of air

and water mass flux rates, and Reynolds number. Several differential pressure transmitters were installed in the test section of the pipe in order to determine the difference between the pressure drop across the straight tube and the upward or downward bent sections. The authors reported that the data obtained were in good agreement with previous research for straight tubes, but for flows in a pipe with a bend there was significant deviation. The maximum difference was observed for the case of two phase flow in an upward configuration of the bend, due to swirled motion. This diminished as the gas phase increased.

In an attempt to define the impact of the constitutive parameters of viscoelastic fluids on the pressure drop and kinematics of flow through an axi-symmetric contraction–expansion geometry, (Pérez-Camacho *et al.*, 2015), developed an apparatus which permitted simultaneous measurements of flow visualisation and pressure measurements. Three liquids with different rheological behaviour (Boger, shear thinning and Newtonian) were tested in contraction-expansion channels of various sizes. Two pressure transducers were built in fully developed zones upstream and downstream of the contraction to avoid vortex influence. It was observed that elastic properties of the test fluids affected pressure dissipation along the flow, which manifested in a greater pressure drop in the case of Boger and shear thinning liquids compared with Newtonian fluids. The intensity of this phenomenon rose as the contraction-expansion ratio increased.

(Rodd *et al.*, 2005), examined fluid behaviour in planar entry flow in order to explore the interaction between elastic and inertial properties. Low viscosity polyethylene oxide solutions and a Newtonian fluid (water) were exposed to deformation in a micro fabricated contraction-expansion channel with a contraction ratio of 16 under conditions of a controlled flow rate conditions. Kinematics of the flow was monitored by video-microscopy and streak imaging which revealed occurrence of vortex growth as a result of combined viscous and elastic properties of the test fluids. Pressure was measured using two differential pressure sensors which were installed into pressure taps upstream and downstream of the contraction part of the channel. The authors emphasized that the geometry used in this particular device allowed them very high shear rates and high extensional flow effects to be achieved. The chosen approach for making pressure drop measurements enabled the researchers to quantify the excess pressure drop for viscoelastic fluids in comparison with a Newtonian fluid. However, the data obtained have not been compared with previous studies or with any existing model.

Craven, Rees and Zimmerman, 2010 presented numerical simulations for the electrokinetic flow of a Carreau fluid in a T-shaped channel. They investigated the optimal pressure sensor positioning in order to enable viscous parameters to be determined by using an inverse method. A T-shaped channel can be used to set up a flow system that generates a range of extensional rates simultaneously, thus enabling the fluids viscosity function to be determined from the study of a single flow. This information can be extracted indirectly by measuring the pressure in the flow at different positions along the channel. The statistical moments of the back wall pressure profile of a Carreau fluid in a T-junction channel were found to map uniquely to some constitutive parameters of the shear viscosity.

A region of high interest is the stagnation point where it is possible to produce a set of extensional rates as a function of the deformation rate. Pressure recordings could be made with the application of pre- calibrated pressure sensors.

Based on the above review, the conclusion could be made that pressure sensors are precise and reliable tools for detecting and recording flow strain information in real time. The range of these types of sensors is very wide in terms of size and measurement scale from micro lab-on-chip devices to industrial size prototypes. The field of application is significantly broad and includes flow pattern determination, phase differentiation, pressure drop assessment and indirect extensional viscosity measurements. At the same time, pressure sensors have some peculiarities which must be taken into consideration. All sensors should be calibrated prior to experiments. The sensors are not compatible with all types of flows and liquids and should be chosen for the particular needs of the research and industrial cases. Pressure sensors are well characterized for steady state flow, whilst their use for the transient flow requires additional manipulation to improve the reliability of the reading.

In this study, in order to provide the opportunity for extracting viscous parameters by means of the application of inverse methods using a prototype rheometer, four pressure sensors were embedded in the channel ceiling: one in the centre of the T-junction and one in each arm of the channel (one in the inlet and one in each of the two outlets). These types of sensors are low cost, can work in high pressure conditions and are suitable for use with opaque liquids.

The above survey leads one to the conclusion that the use of pressure sensors provides an optimal solution for the investigation of viscosity for non-Newtonian liquids under pressure drop flow conditions in terms of preciseness, reliability, applicability for opaque liquids and the potential for use an on-line processes.

2.7. Review of velocity measurement methods

Investigation of fluid flow consists of finding physical fields of the flow based on the property of the liquid and boundary conditions. Flow statistics include pressure value and velocity components. In order to carry out an inverse method it is necessary to define flow kinematic figures prior to finding the constitutive parameters of the flow.

Reliability and accuracy of definition of flow parameters depends on making a suitable choice of sensor system. Many various techniques have been used for investigation of the velocity profile of the fluids flowing under different conditions.

Study of recent research concerning velocity measurements shows that there is a significant diversity of methods which could be used to define the velocity of particles in a gas/solid flow. These methods include digital holographic particle velocimetry (Yang and Kang, 2015), X-ray computed tomography (Bieberle and Barthel, 2016), (Barthel *et al.*, 2015), electrostatic sensors (Seraj, Rahmat and Khalid, 2013), (Li, Xu and Wang, 2012), (Ma and Yan, 2000), electrical capacitance tomography (Wang *et al.*, 2012) and many others. All these methods require that there is a high contrast between the phases of the flow. This significantly narrows their application potential.

In order to investigate two-phase oil/water flow velocity (Dong *et al.*, 2015), applied a continuous wave ultrasonic Doppler method. Oil formed non-rigid droplets in water. An emitted acoustic wave reflected from moving droplets, obeyed the Doppler effect. The testing chamber consisted of a plexiglas pipe with two ultrasonic piezoceramic transducers. One of them emitted an ultrasound wave with a particular frequency and the other received and defined the phase shift of the wave. The wave phase shift was translated to give the mean velocity in the sensing volume. and This estimate could be made with an average error equal to 3.63%. The authors pointed out that this non-invasive ultrasound method could be used to measure the velocity profile of two-phase flows.

Barthel *et al.*, (2015), described X-ray tomography for velocity measurements of two-phase flows. In addition to gas-liquid and gas-solid flows, the researchers investigated the continuous liquid phase by adding a tracer additive to enable X-ray examination. This is a non-invasive imaging method based on X-ray generation. An analysis of a sequence of cross-

sectional images permitted them to define the velocity of the phase of the flow or contrast agent in the fluid stream. This method demonstrated its high efficiency for opaque liquids and included use of the cross-correlation technique for attenuation gradients analysis.

The two phase flow velocity measurements described above are suitable for specific types of flow in which droplets or separate particles could be formed. So the conclusion could be made that they are not suitable for homogeneous fluids such as emulsions, suspensions and other viscoelastic liquids.

Non-invasive imaging techniques have been successfully transformed from qualitative flow visualization tools into quantitative velocity measurement instruments. The combination of illumination, recording equipment and computational image analysis is fundamental to particle-based velocimetry techniques. All particle based techniques require that the test liquid is seeded by fluorescent beads, contrast or radioactive particles. These methods also can be used for the assessment of the stability of the flow field.

Laser Doppler velocimetry makes use of a split laser beam. The two resulting coherent beams are made to cross and form an interference area. The motion of highly reflective particles that cross this area can be recorded. The velocity can be determined from the known time delay (Marvos, 2001).

More reliable and sophisticated methods of particle tracking are particle image velocimetry (PIV) and particle tracing velocimetry (PTV). These methods differ in the principles of data recording used. While PTV determines randomly located velocity vectors, the PIV method delivers velocity vectors on a regular grid. The applicability of PIV/PTV depends on several parameters, e.g., flow characteristics, intensity of illumination, and density of seeding (Li *et al.*, 2013).

The dynamic viscosity in a T-junction micro-rheometer was investigated by Bandulasena, *et al.*, 2011. The velocity field within the microchannel was measured using μ-PIV. The PIV apparatus consisted of a laser, CCD camera, synchroniser, inverted microscope, fluorescent filter block and beam optics. The fluid was seeded with fluorescent particles to track the flow. The velocity field statistics were used as a base for inverse problem solving.

Velocimetry applied to streak images can be used to analyze the flow field dynamics as a function of the flow characteristics: Wiesenberger/Reynolds number correlation (McKinley *et al.*, 2007) (Gulati, Muller and Liepmann, 2008), excess pressure lost (Binding and Walters,

1988) and different flow rates (Campo-Deaño *et al.*, 2011). In these articles the authors investigated parameters of a flow that can cause vortices or secondary motions in contraction flows. The visualization of flow patterns was analyzed using sophisticated methods to determine the elasticity of the tested fluids.

All of the PIV techniques described above involved use of optical methods. However, optical apparatus are generally unsuited for the purpose of on-line process measurement and correction due to their complexity and bulkiness. Complications associated with statistical data collection from the visualisation pose problems for making on-line measurements. Furthermore, all of the experiments listed above involved the use of additives to the liquid in order to make the velocity field traceable. The use of seeded particles can change the properties of a test liquid and is inappropriate for the investigation of consumable goods (food, cosmetics, etc.). Obviously, specific restrictions exist due to the physical nature of the optical approach - the experimental chamber and the liquids of interest must be transparent. This excludes all opaque liquids such as paints, food products and cosmetics from the application field. Setups for the investigation of transparent but very viscous liquids should be constructed from metals or very thick plastic in order to withstand the required high pressures. This makes the application of visual methods very limited. Practically, it is very difficult to implement optical test systems as a suitable alternative for on-line measurements. They measure velocity pattern of the flow only in the optical focused area, which could be insufficiently small compared to the full flow geometry. The optical method was found to be limited its applicability.

Thus one of the targets for this research is the development of a non-invasive, reliable, easy to use examination approach that is suitable for liquids of any transparency. The visualisation methods described herein could be used during the preliminary stages of the research as a supporting methodology to provide further insight into the physical nature of the flow.

2.7.1. Capacitance measurements

Another non-invasive, but reliable method of flow velocity measurement is capacitance sensing. Use of capacitor sensors to obtain physical measurements can be described by the following principle: the process, or parameter, changes the capacity between the electrodes of the capacitor. The electrodes of a capacitance sensor measure the permittivity variation of fluctuation of a fluid flow and the electrical circuit transfers it to the analogue data. Ideally, the electrodes should be assembled in such way that the sensor will

measure the particular characteristic of the process. For the purposes of the present research one of the parameters of interest is the velocity of a flow. To determine the flow velocity two capacitor sensors are installed in the channel such that one is a short distance, ΔL, upstream of the other. Calculation of the cross-correlation between the signals activated in the array of sensors by a propagating pulse permits one to determine the time shift, Δt (fig. 9).

If the distance between the two sensors is known, then the flow velocity can be calculated (Fuchs *et al.*, 2009). Capacitance sensors are characterized by high sensitivity and data transfer rate. This means that they can be used to measure flow properties accurately.

A capacitive approach is a well-known method for controlling and characterizing different types of flows. Demori *et al.*, (2011), developed a microfluidic device with embedded capacitive sensors to investigate flow behaviour and electric permittivity for different liquids. In their work a system of sensors was embedded into the device. The authors compared the device with other techniques for fluid characterization and drew the conclusion that the suggested system has the advantage of being low cost and provides measurements of the signal in real time.

Measurements of water in oil concentrations using straight surface and surface helical plate sensors were carried out by (Hammer, Tollefsen and Olsvik, 1989). Both configurations demonstrated high accuracy of measurements, but the latter showed a lower dependence on water distribution in the mixture.

A seldom used wire-type electrode capacitance sensor was developed and used by (Zhai *et al.*, 2014) to measure the velocity of horizontal two phase oil-water flow. The aim of the research was to make a reliable sensor for use in petroleum industry. The sensing system consisted of two parallel Teflon coated wires placed into the channel, exiting signal, data transition and data acquisition modules. To investigate the sensitivity field of the capacitance probe, computational simulations were undertaken using finite element method. Velocity of the flow was determined using the cross-correlation technique. Experiments demonstrated good performance of the probe in the narrow high sensitivity field area where the response of the system is dependent on the flow structure.

A comparison of four different popular techniques for flow investigation was published by Keska, Smith and Williams, (1999). Different patterns of two-phase air-water flow were investigated with the four most commonly used detection systems: electromagnetic methods (capacitive and resistive), a static pressure method and an optical method. The capacitive

sensor used in the system consisted of two electrodes opposing one another on the inside of the flow channel and defined the spatial concentration of the flow. The authors reported that the optical and pressure based systems were both more sensitive to the concentration and flow pattern compared to the capacitive method.

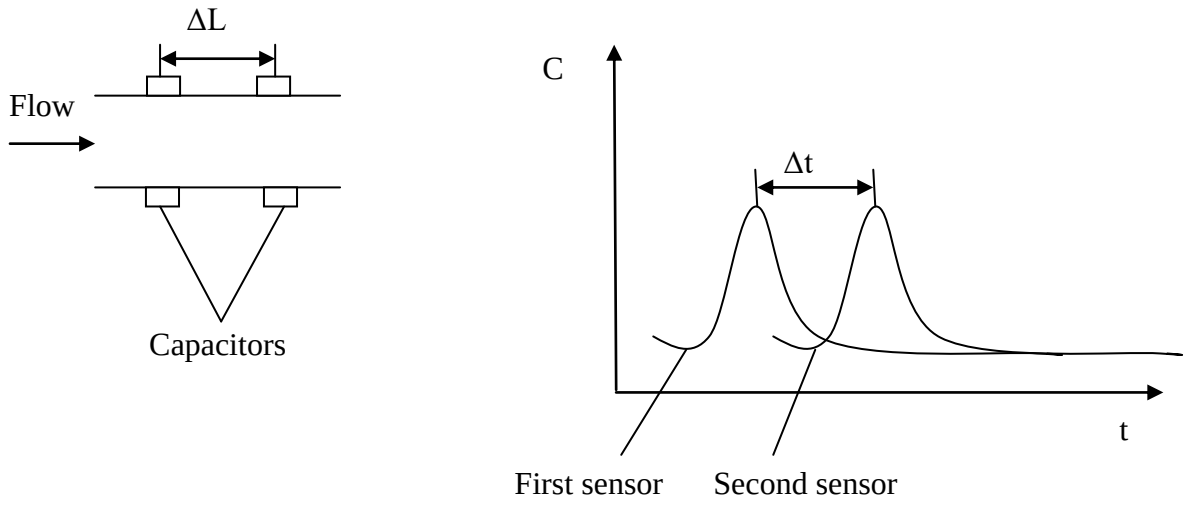

Figure 9. Working principles of capacitive flow velocity sensors. C-capacitance.

Jerry K Keska and Williams, (1999) pointed out that in comparison to capacitive and resistance methods, the pressure fluctuation technique has a lower resolution.

Strazza *et al.*, (2011) applied the capacitive system to determine a holdup in a mixture of high viscous oil and water. Two electrodes in the traditional concave configuration were flush-mounted onto the inner side of the channel. To eliminate any stray capacitance of the connecting cables the authors used AC-based electronics. The authors proposed a configuration for a capacitance system that is suitable for the investigation of the flow with conductive water. Another configuration of a sensor to measure holdup in two phase flow was suggested by (Zhai *et al.*, 2015). A double helix capacitance sensor used for water-oil flow showed a good sensitivity for water predominating flow.

Another work, devoted to the investigation of liquid holdup, described a conductance and capacitance combination sensor. A real time measurement method was realized by installing of four ring conductive electrodes and a pair of copper capacitance electrodes on a plexiglas pipe. They measured fluid fractures of the flow in the same volume and in short time period. Electrical Capacitance Tomography was chosen as the main principle of the sensing system.

The authors reported higher sensitivity of capacitance sensors for more homogeneous flow in comparison with conductive sensors, which worked well with more stratified flows (Wu *et al.*, 2015), (Tan *et al.*, 2015).

A new capacitive flow sensor was developed for respiratory monitoring. They derived a methodology that prevented a stray capacity by use of a monolithic sensor (Liao, Chen and Lu, 2013).

Results from a fluid dynamic study using a T-junction channel geometry for a two-phase air-water flow were recently published by dos Reis and Goldstein, 2013. Capacitive measurements were conducted with both helical and concave plate sensors. Measurements obtained demonstrated the suitability of their experimental setup to work as a gas-liquid separation device.

De Kerpel *et al.*, (2013) described data obtained using a capacitive void fraction sensor for researching the properties of two-fraction flows. Two concave copper electrodes of wide angle (160˚) were glued onto the tube wall. The measurement technique was based on both effects of the void fraction, which defined a capacitance between the electrodes, and on the non-homogeneous electric field that arose due to the curvature of the electrodes. The detected capacitance depended on the spatial distribution of the void fractions. The authors concluded that the form of the electrodes (curvature) had a significant effect on the measured capacitance.

An important problem arising in the petroleum industry concerns the analysis of the concentration of water and gas in crude oil and many articles are devoted to the solution of this problem. A 16-segmented electrical capacitance tomography sensor was used to obtain images of water-oil fractures in pipelines using capacitance data (fig. 10). It is worthwhile to point out that the tomography method requires the placement of capacitance electrodes all around of a pipe to provide flow visualization based on data measured. An acquisition system reconstructed an image of the flow structure from an integral of the measurements from all of the electrodes. The authors noted that they used a cylindrical pipe, but the shape of closed channel could be diverse. The experiments demonstrated consistency of concentration values and flow regime of water-oil mixture (Mohamad *et al.*, 2016).

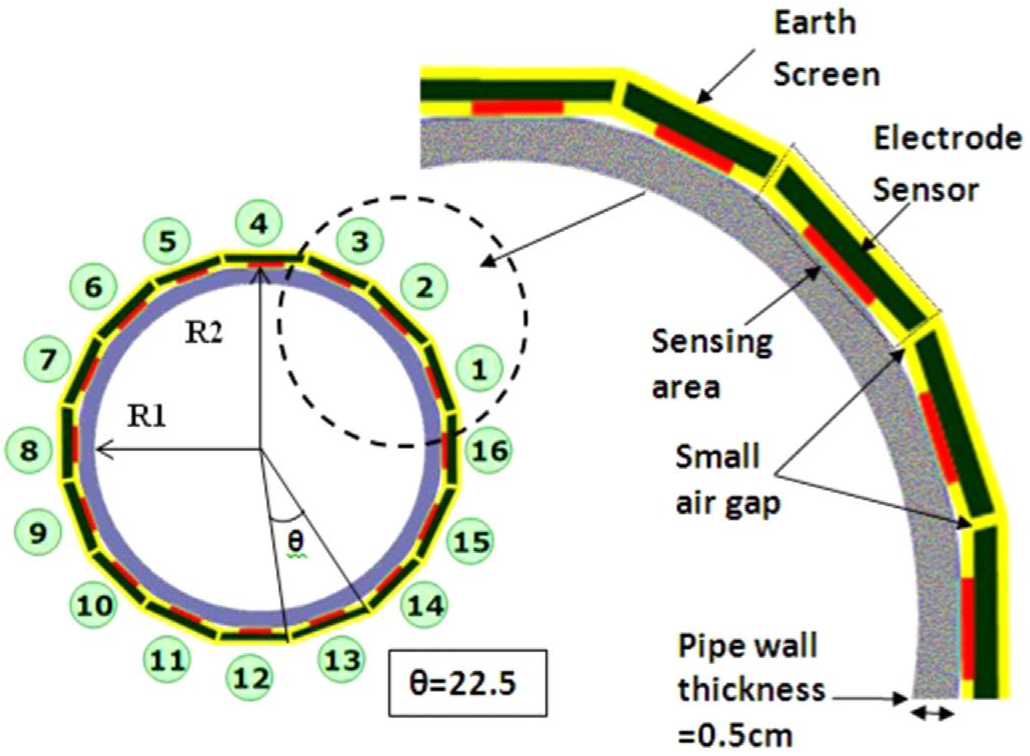

Figure 10. Cross-sectional view of the Electrical Capacitance Tomography sensor with 16-segmented electrodes (Mohamad *et al.*, 2016).

Based on an analysis of all above mentioned types of capacitance sensors and their applications, the following conclusions can be drawn:

- capacitance sensors are non-intrusive and provide accurate measurements with a high rate of data registration;

- capacitance sensors are used mainly to determine a fraction of the flow such as species of the mixture concentration or flow holdup;

- a fast developing field of the application of capacitance sensors is flow visualisation based on tomography techniques involving a large number of electrodes that cover the whole surface of the channel;

- flow velocity measurement is a comparatively new and poorly developed application of a capacitance sensor;

- capacitive sensors are sensitive to the flow patterns and regimes;

- results obtained are dependent on the shape and reciprocal position of electrodes;

- the sensitive field of the capacitance sensors is usually located in the vicinity of the electrodes, so it is recommend that preliminary investigations are carried out using computer simulations.

Capacitive sensors can lead to non-invasive, relatively low cost and reliable measurements of the flow rate, but consideration must be given to possible distortion of the electric signals due to stray capacitance which may be linked to assembly of the experimental setup.

2.8. Cross-slot rheometers and their variations

The T-junction geometry assumes the formation of a stagnation point flow which permits investigation of non-Newtonian effects of viscoelastic liquids through the control of the imposed flow rate. The vorticity-free state of the flow near the stagnation point can result in the large extensional deformation and orientation of the microstructural components of complex fluids. Thus this type of elongation flow allows producing a significant range of extensional rates along the back wall of the channel. A stagnation point flow can be induced by the method of opposed jets method, four roll mills and cross-slot geometries. The T-junction channel device is a particular case of a cross-slot configuration which has been previously widely used in rheological studies of elongation flow (Soulages *et al.*, 2009), (Pipe and McKinley, 2009), (Odell and Carrington, 2006). Cross-slot geometries could generate higher degrees of strain compared with contraction flows, and in some cases can produce an almost complete uncoil of flexible polymer molecules (Rocha *et al.*, 2009).

In contrast to the aforementioned four-rolled mill and opposed jets methods, cross-slot and T-shaped rheometers use field measurements of the channel flow to test liquids. For the purposes of on-line measurements this approach is potentially more reliable. The velocity fields, pressure and mass flow rates can be controlled. In addition, in the vicinity of the stagnation point, a non-homogeneous elongational field is formed by a pressure-driven flow, which enables one to perform information-rich tests. In cross-slot devices, the extensional viscosity manifests as an excess pressure drop upon comparison with inelastic liquids, which makes this geometry promising for the investigation of viscoelastic liquids (Haward S. J., 2012).

In cross-slot devices the stagnation point is located along the line of symmetry that passes through the point of intersection of the channel sidewall and the separating streamline. As a consequence of the no-slip boundary condition and continuity, the local velocity vector and all velocity gradients are zero at the stagnation point (Soulages *et al*., 2009). This type of flow provides both shear and elongation deformations if the Reynolds number of the flow is sufficiently high that viscous effects are confined to the wall region and that a core flow is created which is free of shear and in pure extension (James *et al*., 1990).

Williams and Williams, 1985, described a lubricated cross-slot instrument that could be used to form a planar orthogonal stagnation flow. Use of a lubricant is aimed to eliminate the shear component of a viscoelastic flow due to slip wall conditions. The authors tested Newtonian and Boger fluids, using pressure transducers to assess extensional flow characteristics. They pointed out that the lubricant (sugar and water mixture) affected experimental results under certain conditions. They found that the Trouton ratios for both liquids were in good agreement with theoretical consideration, but the lubricant affected the stability of the flow, so the researchers concluded that further modification of the instrument should be made (Williams and Williams, 1985).

Another type of a parabolic cross-slot stagnation point rheometer was used by (Macosko, Ocansey and Winter, 1982) for the investigation of steady state planar extensional flow. Melted polymer was fed into the channel with mineral oil as a wall lubricant. The sensitivity of the pressure transducers used was above the range of the pressure drop, so the normal stress difference was measured by birefringence. The data obtained demonstrated that wall lubrication decreased pressure on the walls of channel and additionally the flow became a two phase flow, which made theoretical analysis difficult. The authors made an important conclusion that stagnation point rheometers had an advantage compared with stretching type of rheometers because they are capable to cope with higher flow rates which permits the study of low viscosity fluids. Results of birefringence shown that the stress around a stagnation point is similar to one of steady planar extension flow.

A lubricated optical rheometer for analyzing the complex flow of polymer melts was developed by Soulages *et al.,* 2008. This lubricating system enabled effects of shear stress to be eliminated. Measurements of extensional flow were made using flow-induced birefringence techniques and PIV. The depth and width of the channel was 6 mm and 12 mm respectively with arms length of 100 mm. To provide fully developed flow conditions the

total length of the input arms was 360 mm. This instrument was successfully used to test polymer melts. 2D birefringence velocity fields were determined and were assumed to be sufficient to derive constitutive parameters of the tested fluids. A short-coming of this device was that it used a foreign component for the lubrication (in this case - silicone oil), which can influence the data obtained, and further investigation should be carried out to develop a rheometer for viscoelastic fluids.

In order to transform a cross-slot geometry, which forms non-homogenous flow, into one that generates a homogeneous flow, Haward *et al*., 2012 optimized the shape of the channel using numerical simulations. The new geometry induced a constant extension rate along the lines of symmetry of the channel (fig. 11). Measurements of extension parameters of test liquids were obtained from the bulk excessive pressure drop data and from birefringence calculations. This microchannel device demonstrated capacity to measure extensional viscosity of low viscosity polymer solutions in broad range of deformation rates and could be used as a base for extensional rheological measurements.

Another microfluidic cross- slot device was used to study wormlike micelles in elongational flow (Pathak and Hudson, 2006). The kinematics of the flow were investigated using PIV, whilst the behaviour of the molecules was examined by rheo-optic means, measuring birefringence aspects of the flow, which characterized the spacial orientation of the polymer molecules. Because of the specific of microrheometry, shear effects were found to be negligible in comparison with elastic ones. Experiments with controlled flow rates revealed dependence of the birefringence on the extensional flow that decreased exponentially with the distance from the stagnation point. The main conclusion of the research was that if the residence time of a molecule in an elongation flow field was more than its relaxation time, then this would lead to its becoming stretched and orienting along the flow stream lines.

Rheometers containing T-shaped channel geometries are widely used to solve various scientific problems concerning fluid dynamics for both Newtonian and non-Newtonian inelastic liquids. A group of researchers studied the pressure drop of single and two-phase water and N_2 flows in a T-type microchannel under controlled flow rate conditions. The static pressure was measured by two pressure transducers, whilst the pressure drop was directly defined using a water U-tube manometer. The correlation of the experimental viscosity data with those predicted from numerical homogeneous and non-homogeneous models was investigated. The authors admitted weak correlation between empirical and numerical results

for pressure drop experiments and drew the conclusion that further systematic investigations should be made (Yue *et al*., 2004).

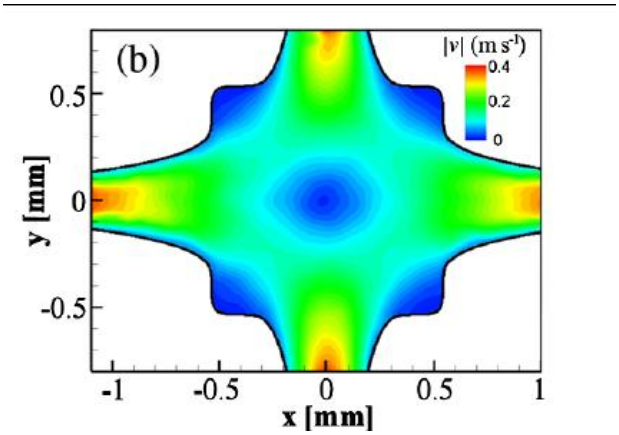

Figure 11. Velocity field of a cross-slot geometry, providing homogeneous stagnation flow (Haward S. J. Alves M. A., McKinley G. H., 2012).

Unsteady flows in a square tube T-junction were examined in another project. The authors focused their attention on the characteristics of recirculation regions in the channel, such as velocity, pressure, and wall shear stress distributions, along with limiting streamlines as a function of time (Anagnostopoulos and Mathioulakis, 2004).

Two modifications of T-shaped microchannel rheometers were investigated by Soulages *et al*., 2009 to examine the stability of viscoelastic stagnation flow. The difference in these geometries was the presence, or absence, of the cavity adjacent to the stagnation point. The geometry of the channel affected the spatial characteristics of a stagnation point: it was fixed at the middle of the backwall in the case of the channel without a cavity, and moved freely in the case of the channel with a cavity. The spatial characteristics of the flow were controlled using streak velocimetry. Different flow rates were implemented in order to investigate the influence of the velocity field on the character of the flow. Steady planar elongational flow of dilute solution of the shear thinning polyethylene oxide was studied in order to investigate the influence of elongational characteristics on symmetry of the flow. Based on the results of the study it was concluded that the elastic component defined the behaviour of the free stagnation points showing that there was a tendency for the symmetry to break down with increasing Weissenberg number.

Viscoelastic constitutive parameters of a polyisobutilene solution were studied by optical methods in a cross-slot microchannel. The velocity field was investigated using laser Doppler anemometry and the stress was measured using birefringence. Experimental parameters of the velocity were in good agreement with data, predicted by Carreau model, whilst viscoelastic stress around a stagnation point was significantly bigger than that simulated by the Phan-Thien-Tanner model (Schoonen *et al.*, 1998).

Also, a T-shaped microchannel was used by (Bandalusena, Zimmerman and Rees, 2010), (Bandulasena, Zimmerman and Rees, 2011) to determine the constitutive parameters of the pressure-driven flow of polymer solutions using an inverse method. Using PIV for measuring the velocity profile of a power-law non-Newtonian liquid (xanthan gum and polyethylene oxide solutions) it was proved that the constitutive parameters of liquids tested could be derived from the flow statistics from a single experiment. Numerical simulation of laminar steady state non-Newtonian flow demonstrated the existence of a unique inverse that maps the global characteristics of the flow onto constitutive parameters of tested liquids. One-to-one mapping of the components of the fluid dynamic equations permitted the constitutive parameters to be derived from the measured flow fields. The feasibility of this approach was proven hypothetically and further experimental studies would be of great of interest (fig. 12) (Bandulasena, Zimmerman and Rees, 2008).

2.9. Concluding remarks

Summarizing the information about stagnation point cross-slot or T-shaped rheometers, several important conclusions could be drawn. Firstly, stagnation-point devices themselves permit the construction of a non-homogeneous flow field that exhibits a with large extensional deformation in the vicinity of a stagnation point, resulting in velocity variation. Hypothetically, this makes it possible to derive parameters of interest from a single experiment around this information-rich region. Secondly, cross-slot and T-junction rheometers have fixed borders (walls of the channel), which enable sensors to be incorporated to measure the physical parameters of liquids. Zimmerman, Rees and Craven, (2006) suggested that the T-channel geometry is suitable for rheometrical investigations if the total pressure drop associated with the steady symmetric flow of a complex fluid could be measured. For unsteady conditions, additional embedded capacitor sensors could be used to provide velocity field data. Thirdly, all works described above studied extensional parameters using optical methods of investigation, which is not always applicable. Additionally, the

researchers used microchannels or lubricated channels, which are not often appropriate for use in industrial on-line conditions.

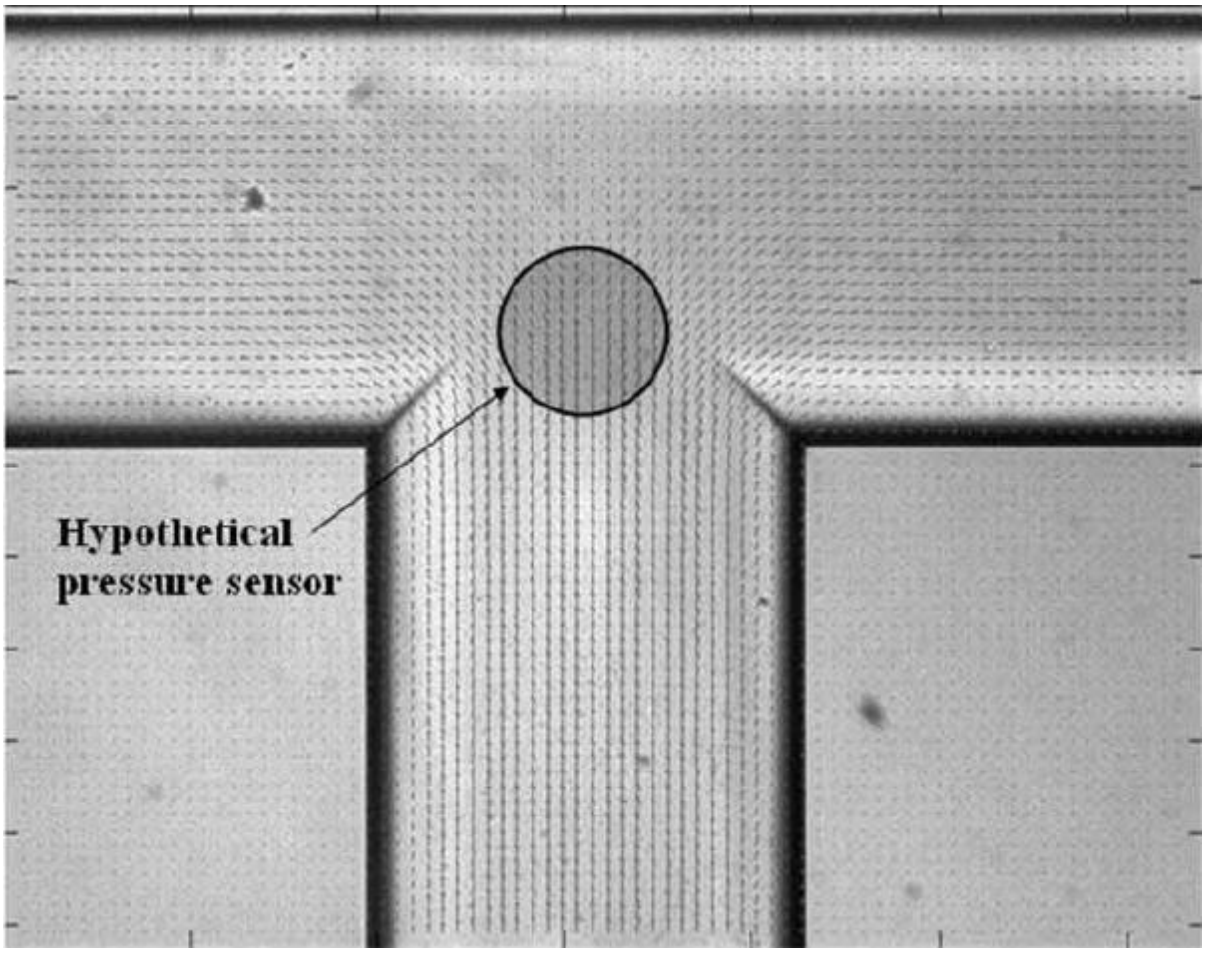

Figure 12.Velocity profile of the flow of pressure-driven xanthan gum in a microchannel T-junction measured using μ-PIV. A hypothetical pressure sensor with diameter 100μm is placed in the region displaying maximum sensitivity to the flow behaviour index of a power-law constitutive equation (Bandulasena, Zimmerman and Rees, 2008).

Thus, T-shaped rheometer could be considered as a robust, reliable and customized device for in-line or on-line control of extensional characteristics of fluid flows that arise in manufacturing processes. The rheometer could automatically operate at a controlled flow rate and is suitable for the testing of transparent or opaque liquids across a wide range of extensional viscosities.

Chapter 3: Methodology of inverse method approach to extensional viscosity definition

Inverse methods are widely used to effectively solve different physics problems (Fu, Caers and Tchelepi, 2011), (Evensen, 1994). The expression “inverse problem” refers to system identification, that is the updating of model parameters based on measurement data (Mainçon and Barnardo-Viljoen, 2013). The inverse approach has proved its effectiveness in problems where there is some kind of disturbance occurring in the tests (Szeliga, Gawad and Pietrzyk, 2006) or large difference between the experimental data and model prediction due to the severe testing conditions corresponding to appropriate industrial applications (Gavrus, Massoni and Chenot, 1996). Also, this methodology could work when it is not possible to measure parameters of interest directly, but it is possible to collect alternative data and map them onto the required parameters using models of the physical processes involved. If a functional dependence exists between the measurable parameters and the parameters of interest, then the latter could be deducted from empirical tests.

The inverse method assumes two consecutive steps:

- forward problem solving or direct analysis, this involves finding the numerical solution of the direct model, taking into account a priori known material properties;

- inverse problem solving or inverse analysis, where the measured parameters are mapped to the constitutive characteristics of a liquid.

The development of computational fluid dynamics (CFD) has made it possible to predict the global statistics of a flow based on continuum mechanics models. Thus the first step of the inverse method, i.e. the forward problem, involves the system description and solution of the governing set of partial differential equations with appropriate boundary conditions. For CFD these are the Navier-Stokes equations and constitutive equations. Boundary conditions depend on the flow geometry and conditions of the experiments.

Verification of the model is an essential stage of the forward problem. The effects predicted by the model should be compared with observational data. In the case of divergence between

experimental and predicted results, the model should be revised to reduce the discrepancy to a statistically acceptable level.

The second step - the inverse problem - begins with the investigation of the existence of a one-to-one mapping of the statistical measurable values to the constitutive parameters of the test fluids. If this mapping is unique and continuous, then the T-shaped rheometer can be used for the characterisation of liquids by a single experiment.

Gavrus, Massoni and Chenot, (1996) presented an inverse method for analyzing a hot metal forming process. They suggested that it was possible to find unknown rheological parameters through a set of values that provided the best fit between experimental data and numerical simulation. For their inverse analysis the authors took torques corresponding to different times, rotation speeds and initial temperatures and derived from them the constitutive parameters for elastic deformation.

Szeliga, Gawad and Pietrzyk, (2006) also worked on a metal forming problem. They described an inverse algorithm that consisted of three main stages: (i) the model of the direct problem, (ii) experiment, (iii) optimization techniques. The authors combined an inverse algorithm with a sensitivity analysis, which enabled them to interpret different parametric tests of cold and hot metal plastic deformation.

Inverse methods are widely used for studies of geological and hydrogeological processes. So Fu, Caers and Tchelepi, (2011) developed an inverse algorithm for the modelling of reservoirs. The large-scale problem was solved using a finite element model incorporating a multi-scale method. A new method, permitting estimations of soil water flux density and soil thermal properties from a heat pulse probe, was suggested by Yang, Sakai and Jones, (2013). The method consisted of an analytical solution coupled with a fitting technique. The direct model took account of inhomogeneity of the strain rate, strain and temperature distributions.
Finite element simulations and optimisation techniques were also used by Zhou, Qi and Chen, (2006) to determine the constitutive parameters of metal composite temperature deformation. Direct methods of measurement for solving this problem could not be made because it was not possible to measure some of the parameters (load or displacement), or the system required special experimental configurations (e.g. to reduce friction, ensure constant train rate and temperature, etc.).

Zimmerman, Rees and Craven, (2006) and Bandalusena, Zimmerman and Rees, (2010) showed that the inverse method based on mapping analysis has the advantage of providing high accuracy for parameter estimation, even for highly sensitive systems.

Since the development of CFD now makes it possible to carry out calculations for very complicated models of fluid dynamics, involving the solution of high order spatial-temporal systems of partial differential equations, it should be possible to work out a procedure for finding constitutive parameters from a knowledge of flow field statistics gained experimentally.

The procedures for finding constitutive parameters and curve fitting for a particular fluid using conventional rheological tests could involve around 20 to 50 experiments performed over a wide range of shear rates, are laborious and require human manipulation followed by curve fitting for extensional viscosity (Guillot *et al.*, 2006). Therefore development of a new approach for the rheometry of complex fluids using inverse methodology might lead to a cheaper and faster way of process control. Zimmerman, Rees and Craven, (2006) presented and theoretically validated an inverse method based on two-dimensional finite element simulations of electrokinetic flow in a microchannel T-junction for a fluid with a Carreau-type nonlinear viscosity. They showed that there exists a single- valued map between the viscous characteristics of the fluid and the end-wall pressure profile for a range of non-dimensionalised Carreau parameters. This theoretical conclusion was further established by Bandalusena, Zimmerman and Rees, (2010) for a power-law fluid in a T-junction microrheometer. A CFD model for simulating velocity fields was verified by comparison with experimentally measured velocity fields obtained by μPIV. Furthermore, the computational model was successfully used to develop an inverse method for characterizing the rheological parameters. In these articles it was postulated that data from pressure sensors or flow rate measurements could be uniquely inverted and thus be used to identify the constitutive parameters of a fluid from actual measurements of the velocity profile of the pressure driven flow.

The goal of this particular research is to check the hypothesis that the inverse method may be used for characterising extensional viscosity processes for elastic, but constant shear viscosity fluids (Boger fluids). The first step is to model viscoelastic flow for a particular geometry of a bespoke T-shaped rheometer (forward problem). The second step, its experimental

verification, and the final stage, is to solve the inverse problem to calculate constitutive parameters using the model from the first stage.

Zimmerman and Rees, (2009) described the inverse problem as a three-stage modelling process:

1) solve the forward problem to predict the global statistics of the field variables from the selected operating conditions and physical parameters;

2) investigate uniqueness of correspondence of global statistics to constitutive parameters of a liquid;

3) solve the inverse problem to estimate the physical parameters from the statistics of the field variables which give a measure of the performance of the system under known operational conditions.

For information-rich experiments, for example, those in which a range of elongation rates co-exist along the back wall of the T-shaped rheometer in a single experiment, it is impossible to obtain a direct measurement of the elastic parameters of a fluid by non-optic methods from a single experiment:

$$\dot{\varepsilon}=f(\sigma_E), \tag{3.1}$$

where $\dot{\varepsilon}$ - extension rate, σ_E - extension (normal) stress.

As far as it is possible to detect the whole range of elongations along the back wall of the T-shaped rheometer, using either optical or electrical means of measurements, in this work we investigate whether it is possible to extend the above studies by considering whether inverse methods can be used to extract the elongational viscous parameters.

The quantities that are directly measurable form a dataset, *d*. We refer to the set of values that is known or to be reconstructed as the image, *f*. The solving function $f \rightarrow d$ is called the 'forward problem'. Conventional modelling could be used to solve the forward problem, which entails the solution of the governing equations of motion. Inversion algorithms can be used to identify the cause of the measured effect. The mapping $d \rightarrow f$ comprises the corresponding inverse mapping. To realize this scenario practically, there must exist an experimental opportunity to obtain the dynamical measures that can be mapped to constitutive parameters. Thus the number of dynamical measures must be consistent with the

number of characteristic parameters in the model. Hadamard, (1923) posed conditions, which must be satisfied:

- for any data, *d*, in the dataset, a solution exists;

- the solution is unique in the image space;

- the mapping $d \rightarrow f$, i.e. the inverse mapping, is continuous.

Thus, if for the case of extensional flow one considers for the forward problem that the extensional viscosity is a function of the extension rate,

$$\eta_e = f(\dot{\varepsilon}), \qquad (3.2)$$

where the functional dependence can be described using constitutive parameters, then for each set of unknown parameters there should exist an equal number of measured outputs.

The components of the stress field of a viscoelastic fluid can be interpreted in terms of shear viscosity and extensional viscosity.

Thus, to solve the forward problem, it is necessary to define the input parameters of a constitutive model. Shear parameters can be measured with a shear rheometer and extensional parameters can be measured using an extensional rheometer or from calculations based on measurable elastic properties of a fluid such as the first normal stress difference or relaxation time. Simulations to find measurable parameters can be implemented. In the case of fluid dynamics, the forward problem usually consists of solvinga system of partial differential equations to find pressure and flow velocity values (p_i, v_i) using physical and constitutive parameters of the fluid and appropriate boundary conditions.

Thus forward function can be expressed as

$$(p_i, v_i). = f(\text{viscoelastic constitutive parameters}). \qquad (3.3)$$

The next stage concerns the verification of the uniqueness of the mapping function from the measured values to the constitutive parameters:

$$(\text{viscoelastic constitutive parameters}) = f^{-1}(p_i, v_i) \qquad (3.4)$$

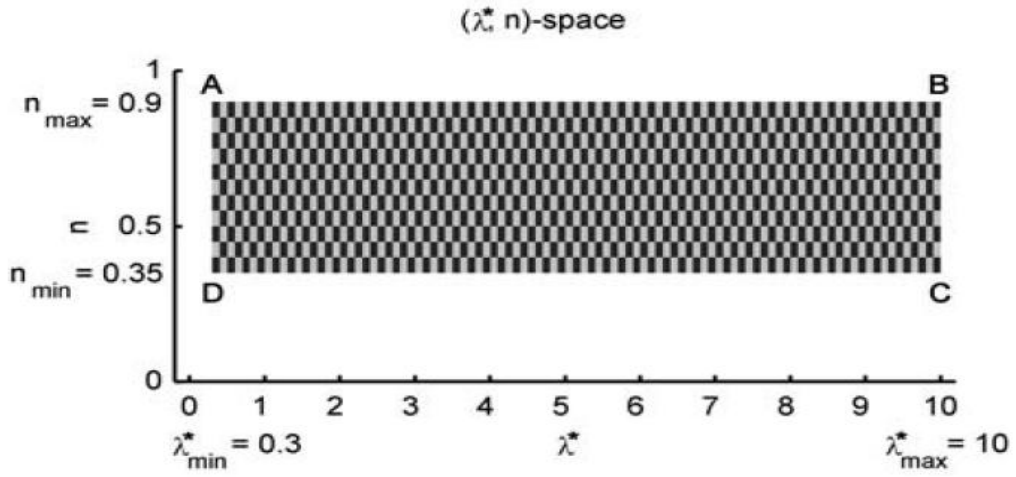

(a)

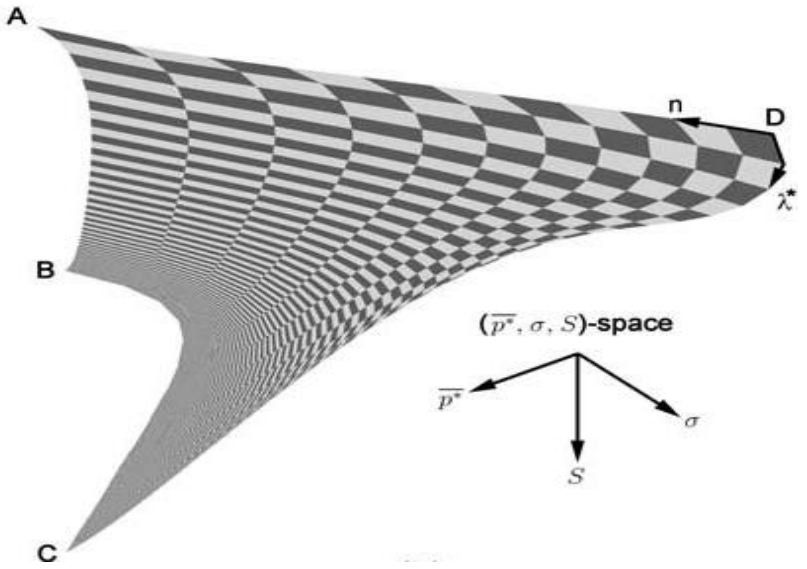

(b)

Figure 13. (a) Forward problem mapping for Carreau-type liquid for n and λ^* constitutive parameters; (b) inverse problem image mapping proving uniqueness and continuousness for global statistics $\bar{p}^*$ (the end wall mean pressure), σ (standard deviation) and S (skewness) of a flow in a T-shaped microchannel (Zimmerman, Rees and Craven, 2006).

This can be achieved by graphic analysis (Zimmerman et al., 2006), which is shown in figure 13. Reciprocal sweeping of input parameters will give a multitude of measured values and will permit a sensitivity analysis to be undertaken. In the picture 13 (a) the space of input

parameters n (flow constituency index) and λ^* (dimensionless relaxation time) is represented. In the part 12 (b) is mapped on to 3D coordinate system of $\overline{p^*}$ (the back wall mean pressure), σ (standard deviation) and S (skewness). These parameters were chosen as most sensitive to the variation of constitutive parameters, thus they were used as global statistics for an inverse problem solution. The figure 12 demonstrates that points ($n;\ \lambda^*$) are mapped to the space ($\overline{p^*};\ \sigma;\ S$) uniquely and monotonously, so the inverse solution could be used for developing a look-up table for deduction of constitutive parameters of the fluid from the global statistics of the flow.

Solution of the inverse problem consists of finding a set of constitutive parameters that correspond to the set of measurable values (pressure drops and velocity profiles). The inverse function theorem states that the necessary criterion for functions to be inverted is

$$det\ J \neq 0, \tag{3.5}$$

where J - Jacobian of the map (p_i, v_i) = f(viscoelastic constitutive parameters).

For this research the Jacobian takes the form:

$$det\ J = \begin{bmatrix} \frac{\partial v}{\partial \lambda} \\ \frac{\partial p}{\partial \lambda} \end{bmatrix} \neq 0, \tag{3.6}$$

where v - velocity of the flow, λ - relaxation time, p- pressure of the flow.

If uniqueness is proved, then the constitutive parameters can be deduced from the statistical measures. The final stage of the inverse problem is the comparison of the input parameters of the model with those derived from the inverse methodology. If statistically accepted agreement is obtained, then the validity of the hypothesis on the applicability of the T-shaped rheometer for use for the purpose of rheometry of viscoelastic fluid will have been demonstrated.

Methodologically, the project can be divided into separate interconnected stages.

For the first phase computer simulation for Oldroyd-B model, describing Boger fluids dynamics, fluids should be undertaken as the forward problem solution (the choice of constitutive model will be examined in details in chapter 4). Model validation will be carried out based on experimental data obtained from a cone-and-plate rotational rheometer. After that viscous response factors will be tested for their sensitivity to the viscoelastic constitutive parameters. The measurable parameters for an inverse function will be defined in accordance with the nature of the extensional viscosity components. If the invertibility of the system could be theoretically proven, then the inverse function will be derived and the parametric mapping can be obtained.

For the second phase viscoelasic behaviour of Boger and Newtonian fluids will be tested in the T-ometer in order to measure flow field parameters at steady state and for transient flows at different flow rates. Constitutive extensional parameters will be estimated using previously developed parametric mappings. If these parameters are in good agreement with those obtained with a conventional rheometer, then the hypothesis of feasibility of the T-shaped rheometer for extensional viscosity measurements based on inverse methodology could be considered to be proved.

Chapter 4: CFD as a forward problem

In this chapter the CFD models for the viscoelastic response to the stress applied in a T-shaped channel are presented. Prediction of the global statistics for Boger fluids is a forward problem which involves solution using an inverse method approach. Since fluid dynamic equations define the pressure and velocity fields of the flow, two kinds of models are used to simulate the steady and transient flows of the complex fluid: (i) the Navier- Stokes equation for the steady state flow of the fluid with a constant shear viscosity and a relaxation time to predict the pressure field and (ii) the laminar pulsing time dependent flow coded with non-steady flow conditions to define the velocity field. The simulated results are compared with experimental results in order to validate the models and to further assess their applicability for the inverse problem solution.

4.1. Preliminary investigation of the models for fluids with a constant shear viscosity and high elasticity

It is possible to describe the viscoelastic behaviour of complex fluids in multiple ways. Fluids with different molecular or compositional structures exhibit different transformations in similar physical and kinematic conditions that manifest in a stress-strain dependence. The property of this dependence is described by an intrinsic material property - viscosity. For viscoelastic fluids the viscosity function is the result of the combination of viscous and elastic components. This ambiguity results in certain difficulties in the theoretical description of the complex fluid dynamics. Fluids with non-linear shear viscosity are some of the most complicated, and many research efforts are being made towards the creation of models capable of reproducing the experimental results. In the case of Boger fluids, i.e. fluids with constant shear viscosity and high elasticity, the theoretical models are well- developed and have been tested across a number of projects and thus could be used for demonstrating the feasibility of an inverse method.

Generally, hydrodynamics of nearly incompressible liquids are described by the following governing equations:

conservation of mass equation $\nabla \cdot u = 0$ (4.1)

where u - flow velocity vector;

conservation of momentum equation for an incompressible fluid

$$\rho \frac{du}{dt} = \nabla \cdot \sigma \,, \quad (4.2)$$

where ρ - density, t - time, σ - total stress;

$$\sigma = -p\boldsymbol{I} + 2\eta_s \boldsymbol{D} + \boldsymbol{T}, \quad (4.3)$$

where p - pressure, η_s - solvent viscosity, $\boldsymbol{D}$ - rate of strain tensor, $\boldsymbol{I}$ - identical matrix, $\boldsymbol{T}$ - polymeric contribution for the deviatoric stress tensor, where

$$\boldsymbol{D} = \frac{1}{2}[\nabla u + (\nabla u)^T] \,. \quad (4.4)$$

The deviatoric stress tensor arises in the by constitutive relationship due to an elastic component. The first model for viscoelastic liquids with constant viscosity was proposed in seventieth and was called the Maxwell model. It included a parameter called the relaxation time which was a characteristic of the elastic component of the flow. The next model developed, the Oldroyd-B model, involved separating the solvent and polymer contributions to the flow dynamics, with an assumption that the polymer molecules had a dumbbell shape in a viscous, but Newtonian fluid (Prilutski *et al.*, 1983). These two models accurately predicted the results for the steady state flow with an inelastic solvent, but the study of PB/PIB Boger fluid (chapter 2.6) revealed, that polybutilene, when used as a solvent, had its own elasticity which manifested in a non-zero relaxation time. Thus, a more sophisticated model was required to describe liquids with a shear-thinning linear or exponential viscosity. The Phan-Thien-Tanner model took into consideration the shear component of general viscosity. Separation of the effects, attributed to the solvent and polymer viscosities of the Boger fluids to simulate its viscoelastic response, is more appropriate for the polyacrylamide in glycerol-water solution, because it deals with both the polymer and the Newtonian solvent. The Phan-Thien-Tanner model is more complex in nature and seems to be not relevant for the purposes of the research, because the shear viscosity of the liquid of interest is constant.

The entry flow simulation was performed by Keiller, (1993), using the Oldroyd-B model. The results have demonstrated the weakness of the model in predicting the vortices for the planar

flow when they occured in an axisymmetric geometry. The author explained this phenomenon by considering the dominating effect of the shear on the extensional stresses and suggested that non-linear models should be used for the prediction of vortices. In addition, similar results were obtained by Phillips and Williams, (2002), where the vortices in the axisymmetric flow were more pronounced when compared with the planar flow. This resulted in a stronger expression of fluid elongation along the axis in the axisymmetric flow. Another shortcoming of the model was highlighted by Davies and Devlin, (1993), who demonstrated the singularities for the corner flow of a Boger fluid. The solution to this problem was proposed by Aboubacar, Matallah and Webster, (2002), where they were able to converge the solution by rounding up the corners of the geometry. At the same time, comparison of the experimental data with computer simulations demonstrated a good agreement of the velocity field and the first normal stress difference with the predicted results (Mompean and Deville, 1997). A few studies have reported a numerical divergence for Oldroyd-B simulations at high Deborah numbers and have suggested multiple methods for overcoming this problem (Alves, Oliveira and Pinho, 2004), (Casanellas and Ortín, 2011), (Thais, Helin and Mompean, 2006), making the model suitable for highly elastic Boger fluids (Tomé *et al.*, 2008). Overall, it has been demonstrated that the Oldroyd-B model has shown reliability and high precision when dealing with constant viscosity - high elasticity fluids, but significant consideration should be made when creating the flow parameters and flow geometry.

Thus, the constitutive equation for the forward problem solution is the Oldroyd-B model, which represents a split tensor for a Newtonian solvent and a polymer. The main assertion is that the general viscosity of the Boger fluid is the sum of the viscosities of the components of the solution:

$$\eta=\eta_s+\eta_p\,, \tag{4.5}$$

where η - general viscosity, η_p - polymer viscosity.

Thus the constitutive Oldroyd-B model for $\boldsymbol{T}$ can be written as:

$$\boldsymbol{T}+\lambda_1\overset{\nabla}{\boldsymbol{T}}=2\eta_p\boldsymbol{D}, \tag{4.6}$$

where λ_1 - relaxation time,$\overset{\nabla}{\boldsymbol{T}}$ - upper-convected derivative.

The upper-convected derivative is defined as:

$$\overset{\nabla}{\boldsymbol{T}}=\frac{\partial \boldsymbol{T}}{\partial t}+\boldsymbol{u}\cdot\boldsymbol{T}-\boldsymbol{T}\cdot\nabla\boldsymbol{u}-\nabla\boldsymbol{u}^{T}\cdot\boldsymbol{T}. \quad (4.7)$$

Thus, the forward problem can be presented as:

$$(\boldsymbol{p},\boldsymbol{v})=f(\lambda_1). \quad (4.8)$$

In order to make the inverse problem feasible, the number of terms contained in the left part of eq.(4.8) should correspond to the number of terms present on the right. If there is one constitutive parameter in the Oldroyd-B model, it is necessary to find at least one parameter that characterises the pressure or the velocity field of the flow that is sensitive to the change in the relaxation time. This can be achieved by finding additional terms using different physical or geometrical parameters of the flow, or their ratios. During the selection of the particular parameters for the inverse function, the dimensions of the sought constitutive parameters must be taken into account.

All of the CFD simulations were performed using the commercially available finite element software package COMSOL 5.2a version on a Windows 10 platform with an Intel I7, 2.4 GHz processor and 8 GB RAM. The computation time varied from 20 min to 2 hours depending on the particular flow problem.

4.2 Computer simulation of the Oldroyd-B model

Computer simulations of the pressure driven Poiseuille flow in a T-junction channel was carried out using COMSOL, version 5.2a. The discretisation of the PDE governing equations was made by using a finite element analysis. The rheological parameters of the Newtonian and Boger test fluids were measured using a conventional cone-and-plate rheometer. These data were used to validate the model. Different concentrations of high molecular number polyacrylamide solutions and glycerol-water solutions were used at different flow rates in order to determine the sensitivity of the flow field statistics to the constitutive parameters of the liquids. A series of meshes with increasing level of refinement were used to determine the sensitivity of the simulation results to the size of the meshing elements.

4.2.1. Geometry and mesh

The construction of the T-shaped rheometer cell will be described in details in section 5.1. The channel itself was mechanically cut in a plate of PEEK, so the resulting cross-section had

a rectangular shape. The stagnation point flow has a symmetric pattern, so in order to save computational time the computational domain was chosen to be a half of the real T-shaped channel, with the line of symmetry lying along the inlet limb (Fig. 14 (a)). The pressure driven Poiseuille flow was modelled as a 2D flow, which in the case of a T-shaped geometry could be defined as a planar extensional flow, resulting in no difference in the neighbouring layers, whilst making boundary effects negligible. Since many researchers have highlighted the numerical singularity occurring in the vicinity of the sharp inner corner of the cross-slot channel, where shear and extension rates are significant, the geometry of this corner was rounded in the model, with radius of 10^{-4} m (2.5% of the channel width) (Fig. 14 (b)).

Preliminary meshing was performed using a physics-controlled method with triangular elements with sides ranging in size from 5.32×10^{-4} m to 1.77×10^{-3} m. The self-consistency of the solution was proven by refining the mesh.

The pressure field was calculated by integration of the pressure value across the footprints of the pressure sensors.

4.2.2. Boundary conditions

A series of tests was carried out to measure the global statistics under different flow conditions, where the inlet flow rate was set as an inlet boundary condition. At two outlets the condition $\boldsymbol{p}$ =0 was established (where $\boldsymbol{p}$ - pressure).

A no slip boundary condition was applied to all walls of the channel:

$$\boldsymbol{u}=0. \tag{4.9}$$

At a symmetry boundary zero normal velocity is prescribed:

$$\boldsymbol{u}\cdot\boldsymbol{n}=0, \tag{4.10}$$

where $\boldsymbol{n}$ is a normal vector,

and the tangential component of the total stress is set to zero:

$$(\boldsymbol{\sigma}\cdot\boldsymbol{n})\cdot\boldsymbol{t}=0, \tag{4.11}$$

where $\boldsymbol{t}$ is a tangential to the boundary vector.

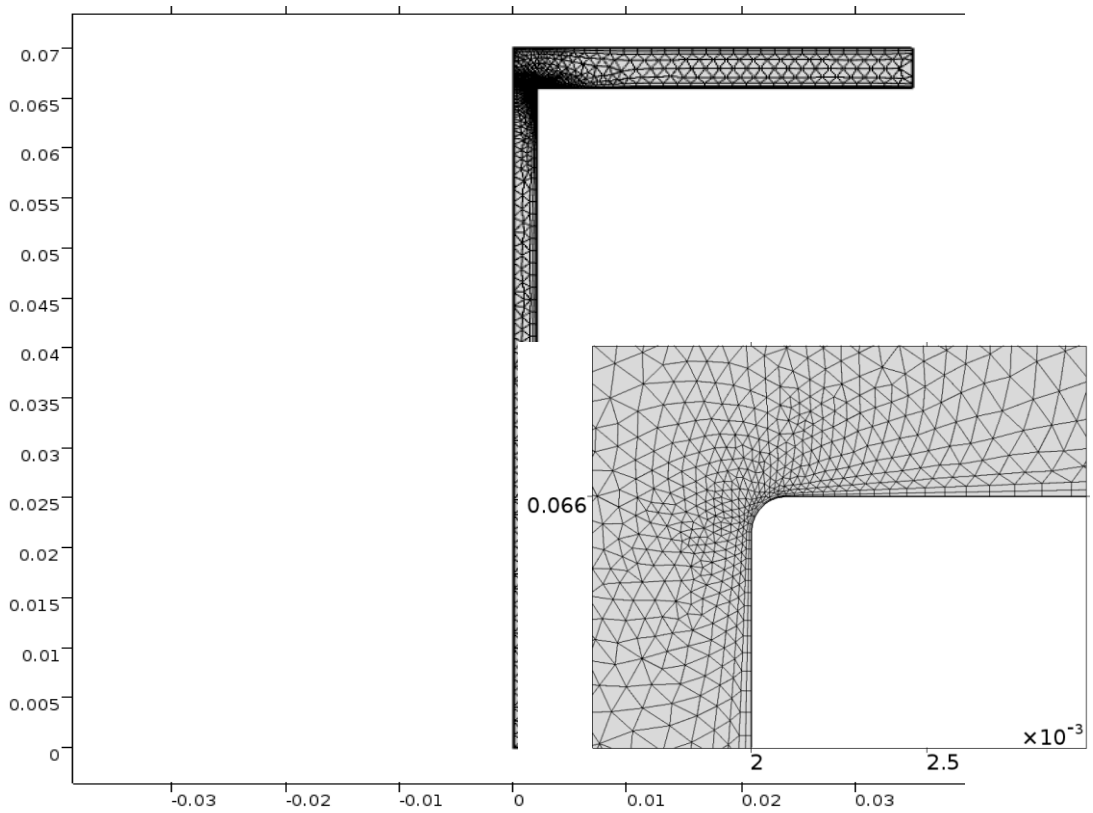

a b

Figure 14.Geometry of the half - channel section, dimension in m (a); rounded corner of the channel (b).

The inlet boundary condition was defined based on the experimental conditions offered by the built-in options in the software:

- velocity;

-pressure;

-laminar inflow;

-mass flow

laminar inflow was selected.

In turn, from the offered option of parameters: "Average velocity, Flow rate and Entrance Pressure", the flow rate was selected as the pressure driven flow was induced with a controlled flow rate using a syringe pump.

The initial conditions of zero pressure and velocity components were set for the entire domain of the flow.

4.2.3. Computer simulation with use of COMSOL

The Navier-Stokes governing equations with Oldroyd-B constitutive equation for the incompressible steady-state flow of the T-ometer geometry were solved using COMSOL, version 5.2a, to obtain the pressure and velocity fields for the viscoelastic Boger fluid. The built-in "Laminar flow" module for the Newtonian fluid (constant dynamic viscosity) was selected to simulate the viscous component of the flow, while the "General form of partial differential equations (PDE)" was used to describe the elastic (non-linear) component of the flow, as it was successfully implemented earlier for the same task by a few authors (Craven, Rees and Zimmerman, 2010), (Baer and Finlayson, 1992). In these articles, the authors have shown that use of the built-in Newtonian Fluid Laminar Flow mode for the momentum equation and the continuity equation solution, combined with the PDE module for the constitutive equation, permits the viscoelastic steady-state flow to be simulated. The modules were coupled through the "Body force" term in the momentum equation.

Parameters of the model are presented in Table 2:

Table 2. Parameters and their notification of the steady state model

Name	Expression	Description
Rho	1.259 kg/m^3	Density
La	0.97 s	Relaxation time
mu_s	0.22 Pa·s	Solvent viscosity
mu_p	0.03 Pa·s	Polymer viscosity
Min	2.1e-4 kg/s	Mass flow rate

Parameters, such as density, relaxation time, and solvent and polymer viscosities were taken from the physical characteristics of the fluids of interest and, additionally, were obtained from the cone-and-plate experiments. For each liquid these parameters were changed to match the fluid dynamics properties of particular liquids. As for the "mass flow rate", its interpretation was based on the test conditions, leading to the range of mass flow rates being used as an input for a parametric sweep study for the sensitivity investigation,

Q_1 = 2.1.kg/s, Q_2 = 4.2 kg/s, Q_3 = 6.3 kg/s.

In the "Laminar flow" module the "Incompressible" flow option was selected, and the extensional conditions for all the simulations were defined as the atmospheric pressure (1 atm) and room temperature (293.15 K). "User defined" values for density and viscosity were selected in order that these parameters were to be taken from the "Parameters" unit. The general viscosity of the liquid to be simulated was calculated by adding the solvent viscosity (mu_s) to the polymer viscosity (mu_p).

The elastic components of the flow are presented in the table 3. They were implemented in the "Variables" unit, as well as some post-processing parameters, such as the Reynolds number and the Weissenberg number.

Table 3. Variables of the Oldroyd-B model

Name	Equation	Parameter
e11	$\frac{\partial u}{\partial x}$	Strain rate 11
e12	$0.5\cdot(\frac{\partial u}{\partial y}+\frac{\partial v}{\partial x})$	Strain rate 12
e22	$\frac{\partial v}{\partial y}$	Strain rate 22
s11	*-p+2·mu_s·e11+T11*	Total stress 11
s12	*2·mu_s·e12+T12*	Total stress 12
s22	*-p+2·mu_s·e22+T22*	Total stress 22
f11	$2\cdot mu\_p\cdot e11-T11-La(u\cdot\frac{\partial T11}{\partial x}+v\cdot\frac{\partial T11}{\partial y}-2\frac{\partial u}{\partial x}T11-2\frac{\partial u}{\partial y}T12)$	Source term 11
f12	$2\cdot mu\_p\cdot e12-T12-La(u\cdot\frac{\partial T12}{\partial x}+v\cdot\frac{\partial T12}{\partial y}-\frac{\partial v}{\partial x}\cdot T11-\frac{\partial u}{\partial y}\cdot T22)$	Source term 12
f22	$2\cdot mu\_p\cdot e22-T22-La(u\frac{\partial T22}{\partial x}-v\cdot\frac{\partial T22}{\partial y}-2\cdot\frac{\partial v}{\partial y}T12-2\cdot\frac{\partial v}{\partial y}T22)$	Source term 22
Wi	$La\cdot\frac{\partial v}{\partial x}$	Weissenberg number
Re	*Rho·u·L/(mu_s+mu_p)*	Reynolds number

where *T11, T12* and *T22* are $\frac{\partial u}{\partial x}$, $\frac{\partial u}{\partial y}$ = $\frac{\partial v}{\partial x}$ and $\frac{\partial v}{\partial y}$ respectively.

The "General form PDE" module allows one to define the coefficients of the general equation (4.12), which correspond with physics of the flow:

$$e_a\frac{\partial^2 \boldsymbol{u}}{\partial t^2}+d_a\frac{\partial u}{\partial t}+\nabla \cdot \Gamma=f \quad (4.12)$$

Under conditions of the steady state and incompressible flow, e_a (mass coefficient), d_a (damping of mass coefficient) and Γ (conservative flux) are equal to zero, while the components of f (source term) are *f11*, *f22* and *f12* from the table 3. Zero flux was defined for every boundary of the domain, and all the initial values were set to zero.

The geometry of the channel was meshed using the physics-controlled mesh, meaning that mesh elements were finer around the corner with a maximum element growth rate of 1.2. A sensitivity test was carried out in order to investigate how the mesh size affected the accuracy of the results. Thus with 1801 non-uniformed triangular elements in the mesh, the minimum element size of 2.35×10^{-3} m and maximum size of 1.05×10^{-5} m were taken as the bench mark solutions (fig. 14 (a)).

A stationary linear solver, implemented with the default Newton's method found the number of iterations necessary for convergence to a solution to be a 100 with the minimum damping factor of 1e-6. The solver algorithm in COMSOL used was MUMPS (multifrontal massively parallel sparse direct solver), which reduced the amount memory required by the unpivoted system. The dependent variables for the system of PDE Navier-Stokes equations were the pressure field, the velocity field and components of velocity tensor *T11*, *T12* and *T22*.

A mesh-size sensitivity investigation was carried out prior to the model validation study in order to find an optimal meshing procedure that would not corrupt the results of the simulation. The results of the computer simulation of the velocity magnitude along the symmetry line are presented in fig. 15. For this simulation the input mass flow rate M_{in}= 1×10^{-5} kg/s was used. It can be seen that the stability of the solution is increasing with the diminishing number of meshing elements. Additionally, there is a limit after which any further mesh refinement does not lead to a solution correction (results at 13771 and 18828 number of elements are virtually identical). The number 13771 corresponds to the "Extra Fine" meshing options in this simulation system, where uneven triangular and quadrialateral elements with average growth rate of 1.2, with element size varying from 5.25×10^{-6} m to 4.55×10^{-4} m. Thus, in order to save computer simulation time, but not to compromise the accuracy of the results, the "Extra fine" mesh size was assumed to be sufficient for the further investigation of a forward problem of steady state and time dependent fluid flows.

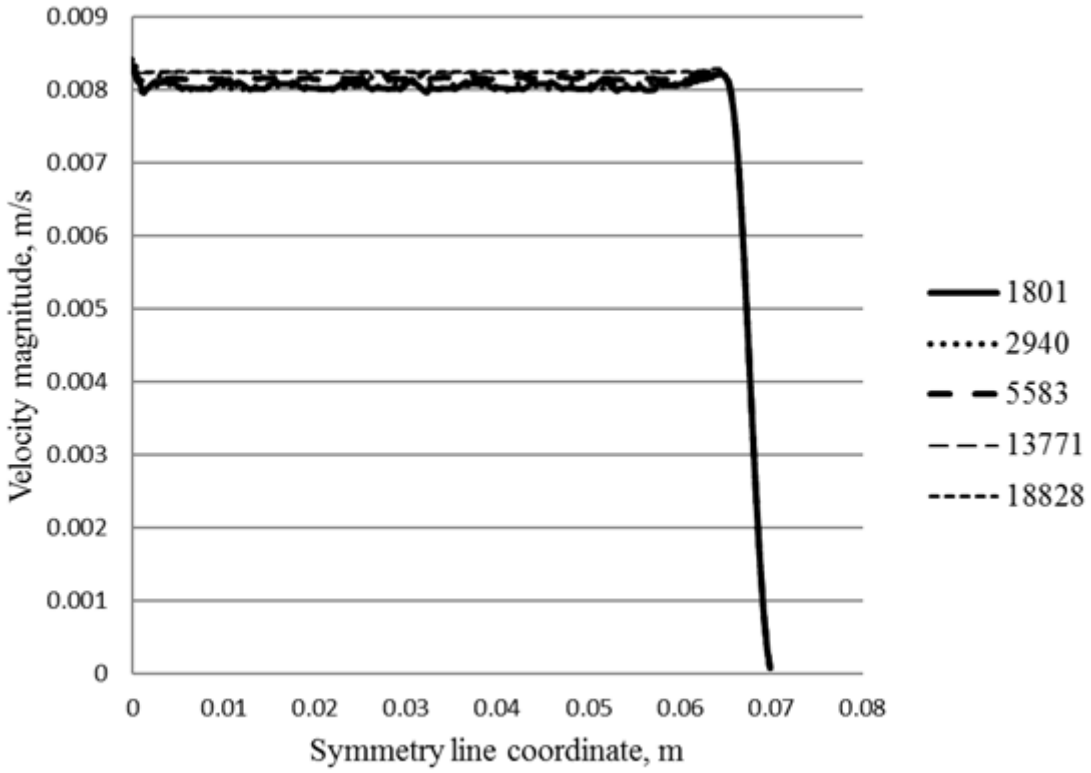

Figure 15. Dependence of accuracy of computer simulation of velocity magnitude on size of meshing elements, represented by their number.

To simulate the velocity field measurements, the pulsing inflow conditions were modelled. For this purpose the inlet mass flow rate was described by a Gaussian pulse function, which is included in COMSOL:

$$y = \frac{1}{\sigma\sqrt{2\pi}} e^{\frac{-(x-x_0)^2}{2\sigma^2}}, \qquad (4.13)$$

where x - input parameter, time, t; σ - standard deviation, x_0 - the location (mean).

Whilst the pressure fields were measured under a steady state conditions, the stationary solver was applied. Since the pulsing flow had a transient nature, the time dependent solver was implemented. The parameters of the Gaussian function were determined as follows (fig. 16):

pulse location 1.2 s;

standard deviation 0.4.

The mass flow rate was modified to form the pulsing inflow along the time range from 0 to 3 s, following the experimental conditions.

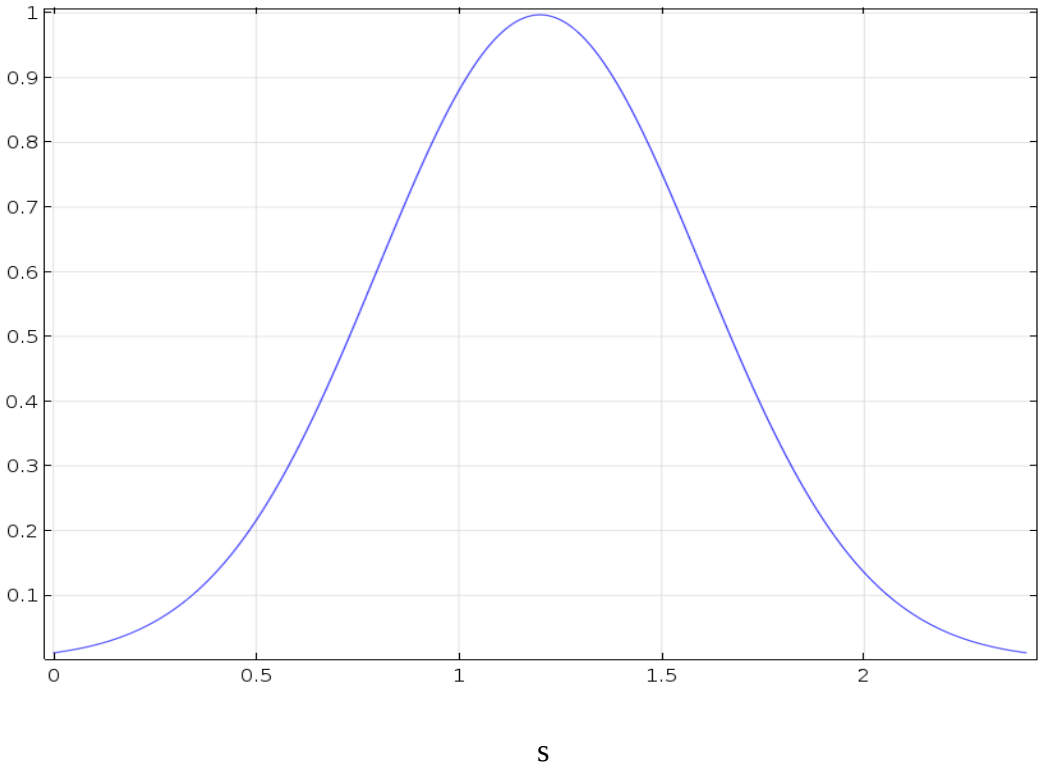

Figure 16. Gaussian function for pulse flow rate modification.

The transient fluid flow of the PAA300 liquid was modelled with the input parameters listed in the Table 2, within the time range of 0 to 3 s and with time steps of 0.01 s. For the two other tests the liquids' input parameters were adjusted in accordance with their to their rheological and physical properties.

The velocity profile solutions were found in points corresponding to the capacitance sensors' placement and by measuring the time delay between the signals.

4.3. Rheological tests

To make sure that the model described above was suitable for a forward problem solution the results of the Oldroyd-B fluid steady flow simulation were compared with the data obtained using the conventional cone-and-plate rheometer.

4.3.1. Experimental fluids

As outlined in chapter 2.5, two Boger polyacrylamide fluids and one glycerol-water Newtonian fluid were used in this research project. The constitutive properties, both being shear and extensional, were measured prior to carrying out the inverse problem experiments.

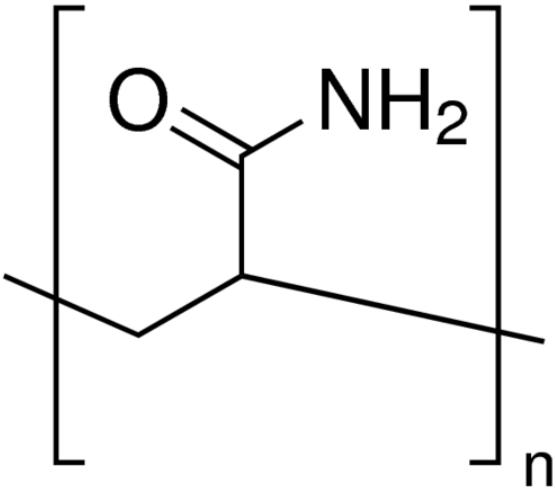

Figure 17. A repeating unit structure of polyacrylamide polymer

(https://www.sigmaaldrich.com/catalog/search?term=Polyacrylamide&interface=Product%20Name&N=0+&mode=mode%20matchpartialmax&lang=en&region=GB&focus=productN=0%20220003048%20219853286%20219853121).

Polyacrylamide (www.sigmaaldrich.com) is a water-soluble polymer, which is able to form long linear or branched molecules from repeating subunits, shown in fig. 17. When added to water, it can sufficiently increase the viscosity of the solution. The PAA solution is a transparent, non-toxic liquid that is stable at wide range of temperatures, degrading at 110^{o}C, but is incompatible with strong oxidizing agents, some metals and their salts. Solutions at concentrations lower than 17% could be stored for a long period of time. The viscosity of the solution linearly increased with the growth of the molecular weight of the polymer.

The PAA used in this study was supplied by Sigma Aldrich, the molecular weight of which was $5e^{6}$ - $6e^{6}$ Mw. Glycerol was provided by the same supplier, with a 99% purity.

Table 4. Ingredients of test fluids

Name	Polyaclylamide, ppm	Glycerol, %	Water,%	Salt, %
Glycerol/Water	___	90.99	7.51	1.5
PAA100	100	90.99	7.5	1.5
PAA300	300	90.97	7.5	1.5

The test fluids' compositions are listed in table 4. The glycerol/water mixture was prepared by utilising a magnet stirrer at room temperature for 24 hours. The PAA in given proportions was dissolved in water by stirring for 72 hours at low speed and room temperature, as long polymer chains could get mechanically damaged. Salt was added to avoid any biological degradation and to eliminate shear thinning viscosity effects. Additionally, some authors (Campo-Deaño *et al.*, 2011) reported that NaCl could decrease the size of the polymer macromolecules and therefore diminish the shear thinning effects of the flow. Dark glass bottles were used to protect the liquids from light decomposition.

The densities of the solutions of interest were measured using a "gravity bottle" test at 20˚C. The test system was calibrated by using deionised water with a density of 998.2 kg/m^3. Each test was repeated five times with each sample of 5 ml placed in pynkometers and then the average values were recorded (table 5).

Table 5. Density of tested liquids

Liquid	Density, kg m^{-3}
Glycerol/water	$1.25 \cdot 10^3$
PAA100	$1.26 \cdot 10^3$
PAA300	$1.259 \cdot 10^3$

4.3.2. Rheological tests

The shear viscosity and stress of viscoelastic and the Newtonian liquids were measured using a cone-and-plate rheometer at a temperature of 22˚C, as well as a relaxation time. An ARG2 rheometer (TA Instruments) and MCR502 (Anton Paar), fig. 18 were used for this investigation.

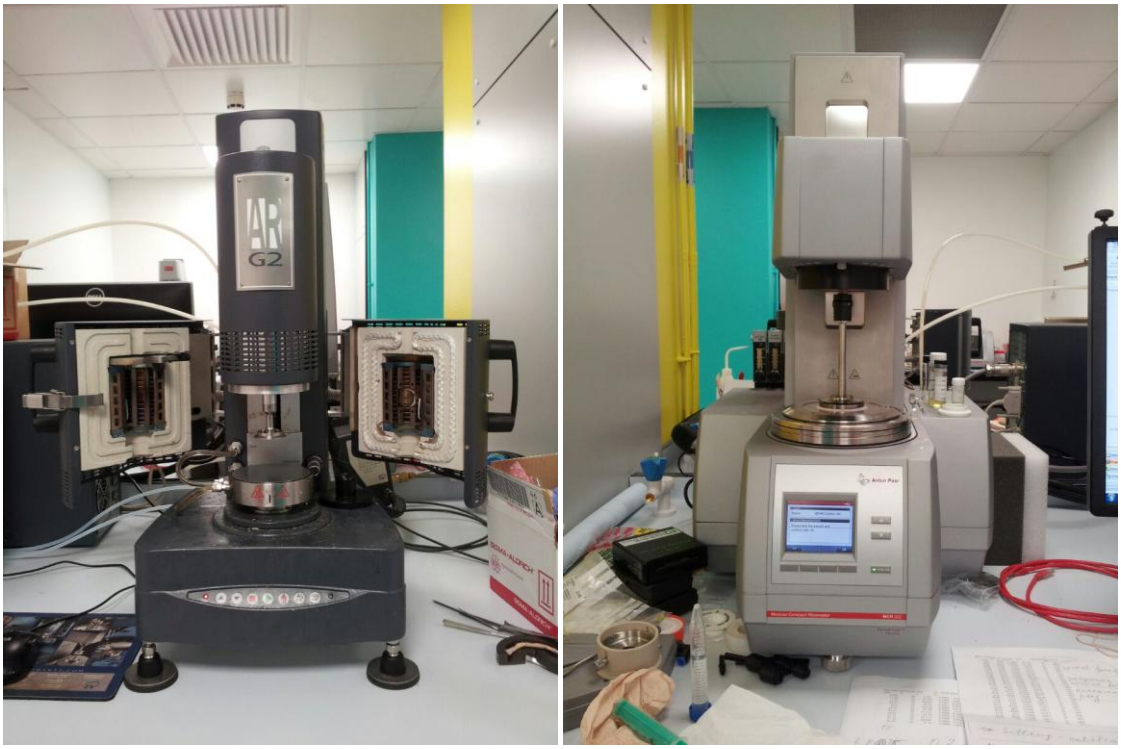

a b

Figure 18. TA Instruments Rheometer ARG2 (a), Anton Paar MCR502 (b).

A small amount of the liquid was placed on a plate held at a controlled temperature without pre-shearing, and three different regimes: simple shear, relaxation time test and oscillation were applied to obtain the data of interest. A cone-and plate geometry was used in both rheometers, since it was recommended for the liquids with low viscosity. The angle of the cones was 2^{o}, with their diameters being 40 and 50 mm for the TA and Anton Paar rheometers respectively. All three liquids were tested three times in both types of rheometers to exclude the influence of measurement bias.

Results of the shear tests are shown in fig. 19. Viscosities of all three liquids exhibited a slight shear thinning: glycerol/water of 8.8%, PAA100 of 6.7% and PAA300 of 8.9%. This confirms that PAA100 and PAA300 could be Boger fluids with an almost constant shear viscosity. In addition, it can be seen from the fig. 19, that adding polyacrylamide to the glycerol/water mixture increases the viscosity of the liquid PAA100 and PAA300, meaning that the general viscosity of these liquids is the sum of the Newtonian and polymer viscosities. Therefore, the average values of the viscosities of the test liquids are:

$\eta_{Glyc/water}$ = 0.22 Pa·s,

η_{PAA100} = 0.23 Pa·s,

η_{PAA300} = 0.25 Pa·s.

Relaxation time was used in constitutive equations for the CFD simulation. In general, the relaxation time defines the time required by the system to return to its initial conditions. Relating it to the viscoelastic fluids, this criteria reflects the time needed for the molecular chain to relax back to the state prior to the stress application. During the test, a step-like constant strain is applied to the sample and the resulting stress decay is measured as a function of time. Note, in addition, that for Newtonian fluids relaxation time tends to zero.

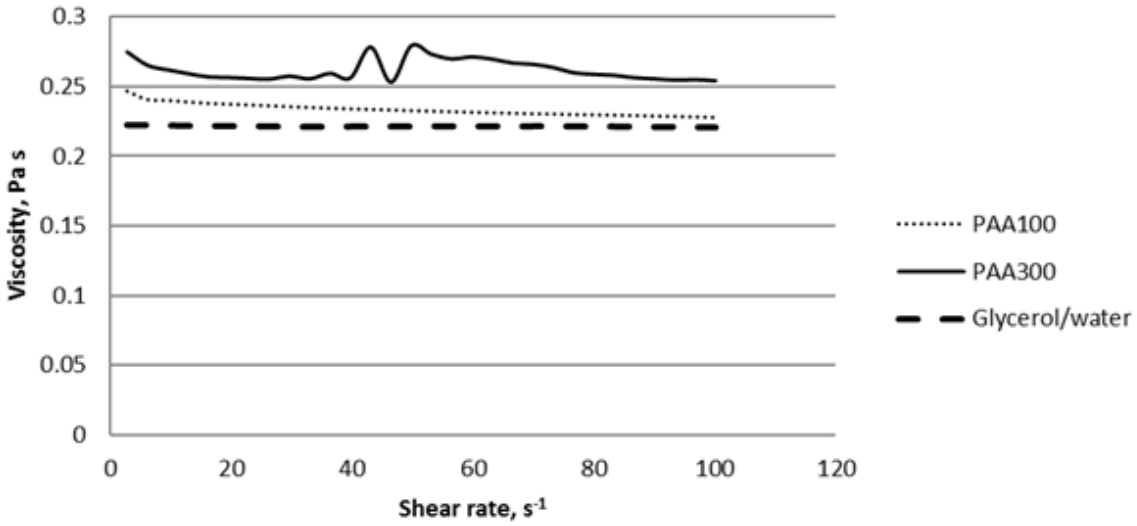

Figure 19. Results of shear tests of glycerol/water mixture, PAA100 and PAA300, average curves.

The correlations of the numerical and experimental data are shown in fig. 20. The discrepancy for all three liquids does not exceed 5%. Additionally, polymer solutions demonstrate shear thinning, whilst the viscosity of Newtonian glycerol/water mixture is almost constant. Shear thinning of polymer based fluids is explained by stretching of coiled

polymer molecules when stress applied. A close similarity between the simulated and measured data could be accepted as a proof of the model validation. In chapter 6, devoted to the results and discussion, the results of the computer simulations, based on this model, will be compared with the experiments for the pressure and the velocity measurements.

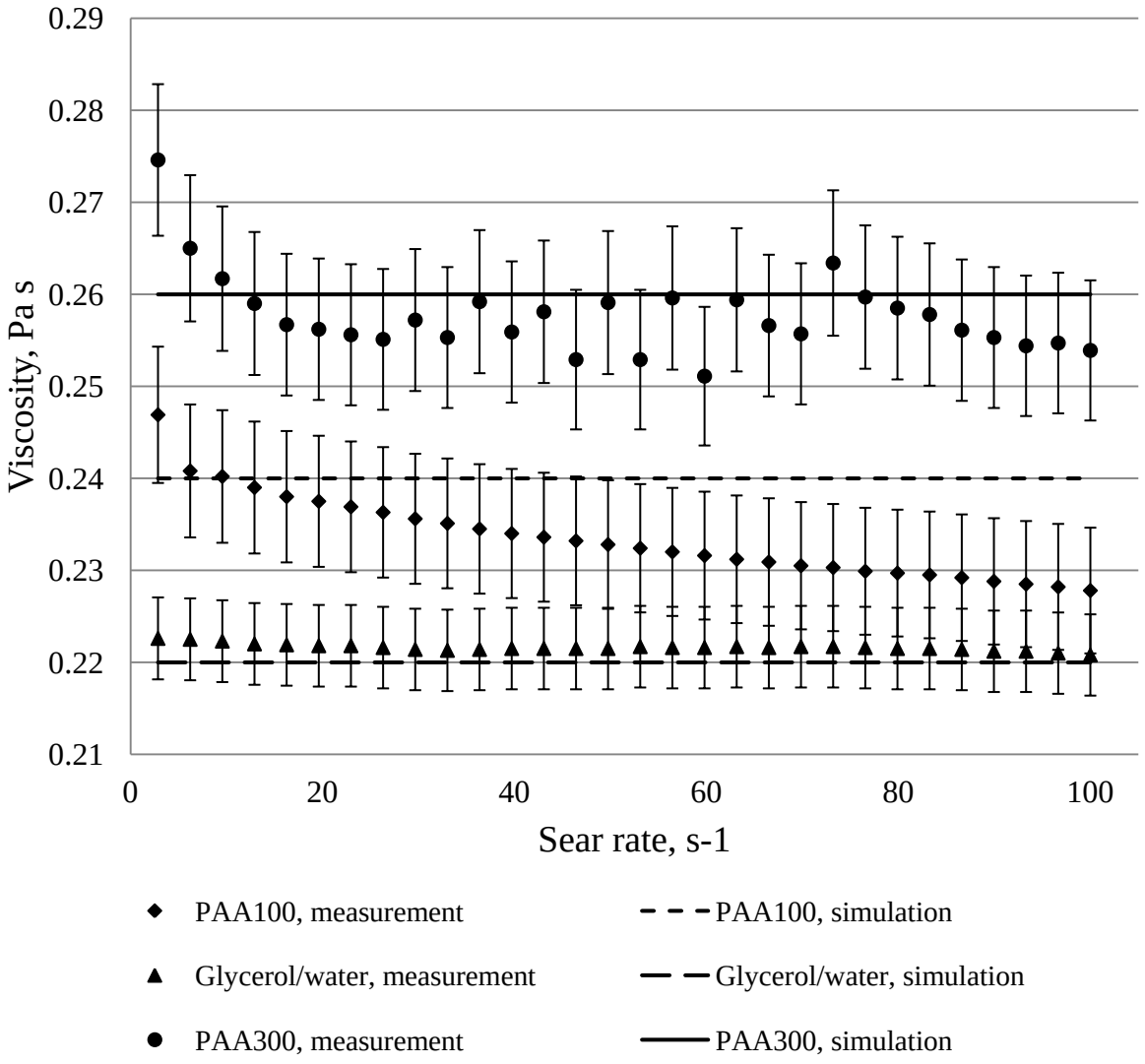

Figure 20. Simulated and measured viscosity dependent on shear rate.

Chapter 5: Experimental methodology

5.1. Design of the experimental T-shaped rheometer

A peristaltic syringe pump unit was used to generate a pressure driven flow through the T-shaped flow channel of the rheometer, thus controlling the shear and normal stresses of the fluid. The T-shaped rheometer design was based on the pioneering studies in the research area of interest, in particular on the work by Zimmerman, Rees and Craven, (2006) and (Bandulasena, William and Julia, 2011).

The new version of our T-shaped rheometer is shown in fig. 21. The apparatus is named T-ometer after the shape of the T-junction flow channel. The device was developed by Dr D. Kuvshinov and produced in the central mechanical shop of the Sheffield University (i.e. it was produced in house).

The flow channel is shown in fig. 21 (a). The channel itself is cut into the plate of PEEK which had a thickness of 20 mm. the inlet/outlet steel-made connectors were threaded into the channel. PEEK was chosen due to its excellent mechanical and chemical resistance properties that are retained at high temperatures. It was theorized that the measurements could be conducted at temperatures of up to 200˚C. The melting point of the PEEK is 343˚C which suits the experimental requirements. Additionally, PEEK is highly resistant to thermal degradation and chemical impact. Three couples of mutual electrodes, made out of copper, are embedded into the base of the device, located close to the stagnation point area of the flow, and they form three capacitance sensors. These sensors were connected to an external data acquisition system by the means of wires that were soldered to the bottom of the sensors.

The next layer comprised a membrane made of plastic (PTFE or PEEK). It covered the channel and made up its ceiling. Due to plastic's plasticity, when being pressed to the base of the rheometer by clamping bolts the membrane acted as a seal, preventing the liquid from leaking outside of the channel. PTFE has melting point at 327˚C and additionally has a very low coefficient of friction. Both PTFE and PEEK are dielectric materials.

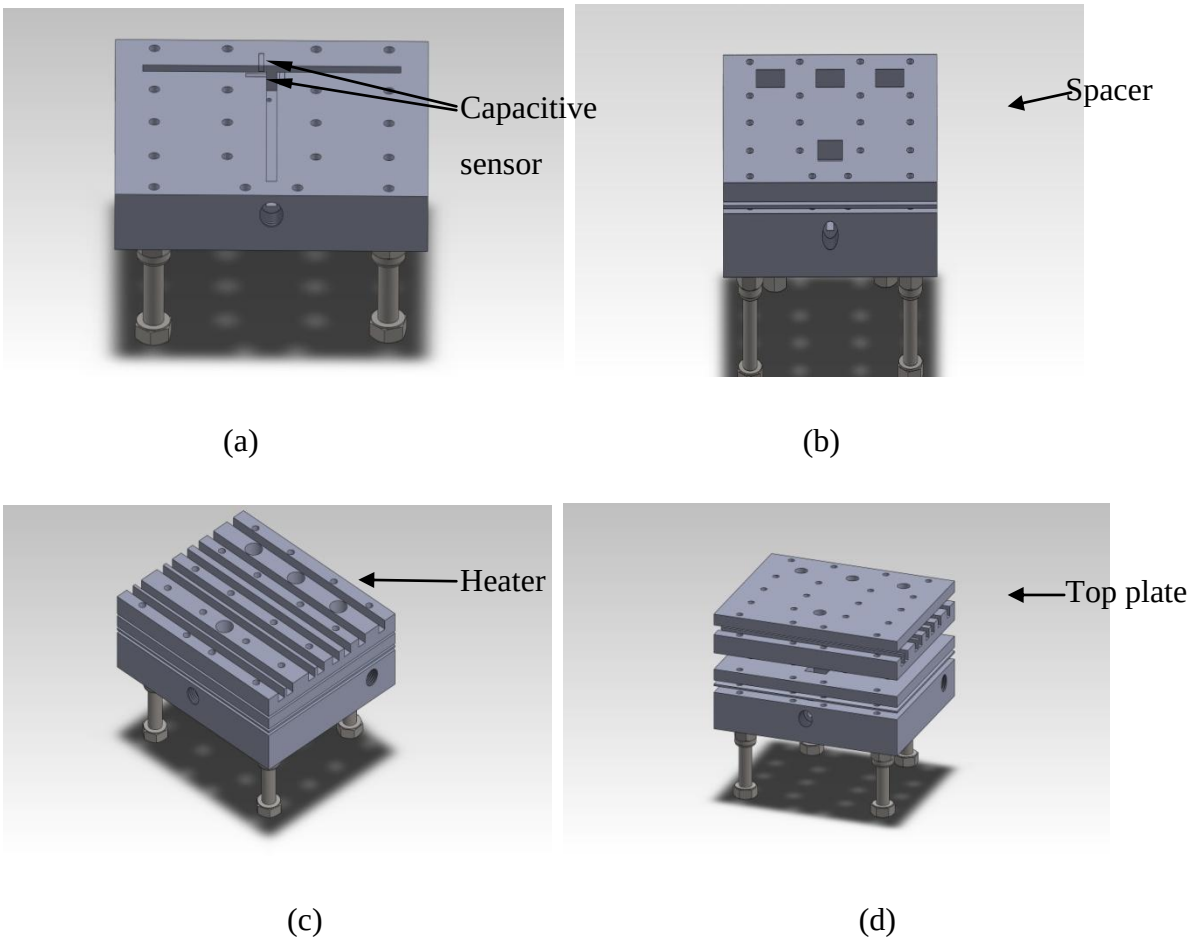

Figure 21. The T-shaped rheometer. (a) - the channel plate, (b) - the spacer, (c) - the heater, (d) - the top plate.

The spacer (shown in fig. 21 (b)) was made of copper and had a thickness of 6 mm. Four windows were made for positioning the strain gauges (pressure sensors) and numerous holes were put in place for wiring purposes. Pressure was distributed along the surface of the base of the device with the use of 20 clamping bolts. The spacer acted as one of the key elements of the heating and thermo stabilisation systems of the device. Due to the high thermal conductivity of copper and the significant thickness of the spacer the component could be treated as a thermal sink, thus dramatically reducing the temperature gradient along the surface of the device. The spacer may be adapted to fit the particular configuration (geometry) of a pressure sensor.

A slotted, flat single heater is placed along the top of the spacer (Fig. 21 (c)). The top of the spacer contains a set of holes to accommodate the wiring associated with the strain gauges.

Straight slots are also cut to accommodate a heating rope. Based on material properties, we performed numerical simulation (see section 5.2) to verify that the heater permits a uniform temperature distribution.

The nichrome heating rope is a resistant heater with an internal thermocouple. It is operated by an external temperature controller.

The top cover of the T-ometer was a 3 mm thick plate made out of PEEK. It contained a set of holes through which the sensors could be connected, accommodating the clump bolts. The plate served as an upper thermoinsulation layer of the whole device.

The proposed experimental procedure required a precise horizontal positioning of the device, for the purpose of which the T-shaped rheometer was equipped with four adjustable legs.

The pressure driven flow was generated by using a high pressure peristaltic KDS 410 syringe pump. The device is capable of providing flows of high accuracy (1% or less) with a broad flow rate, values of which range from 0.001 µl/hr to 145.5 ml/min. A built-in digital module controls the flow rate by taking into account the inner diameter of the syringe. Due to the length of a wide plunger the syringe is able to provide a continuous fluid supply over a long period of time when set to a low flow rate, ensuring a stable, fully developed steady state flow. The programming option allows one to choose between an incremental or a smooth change in the flow rate.

Selection of a suitable syringe was crucial in achieving high accuracy measurements. A large syringe fluid volume would enable one to carry out the experiment over long timescales, and a rigid syringe material would absorb the shockwaves without deformation. Based on these requeirements a glass 100 ml syringe was chosen, supplied by SEWA Medical Ltd. The syringe was made from a borosilicate chemical and heat resistant glass, where the metal nozzle was used to adjust channel connectors. The inner diameter of the syringe was 2.4×10^{-3} m.

5.2. Development of the temperature controlling system

Many rheological studies have been devoted to the investigation of the influence of temperature on the viscoelastic properties of fluids. Complex fluids include the widely-used

class of polymer solutions which are very sensitive to temperature variation. Thus it is important that our prototype rheometer is equipped with a built-in system temperature control.

Chan *et al.*, (2007) observed weakening resistance to shear and extensional flow with increasing temperature in biopolymers. They deduced that temperature had a much stronger effect on shear, than it had on the extensional flow of starch samples.

Núñez, Della Valle and Sandoval, (2010) investigated viscous and elongation behaviour of a ready-to-eat blend at temperatures below its melting point 100 - 120ºC and above its melting point 140 - 160ºC using a capillary rheometer. The experiments showed that the dependence of wall shear stress on apparent shear rate is a function of temperature that is the linear coefficient of the relationship increases with the temperature of the blend.

Significant dependence of flow properties on temperature was shown by (Schweizer *et al.*, 1990). These authors studied M1 fluid in an opposed jet rheometer that generated a stagnation point flow. Measurements of an effective extensional viscosity and optical birefringence were implemented at three temperatures: 20, 30 and 40ºC. A direct dependence of apparent strain rate/apparent viscosity relationship on temperature was found.

An emulsification process for concentrated oil-in-water emulsions was studied in the article of (Sánchez *et al.*, 1998) in the temperature range from 5 to 50ºC. The results obtained confirmed the importance of temperature an emulsification. It was shown that an increase in temperature is associated with a decrease in the linear viscoelasticity properties of the final emulsion.

Thus, from these studies the conclusion can be drawn that temperature affects the viscoelastic properties of liquids. Therefore temperature control is the one of key features of our experimentation.

A 3D numerical model simulating the temperature distribution in the prototype rheometer was developed using COMSOL 4.3b software, "Heat transfer in solids" module. A finite element scheme was used to predict the temperature field for a copper plate with embedded aluminium cylindrical electrodes arranged in several different combinations. The governing equation for heat transfer for the steady-state problem in a solid is:

$$\rho C_p \mathbf{u}\cdot\nabla T = \nabla\cdot(k\nabla T)+q, \qquad (5.1)$$

where ρ - the density from the material properties, C_p - heat capacity from the material properties, $\boldsymbol{u}$ - velocity field (for a moving coordinate system), T - temperature, k - thermal conductivity from the material properties, q - heat source.

Because the heat source is fixed, **u** = **0**.

The heat source is defined for electrodes as

$$q=\frac{Ptot}{Vol}, \quad (5.2)$$

where P_{tot} - heat source power, Vol - total volume of the heat sources.

The total power for the model P_{tot}= 100 Watt.

Boundary conditions for this model are of two types: thermal insulation and convective cooling.

The thermal insulation boundary condition is the default boundary condition for all heat transfer interfaces. This boundary condition means that there is no heat flux across the boundary:

$$-\mathbf{n}\cdot(-k\nabla T)=0. \quad (5.3)$$

This condition is applied over the surface between the heating electrodes and the outer material.

Uniform convective cooling boundary conditions were applied for all other surfaces of the geometry:

$$-\mathbf{n}\cdot(-k\nabla T)=h\,(T_{ext}-T), \quad (5.4)$$

where h - heat transfer coefficient, T_{ext} - external temperature.

The heat transfer coefficient controls the type of convective heat flux in the heat transfer model. The research programme will be carried out in air (as opposed to in vacuum or underwater), so h is a heat transfer coefficient in air. The external temperature is taken as T_{ext}=20ºC.

These equations were solved using a Galerkin finite element method. Grid mashing was made using a physics controlled mesh. Mesh cells were finer along the electrodes (the boundary of

the heat flux). Computer simulations were made for configuration of two, four, six and eight heating elements. The results of the calculations are presented on the fig. 22.

It can be seen that that the most uniform temperature field is achieved from implementation of the configuration eight heating elements whilst for the case of the two element configuration, for example, the temperature difference across two points of the channel can reach 50 K.

The drilling of 8 holes in the reactor base could lead to the construction difficulties of the device. In addition, if the channel body was to be made of copper, it should be noted that this element is not chemically neutral. Thus the decision was taken to construct the channel using PEEK and to make an external heating plate.

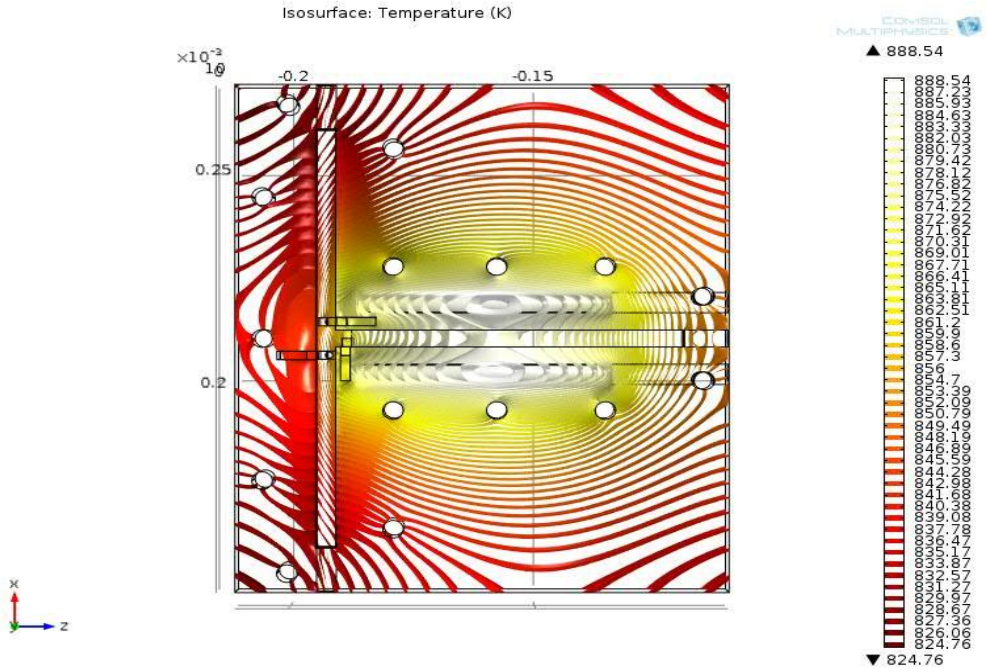

a

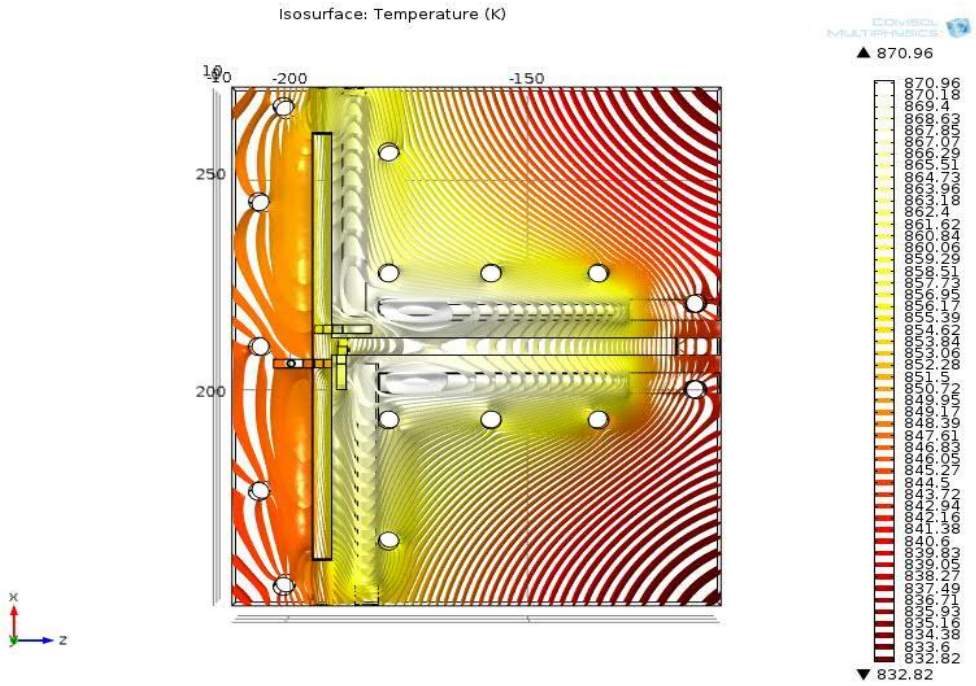
Isosurface: Temperature (K)
-200
-150
250
200
▲ 870.96
870.96
870.18
869.4
868.63
867.85
867.07
866.29
865.51
864.73
863.96
863.18
862.4
861.62
860.84
860.06
859.29
858.51
857.73
856.95
856.17
855.39
854.62
853.84
853.06
852.28
851.5
850.72
849.95
849.17
848.39
847.61
846.83
846.05
845.27
844.5
843.72
842.94
842.16
841.38
840.6
839.83
839.05
838.27
837.49
836.71
835.93
835.16
834.38
833.6
832.82
▼ 832.82
x
z

b

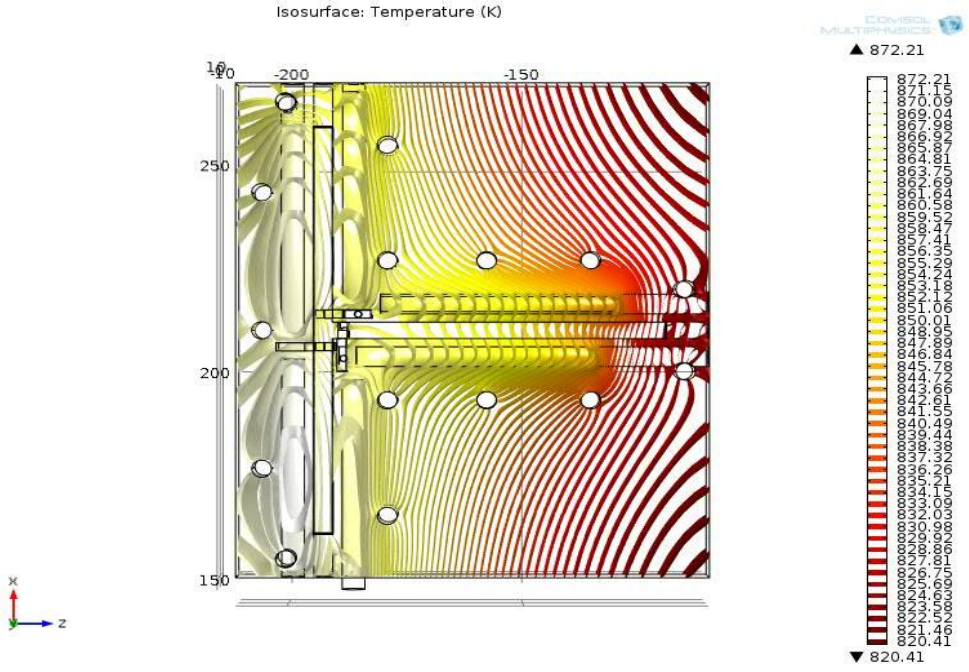
Isosurface: Temperature (K)
-200
-150
250
200
150
▲ 872.21
872.21
871.15
870.09
869.04
867.98
866.92
865.87
864.81
863.75
862.69
861.64
860.58
859.52
858.47
857.41
856.35
855.29
854.24
853.18
852.12
851.06
850.01
848.95
847.89
846.84
845.78
844.72
843.66
842.61
841.55
840.49
839.44
838.38
837.32
836.26
835.21
834.15
833.09
832.03
830.98
829.92
828.86
827.81
826.75
825.69
824.63
823.58
822.52
821.46
820.41
▼ 820.41
x
z

c

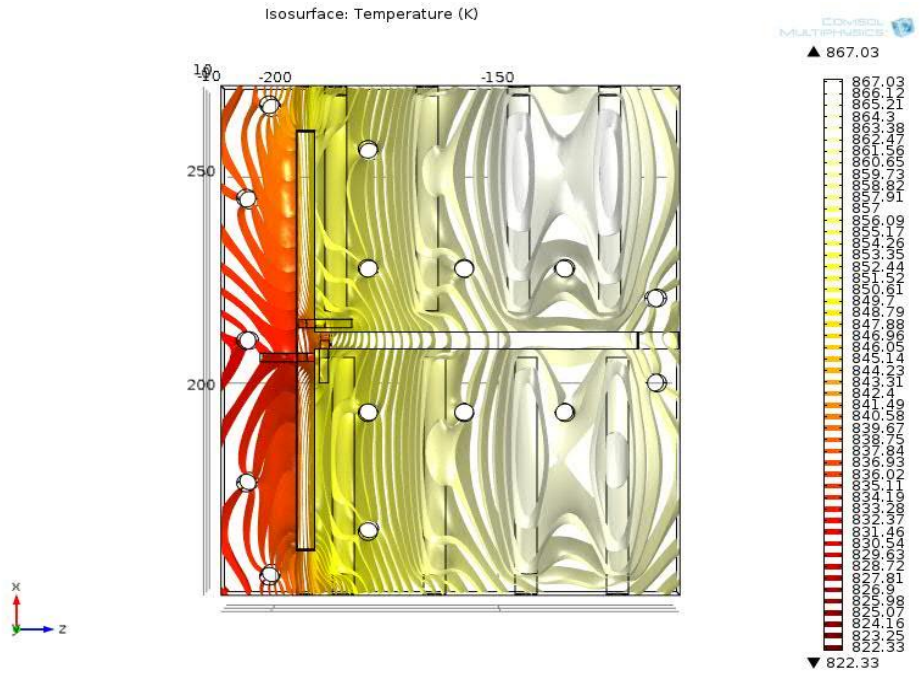

d

Figure 22. Temperature distribution in the domain: (a) - 2 heating elements, (b) - 4 heating elements, (c) - 6 heating elements, (d) - 8 heating elements.

5.3. The measuring network

In chapter 3 an explanation for the forward and inverse problem was provided. It was stated that for the inversion to be able to be used constitutive parameters the flow fields that were measured were the pressure and velocity fields. The former was measured by the membrane strain gauges and the latter by the flash-mounted copper electrodes.

5.3.1. Pressure measurement

For the pressure measurement along the T-shaped channel four high precision pressure transmitters were flash mounted into the bespoke made spacer. The transmitters were supplied by the STS Sensor Technik Sirnach, modification ATM.1ST (fig. 23). The operating temperature range for these sensors is between -40 and 125 °C, while the digital temperature compensation algorithm provides a high accuracy between 0 and 70 °C. The diameter of the footprint of the measuring cell was 1.5×10^{-2} m. The transmitters were made from stainless steel, which made them suitable for the operation in a chemically aggressive environment. Furthermore, dynamic measurements were made possible due to the short response time of

the acquisition system. The pressure range is from 0 to 1 bar, and this provided an opportunity to test liquids with different viscosities.

Figure 23. High precision pressure transmitter ATM.1ST (www.stssensors.com).

The principle of operation was as follows: as the membrane deformed under pressure the pressure level was recorded as a function of the pre-calibrated signals from the strain transmitters. The wiring was implemented using the 2 m connectors supplied. The configuration of the sensors is shown in fig. 24. The pressure transmitters were installed at the inlet, both outlets and exactly under the stagnation point area to provide the pressure drop measurement along the channel.

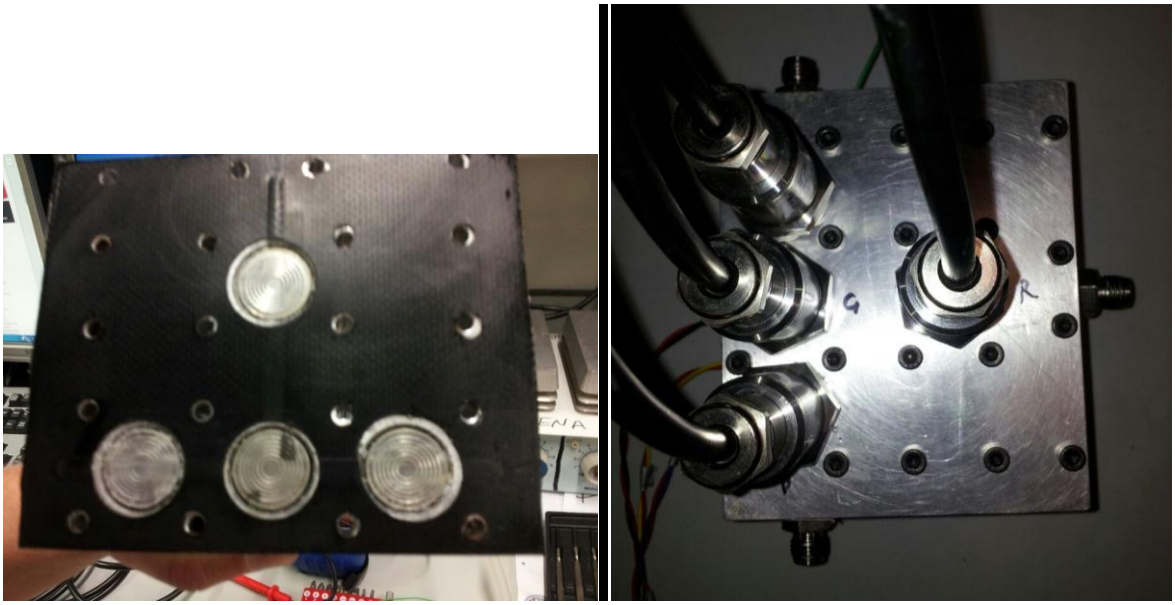

a b

Figure 24. Operating surface of the pressure measurement system (a); T-ometer pressure sensors configuration (b).

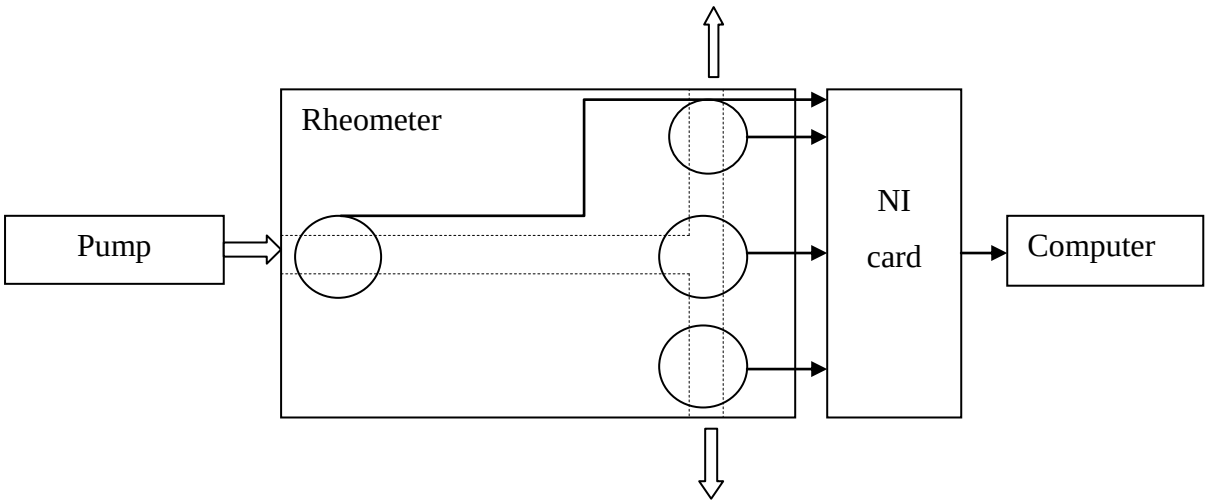

Figure 25. Principal diagram of the pressure sensing system.

The signals from the pressure transmitters through the full bridge mode circuit were transferred to the data acquisition module, (fig. 25) NI USB-6211 device. The device has a USB interface connection to a desktop computer which was to be used as an analogue signal

collector. A LabVIEW program was written for the data collection. The data collection frequency was set to 10 Hz.

5.3.2. Capacitance measurement

The velocity field tracking system was made of copper electrodes embedded in the channel walls. Six electrodes were positioned in the plane parallel to the channel wall to avoid any distortion to the flow. The positions of the electrodes cover the most crucial information parts of the device, which include the stagnation point and the corner area.

The single wall embedded copper electrode forms one part of the single capacity electrode of the rheometer. The second capacity electrode was embedded in the bottom of the rheometer channel. The electric field covered the channel corner, as capacitance of the electrodes form a 90° angle, effectively creating a single capacitance sensor. The wiring of the capacitance sensors was achieved by using 2 mm diameter wires connected to the ends of the external electrodes. The data collection was carried out by NI USB-6211, which is similar to the pressure sensing system described earlier in fig. 25, the velocity sensing system and configuration of the sensors as shown in fig. 26.

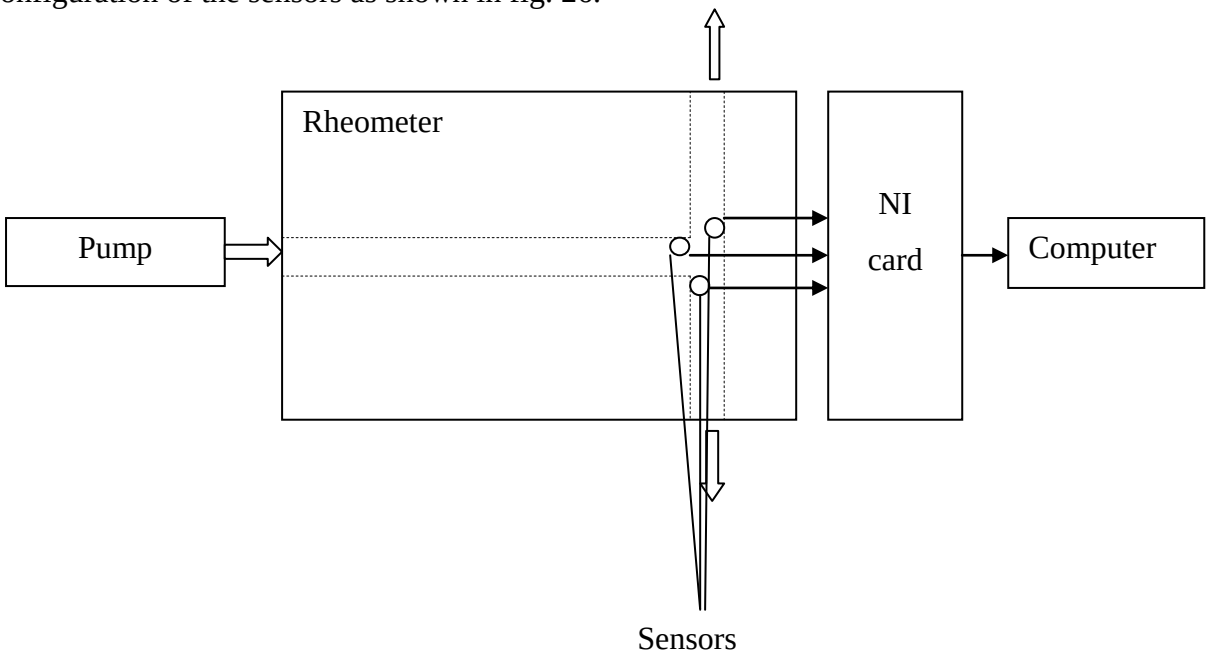

a

b

Figure 26. The principal diagram of the velocity sensing system (a), capacitance sensors configuration (b).

The principles for making measurements of the velocity were described in chapter 2. Knowing the time of the pulse propagation and the distance between the sensors makes it possible to calculate the velocity of the flow. The configuration of the sensors, shown in fig. 26 (b), provides the sought parameter (distance) equal to 5×10^{-3} m.

5.4. Calibration process

5.4.1. Pressure sensors calibration

The assembled rig is shown in fig. 27, consisting of the T-ometer cell, the pump and connected syringe.

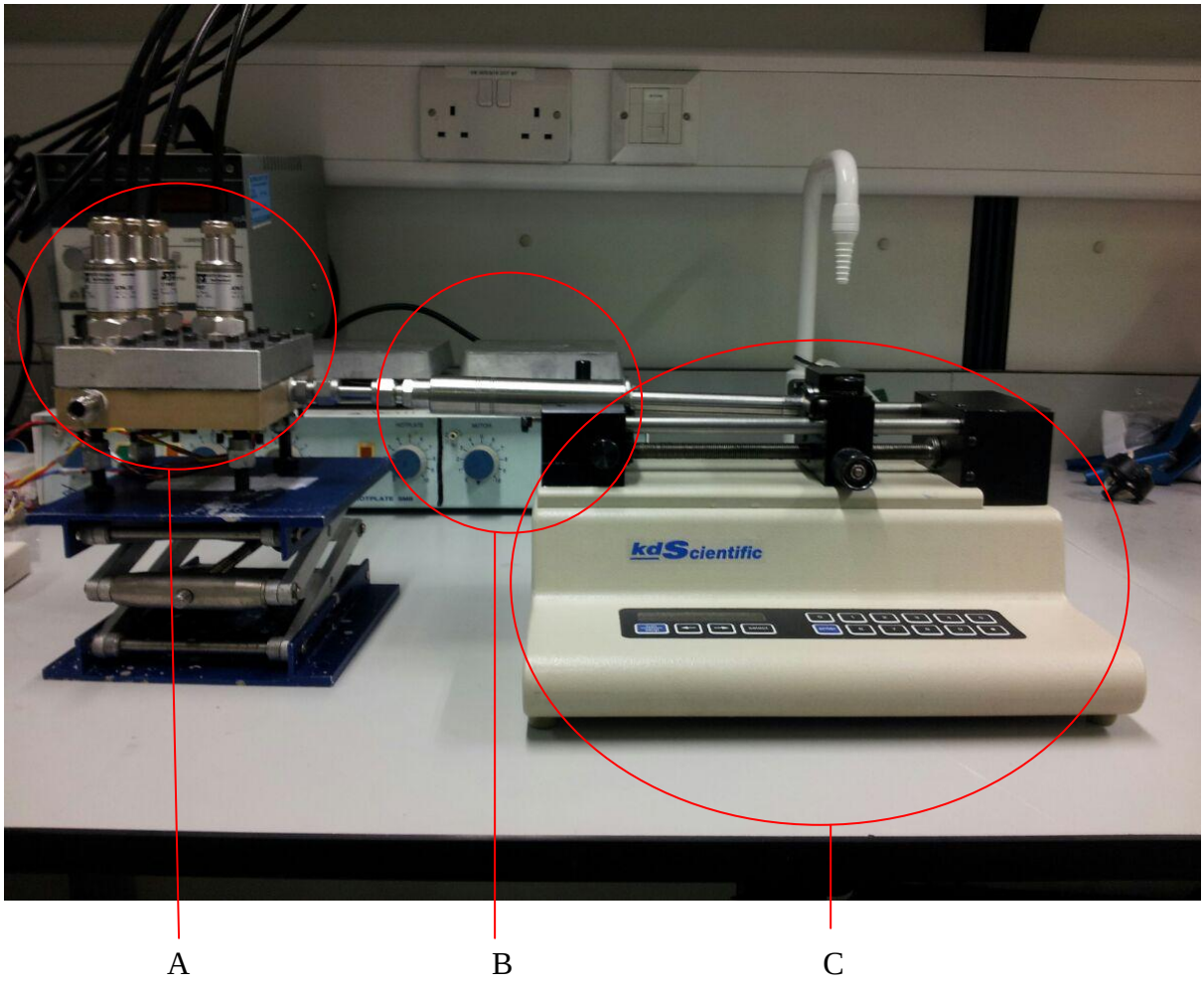

Figure 27. Assembled experimental apparatus: A - T-ometer, B - syringe, C - pump.

The measurement of the velocity is based on measuring the change in capacitance between two sensors over time, thus removing the need in preliminary calibration of the detecting system. As for the pressure sensors, the values were measured in volts which were then converted to Pa. For this purpose a conversion function was defined by carrying out the calibration procedure. A static pressure head was used to calibrate the pressure gauge sensors.

Two liquids, with different densities, were used for the calibration purposes: water and glycerol. The static pressure was calculated by using the following equation:

$$p=\rho gH, \tag{5.5}$$

where ρ - density, g - gravimetric constant, H - length of a pressure head.

The sensitivity investigation was implemented along with the calibration procedures. For this purpose the height of the pressure head was gradually increased in steps of 5×10^{-2} m. Thus, knowing the density of the liquids used for the calibration, the conversion function for the given pressure gauges was found. Examples of readings from the sensors in volts are shown in fig. 28. Each liquid was tested 3 times, and then averaged ratios of volts to Pa were calculated.

It can be seen in fig. 28 (b) that for the glycerol probe the curve has a saw-like shape. This could be explained by the fact that the pressure head pipe was made out of a silicone tube, so the shape of the graph demonstrates an expansion-relaxation process of the tube occurring due to the shock wave from a liquid travelling with a significantly high viscosity. This problem was taken into account by the syringe-T-ometer adjustment system. Further, all of the connecting elements were made out of rigid materials such as stainless steel.

Knowing that the density of the liquids used for the calibrations are:

$\rho_{water} = 1 \times 10^3$ kg/m^3,

$\rho_{glycerol} = 1.26 \times 10^3$ kg/m^3,

the conversion function was calculated as

2.041 Pa=0.0001 V.

The above ratio of voltage to Pa was used for defining pressure measurements.

5.4.2. Sensitivity and stability tests

For the fluid property investigation the flow pattern is one of the most important parameters to consider. The pressure drop was measured in a fully developed steady state flow, i.e. when the pressure field was kept constant throughout the duration of an experiment at a given flow rate. The time required for the flow development and pressure gauge stability were tested at a

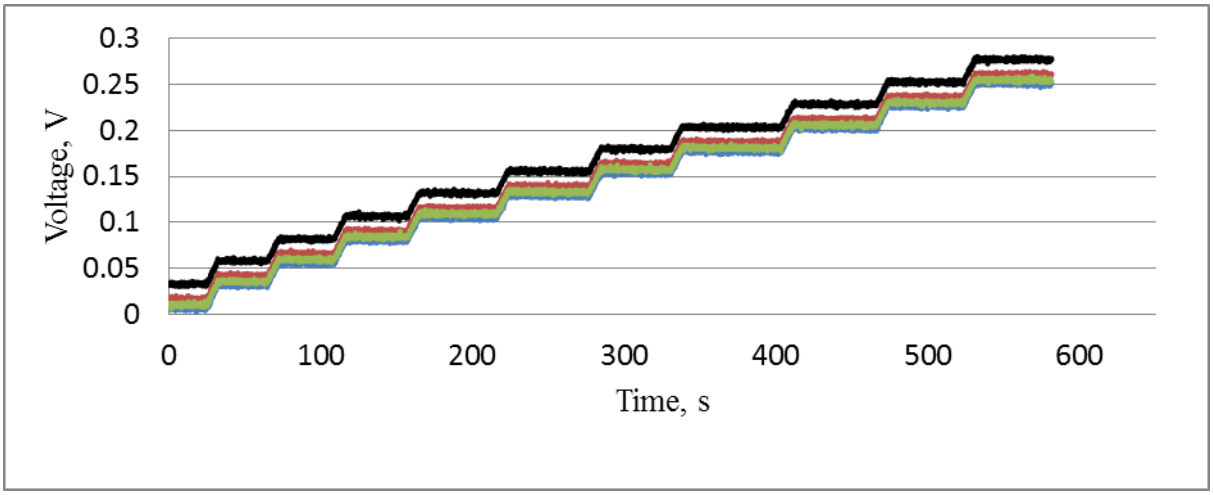

a

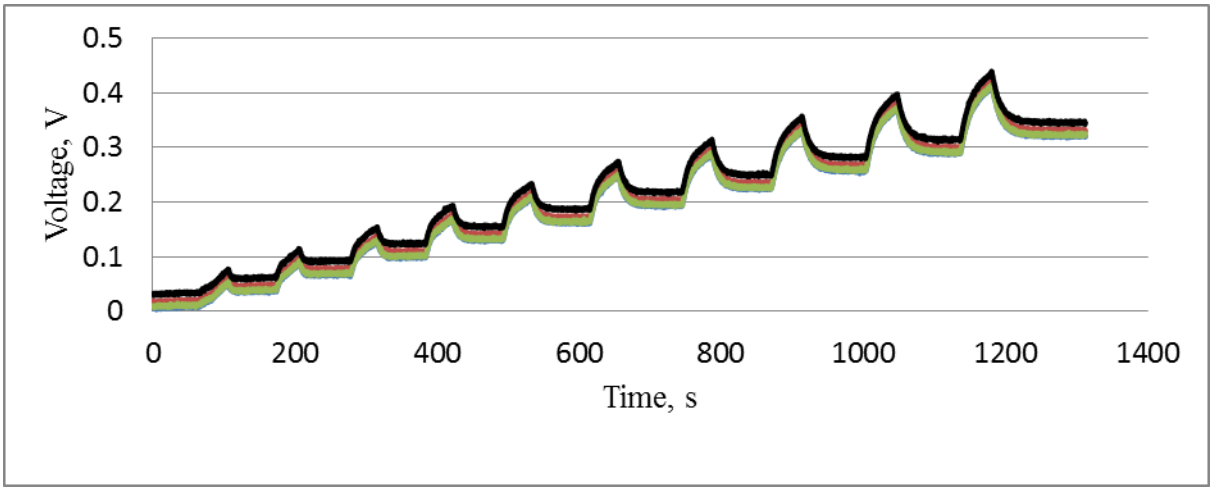

b

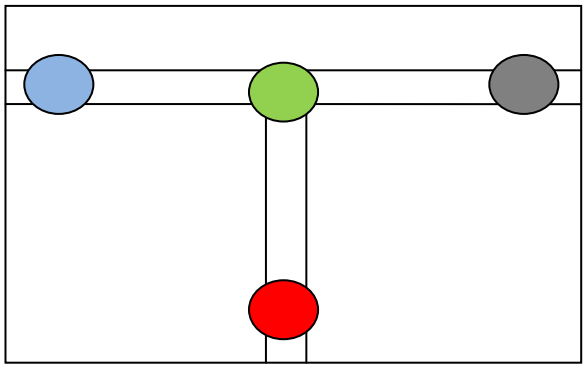

c

Figure 28. Voltage readings for water (a) and glycerol (b) steady pressure head, made by steps. Colour coding for the sensors configurations (c). Time is shown in points taking 10 points every single second.

flow rate of 10 ml/min for 10 min. In fig. 29 the readings for a stability test are shown. It can be seen that the value of pressure measured by all four sensors changed almost immediately and remained constant over the whole duration of the test. Following these results an experimental procedure was planned.

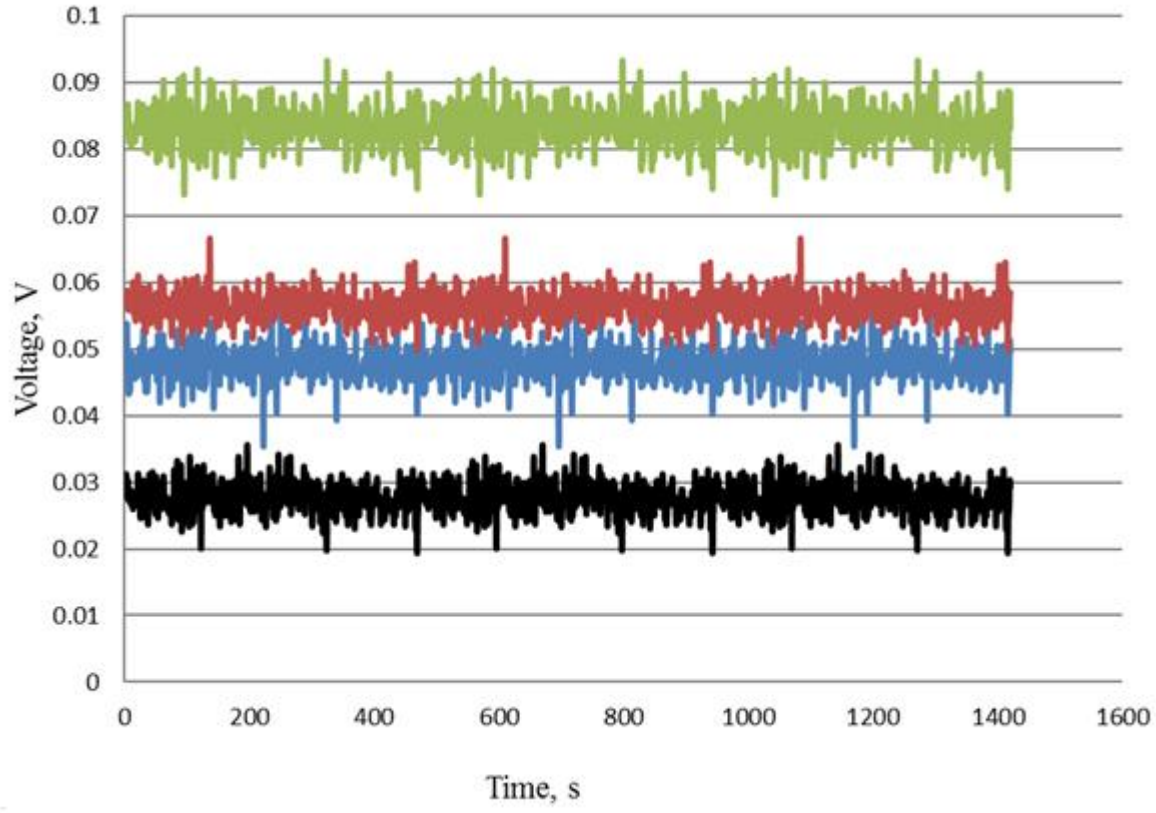

Figure 29. Pressure sensors reading, stability test.

The planning of the experiment was made taking into consideration the sensitivity of the pressure sensors. The voltage measurements at different flow rates are shown in fig. 30.

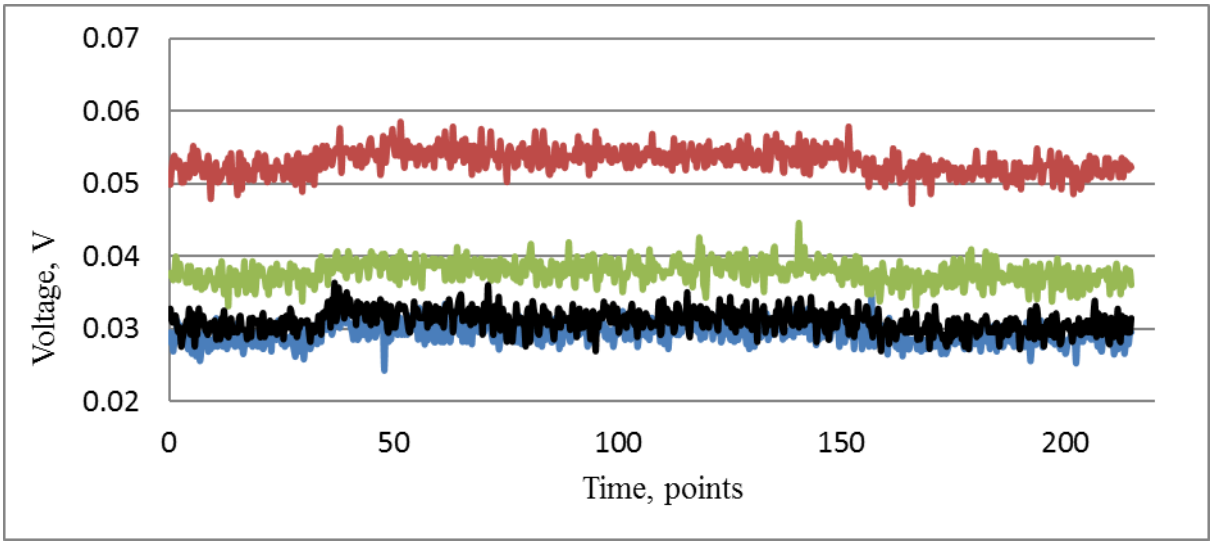
0.07
0.06
0.05
0.04
0.03
0.02
Voltage, V
0
50
100
150
200
Time, points

a

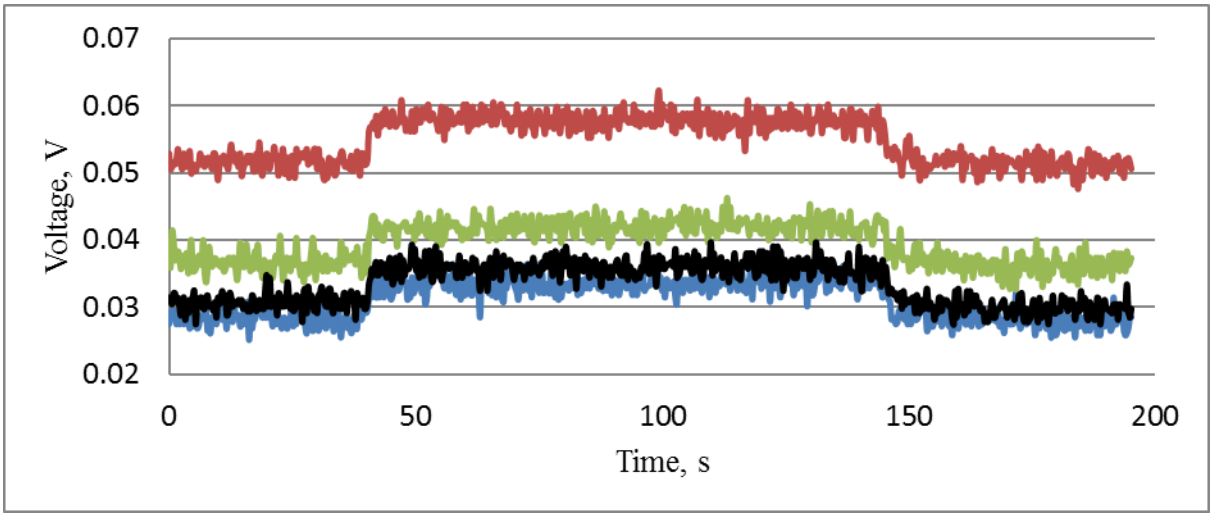
0.07
0.06
0.05
0.04
0.03
0.02
Voltage, V
0
50
100
150
200
Time, s

b

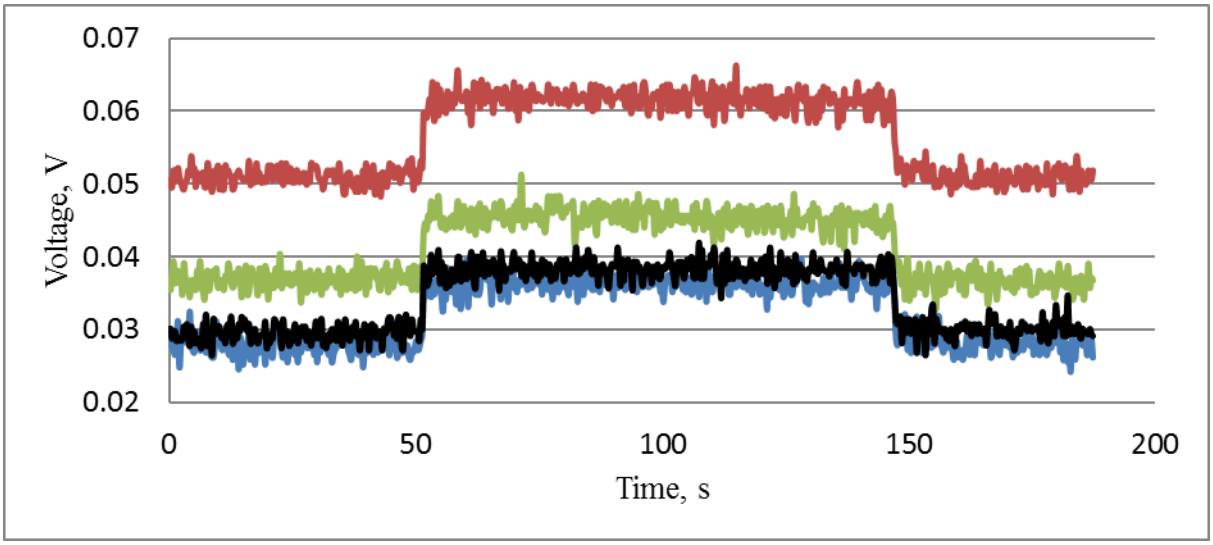
0.07
0.06
0.05
0.04
0.03
0.02
Voltage, V
0
50
100
150
200
Time, s

c

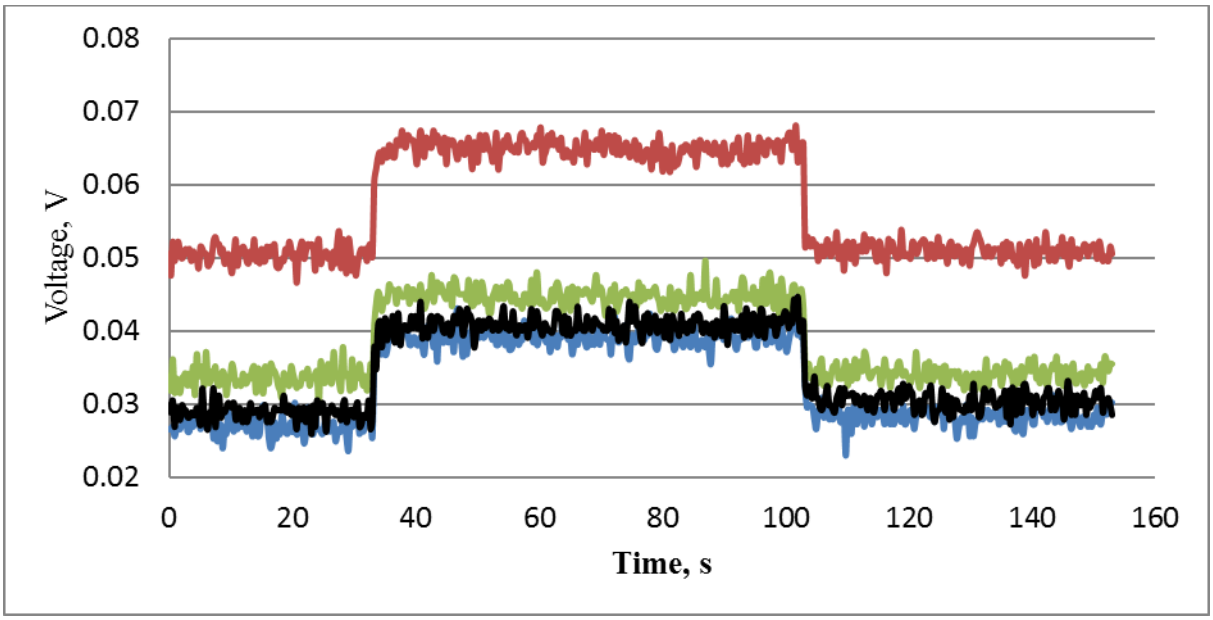

d

Figure 30. Sensitivity test data: (a) 1 ml/min, (b) 4 ml/min, (c) 7 ml/min, (d) 10 ml/min.

The flow system of the device was filled with test liquid. Then stress was applied at the inlet of the channel at controlled flow rate. Measured voltage differences for given flow rates were:

ΔV(1 ml/min) = 0,0013 V = 26.53 Pa;

ΔV(4 ml/min) = 0.005 V = 102 Pa;

ΔV(7 ml/min) = 0.0085 V = 173.48 Pa;

ΔV(10 ml/min) = 0.012 V = 244.92 Pa.

Though the meaningful change of voltage exposed at all flow rate applied, the experimental procedure was developed for mass flow rates with the step of 10 ml/min.

5.4.3. Flow visualisation

Flow visualization is an important branch of fluid dynamics research that can provide an immediate picture of the nature of a fluid flow. The development of optical and electronic

technologies have considerably improved the visualisation techniques available, which can now provide some powerful tools for solving rheological problems.

Flow visualization techniques can be divided into qualitative (understanding the physics of the flow) and quantitative (gaining the flow statistics) methods. Optic techniques are comparably non-intrusive, based on the optical properties of light such as refraction and polarisation. Tracing techniques involve the addition of foreign materials into the sample such as fumes for gases and fluorescent beads or dyes for liquids. The combination of illumination, the recording equipment and the computational image analysis is fundamental to the particle-based techniques. All particle-based techniques require that the test liquid is seeded with fluorescent beads. These methods also can be used for assessment of the stability of the flow fields. Particle streak velocimetry records the motion of particles over a period of time using a single exposure (single shot measurement). This leads to the appearance of a streak image and a map of the flow dynamics. However, this method does not produce reliable quantitative data. On the other hand, this method can be used to obtain streamlines of the flow.

The quality of the stagnation point flow was investigated by the means of flow visualisation. The flow was tested at different volumetric flow rates to investigate the flow pattern stability. For visualisation purposes a transparent chamber, replicating the geometry of the original T-shaped channel, was made out of perspex, as shown in fig. 31 (a). The device was equipped with a high pressure KDS 410 syringe pump, a Dolan-Jenner MI-150 Fibre Optic Illuminator light source and a Canon DS126071 digital camera for streak photography. The optic light source was coupled by an optical fibre into the ring shaped white light reflector. The optical layout of the rig is shown in fig. 31 (b).

For the flow field visualization, 120 ml of glycerol/water solution was seeded with 3 grams of titanium carbide (code 636967, purchased from Sigma-Aldrich) and tested over a range of different flow rates (fig. 32). The exposition time for streaking photography was 1 s for low flow rates (up to 10 ml/min) and 0.6 s for higher flow rates.

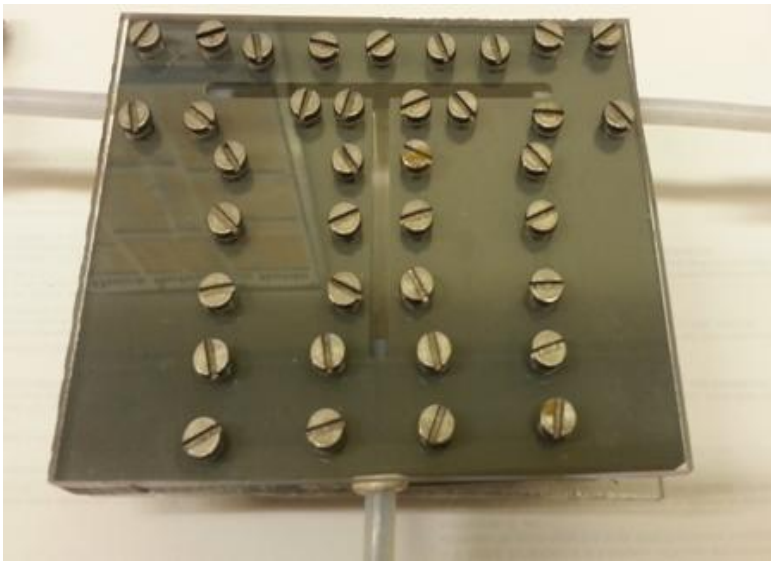

a

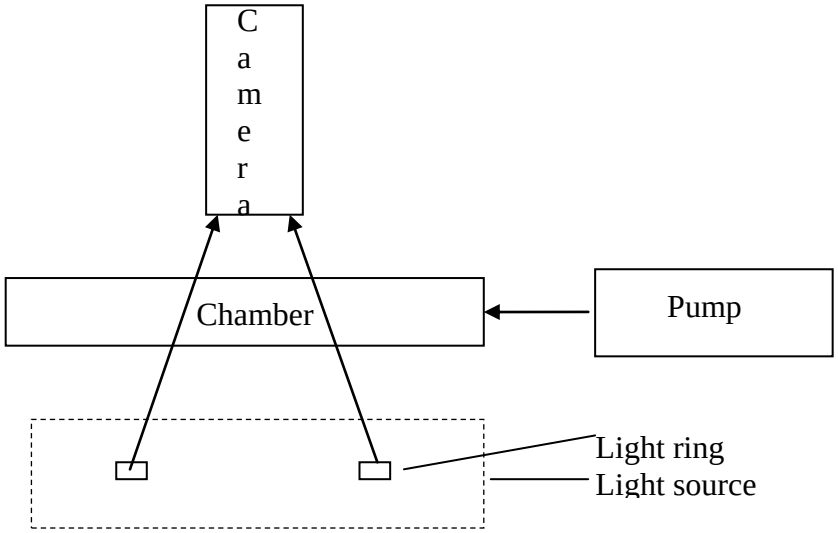

b

Figure 31. General view of the chamber constructed to facilitate flow visualisation (a); optical layout for pressure driven flow imaging (b).

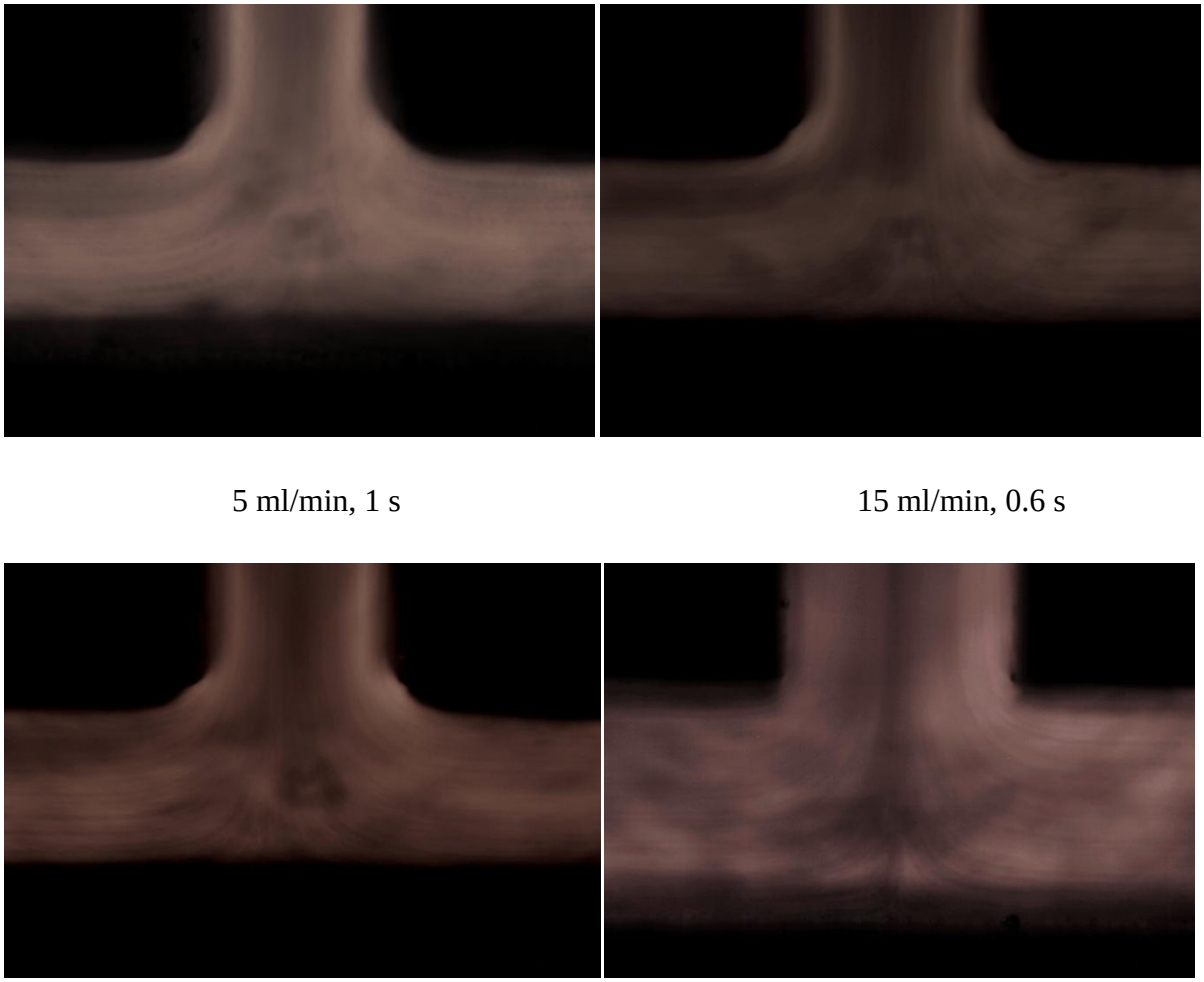

5 ml/min, 1 s 15 ml/min, 0.6 s

25 ml/min, 0.6 s 40 ml/min, 0.6 s

Figure 32. Streaking photography glycerol/water solution.

For all considered flow regimes the flow fields proved to be symmetric, stable and laminar, with the clear stagnation point visible at the back wall of the channel. The maximum investigated flow rate (40 ml/min) was not enough to create a turbulent flow.

5.5. Capacitance sensing system calibration

Whilst the pressure sensors were calibrated by converting the voltage measurements to pressure data, the only requirement for the capacitance system was to define a wave propagation time. For this purpose it was verified whether the electrodes used were capable

of detecting a change in electrical charge of the medium between the electrodes during a pulsing flow pattern.

The capacitance sensors were tested with one of the test liquids at different, non-steady state flow patterns. Fig. 33 (a) shows the principal electric circuit, and fig. 33 (b, c) shows the voltage measurements for the different, non-steady state flow patterns when a potential difference of 1 V was applied. Short repeated pulses (fig. 33 (b)) and a single graduate increasing of the flow rate (fig. 33 (c)) were realised in order to investigate better flow pattern for velocity field measurement.

Cross-correlation analysis was used to measure the similarities between the two data series. If there are two continuous functions, *f(t)* and *g(t)*, describing time series, then cross-correlation is defined as:

$$R_{fg}(t_{dif})=\int_{-\infty}^{+\infty} f(t)g(f+\tau)dt, \qquad (5.6)$$

where t_{dif} - lag (displacement) between two similar patterns of signals, R_{fg} - correlation coefficient.

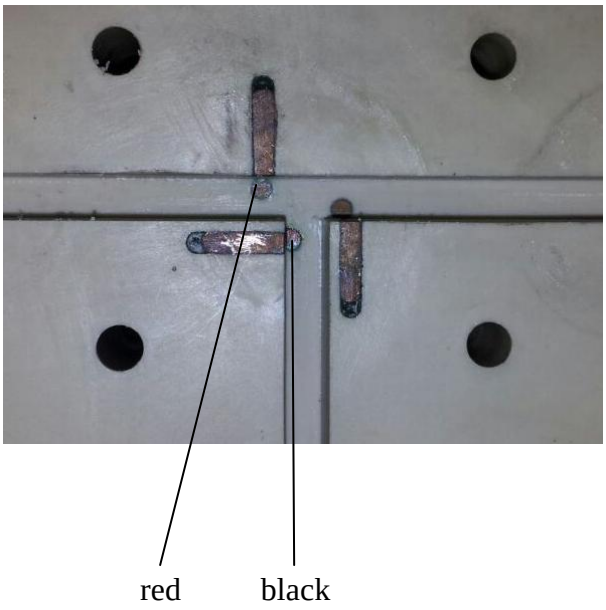

a

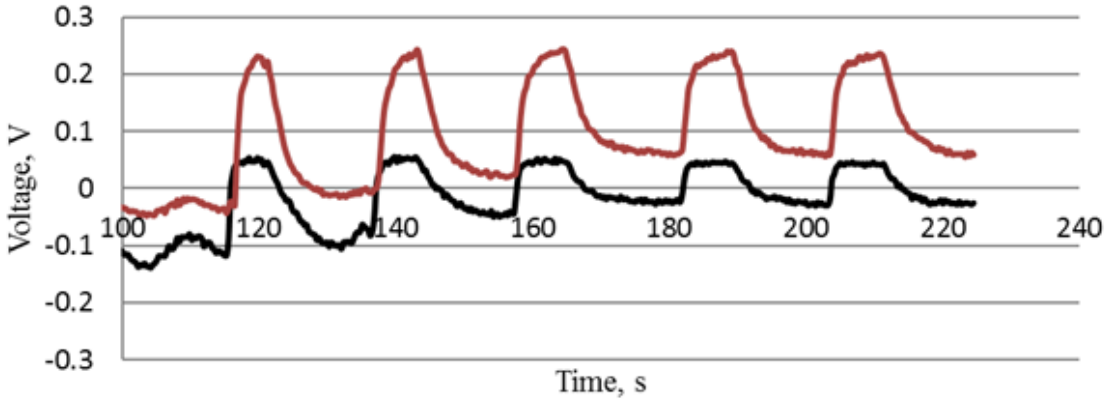

b

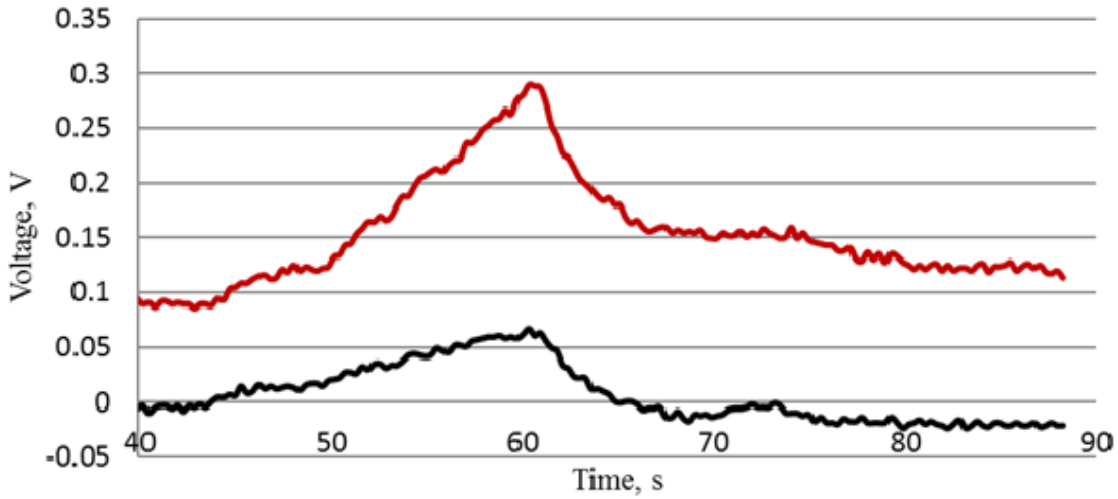

c

Figure 33. Colour coding of signals of the capacitance electrodes (a); pulsing flow of glycerol/water solution (b); gradual rising of volumetric flow rate of glycerol/water solution (c).

Two approaches for the wave formation, demonstrated in fig. 33 (b, c) allowed one to exclude the possible shock wave in the case of pulsing flow. This could be seen from the fact that the measured voltage values are negative, but this does not affect the detection of the displacement time.

5.6. Planning of experiments

Based on the calibration results of the measurement systems of the T-ometer, the following experimental procedure was developed.

1. A fully developed steady flow is immediately formed as can be seen in (fig. 30). Additionally, no expansion-contraction processes were encountered through 0.07 m to the back wall of the channel (length of the inflow limb). Thus, the pressure change was measured one minute after the flow initiation.

2. Taking into account the sensors' measurement rang, sensitivity and the volume of the syringe, pressure drop for several flow rates with step of 10 ml/min was measured. For the given conditions (the compromise of the flow development time and the volume of the syringe) the possible pressure values for reasonably slow flows would be situated at the beginning of the measurement scale, which could affect the accuracy of the experiments. All of the tests were repeated three times, after which the average values for the pressure were calculated.

3. Three pulsing flow regimes and the three increasing/decreasing flow regimes with the different maximum flow rates were carried out in order to obtain velocity measurements. After which time displacement for each flow type and each fluid was defined using a build-in cross-correlation function in MatLab.

Chapter 6: Results and discussion

6.1. Forward problem - research of viability

It has been shown earlier that the pressure drop and velocity profile of a flow is sensitive to the constitutive parameters of non-Newtonian liquids (Zimmerman, Rees and Craven, 2006), (Pérez-Camacho *et al.*, 2015), (Zatloukal *et al.*, 2002) and others. In this chapter the hypothesis in checked that constitutive parameters of test fluids can be unicly inverted through global physical parameters of stagnation-point flow in a T-shaped channel. In this case the one-to-one mapping of parameters is possible, which would demonstrate that this measurement system (the device and inverse calculation) could be used for extensional constitutive parameters determination.

The first step in the process of technology development is the model validation, when experimental data are compared with computer simulation results. In their research (Craven, Rees and Zimmerman, 2010) showed that the pressure and velocity fields were not sensitive to Weissenberg number. The dependence of global physical parameters on elastic responce was investigated using Comsol version 3.2, and at that time the built in stabilising tool allowed them to carry out simulations only for a narrow range of Weissenberg number less than 2. Implementation of the Oldroyd-B model in more developed version of the computer simulation software for a wider range of extensional parameters could open the possibility for applying the viscoelastic model for the inverse method of extensional viscosity measurement.

In this chapter results of computer simulations of steady state flow are compared with experimental flow profiles for the three liquids of interest, and afterwards the accuracy of the predictions is investigated.

Flow velocity is analysed by a cross-correlation technique using data obtained by capacitance sensors, based on principles of capacitance tomography. Combined with a model of an Oldroyd-B fluid under pulsing stress, i.e. non-steady state flow, hypothetically this provides retardation of wave propagation between sensors, separated by a certain distance, due to viscous and elastic effects, which are characteristics of Boger fluids.

As a result of the simulations and analysis undertaken one will be able to define a relaxation time which takes into account other characteristics of liquids of interest obtained in rheological tests.

In the final part of the chapter a conclusion is drawn on the possibility of implementing the inverse method for determinating the relaxation time based on the rheological properties of Boger fluids and global physical parameters, such as pressure and velocity, measured by the T-ometer using developed approach.

6.2. Approximations and assumptions

Modeling usually includes a range of assumptions, because it describes an idealised process. Additionally, manufacturing always involves different irregularities that can affect the precision of measurements. Thus, the approximations of the model 1) smooth walls with no slip conditions, whilst the channel was cut in the PEEK block, that provided a certain level of roughness, and long polymer molecules stuck to the channal walls; 2) that steady laminar flow developed downstream of the flow inlet, not taking into account extension phenomenon; 3) the inner corner of the channel at the junction in the model geometry was rounded to avoid singularities due to a sharp corner; 4) the Oldroyd-B model itself was based on the assumption that polymer molecules in a solvent behave as dumbbells with elastic connections, whereas, molecular movements and their interaction could be more complicated than it was possible to include in the computer simulation model. Hence, it was reasonable to expect that there would be a deviation of the computer simulation results from the experimental data, which might be caused by these approximations. Nevertheless, the model has shown a sufficiently close agreement with the experimental results to enable one to prove the model validation, and, as a consequence, feasibility of the inversion problem.

Also, in addition to the simulation approximations, deviations could arise from the fact that the experimental process itself causes errors because of the specification of measurement sensors and variation of experimental conditions. Presicion and range of measurement is described in the specification of a particular sensor and should be taken into account. In order to decrease of the experimental errors all measurements were carried out three times and then average values were used for the purpose of model validation.

6.3. Agreement between pressure measurements and model prediction

6.3.1. Pressure flow field

Pressure measurements are presented for three liquids at three different flow rates, the average from three tests for each experiment was derived. The Newtonian fluid (glycerol/water) was used as a base fluid for comparison of measurements and in order to determine effects caused by the elastic component in viscoelastic flows. Standard deviation for measured pressure is 16%, and this error propagation is demonstrated in the graph.

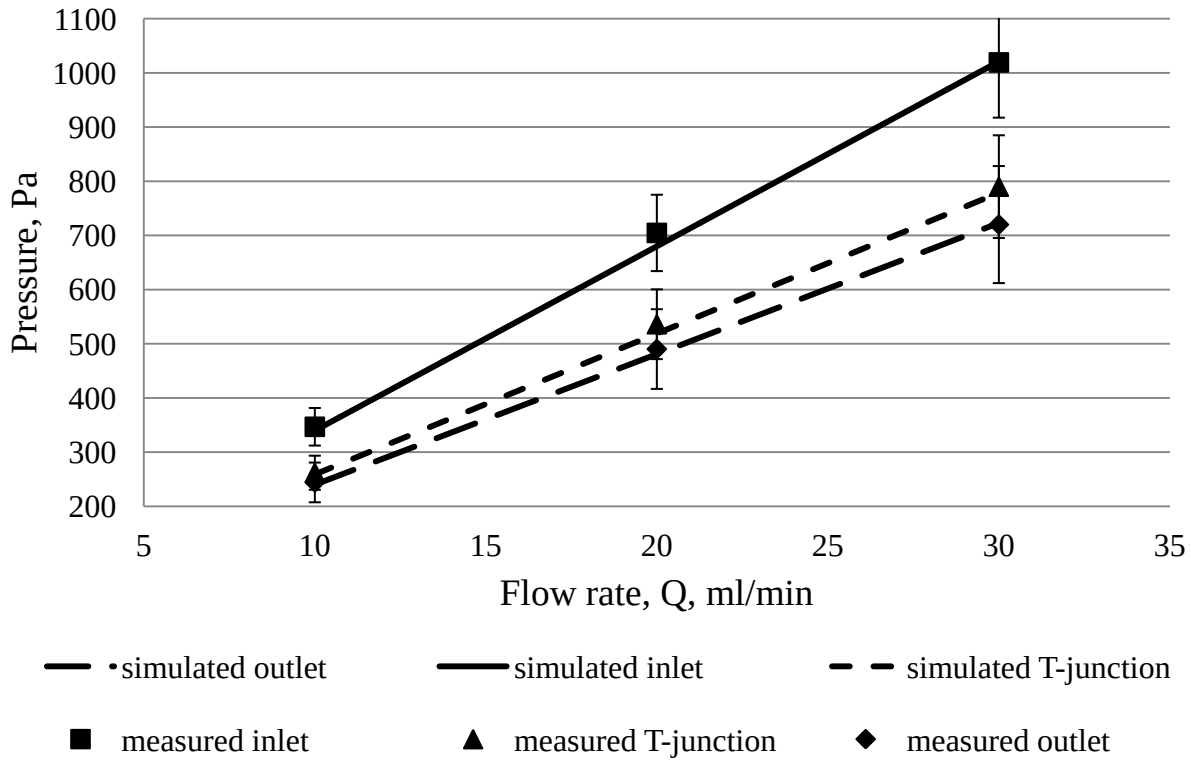

Figure 34. Pressure for glycerol/water solution at different flow rates.

In figure 34 results of the computer simulation and measurement of pressure for glycerol/water solution under different flow rates are shown.

Glycerol/water solution is a Newtonian fluid by its rheological characteristics, where viscosity is defined only by inertial processes when the stress applied, whilst for polymer solutions the viscosity is formed by viscous and elastic components and potentially could exhibit non-linear dynamic viscosity under the stress. The numerical pressure data for PAA100 and PAA300 liquids were simulated using an of Oldroyd-B viscoelastic model which was described in chapter 4.

Comparison of numerical and experimental data are presented in fig. 35. Input and constitutive parameters were obtained by rheological tests and pychometry (table 5) and are summed up in the table 6. As far as the global viscosity of polymer solutions consists of the viscosity of the polymer and of the viscosity of the solution (glycerol/water), the polymer viscosity was calculated by substruction of the viscosity of the solution from the global measured viscosity.

The relaxation time as a constitutive parameter is an intrinsic characteristic of a fluid that could vary across a broad range. For example, Lanzaro and Yuan, (2011) reported that for polyacrylamide solution the relaxation time, measured by small amplitude oscillatory shear, changed from 0.0027 ms to 83.93 ms. Traditionally, the biggest measured relaxation time is used for determination of the parameters of viscoelastic fluid flows. The biggest relaxation time measured for the fluids of interest is presented in Table 6.

Table 6. Input parameters of Oldroyd-B model

Liquids	Density, $kg \cdot m^3$ ρ	Relaxation time, s λ	Solution viscosity, Pa·s μ_s	Polymer viscosity, Pa·s μ_p
PAA100	$1.26 \cdot 10^3$	0.57	0.22	0.01
PAA300	$1.259 \cdot 10^3$	0.98	0.22	0.03

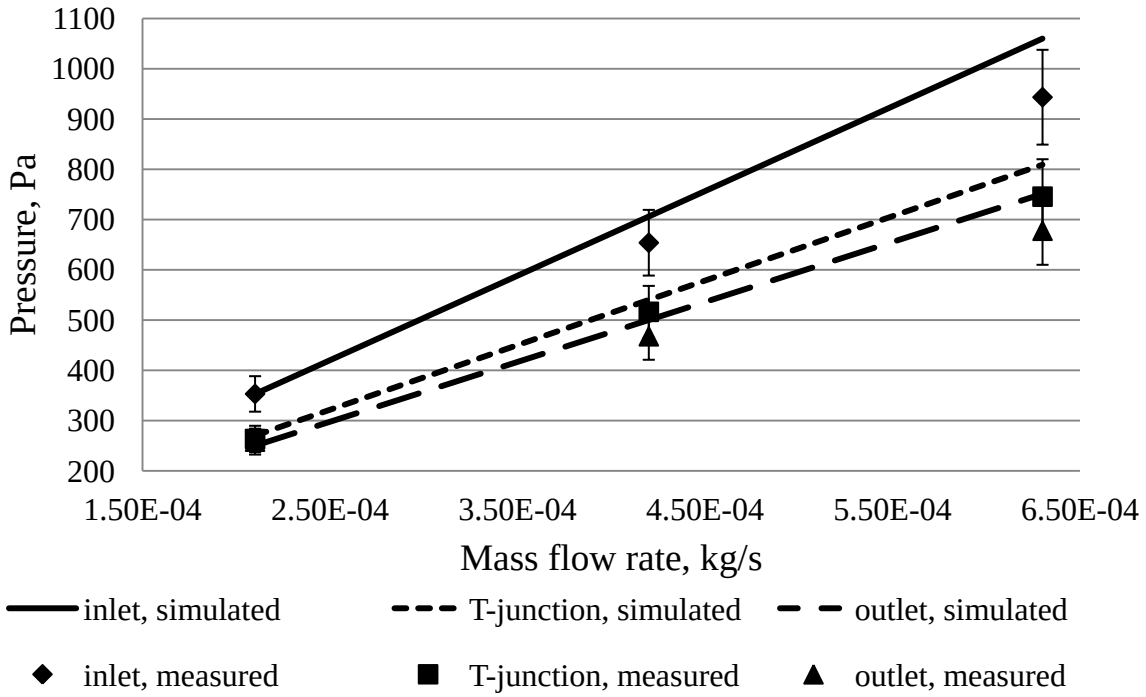

a

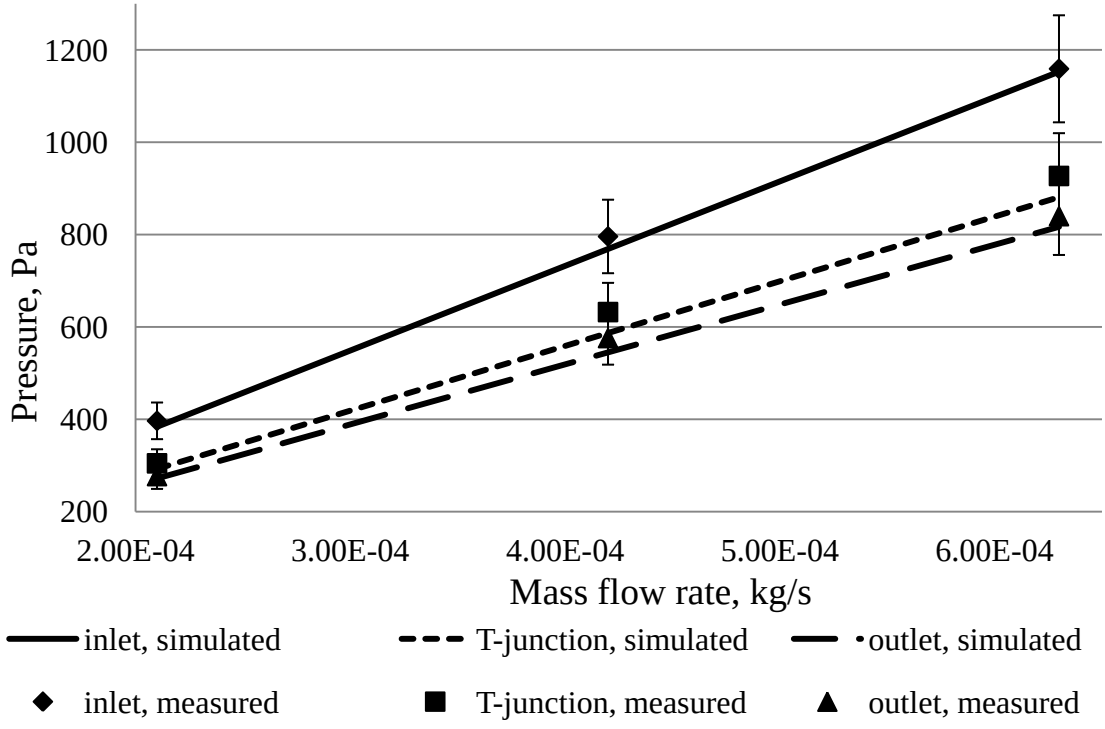

b

Figure 35. Simulated and average experimental data of pressure of the flow, measured at the inlet, T-junction and outlet, at different flow rates for PAA100 (a) and PAA300 (b).

In order to prove an applicability of the Oldroyd-B model for the inverse method the agreement between experimental results and numerical prediction should be analysed. The accuracy of the inverse method depends on both the precision of measurements and assumptions and simplifications of the model described in 6.2. The error accumulation could significantly affect the accuracy of the developed method. The agreement between the two sets of data could be defined by calculation of percentage deviation of numerical results from measurements.

Percentage deviation = ((experimental pressure - predicted pressure)/predicted pressure)·100%

The results of the deviation are presented in table 7.

Table 7. Percentage deviation of pressure for glycerol/water, PAA100 and PAA300 liquids, %

Sensor position	Glycerol/water			PAA100			PAA300		
	$2.1\cdot10^{-4}$ kg/s	$4.2\cdot10^{-4}$ kg/s	$6.3\cdot10^{-4}$ kg/s	$2.1\cdot10^{-4}$ kg/s	$4.2\cdot10^{-4}$ kg/s	$6.3\cdot10^{-4}$ kg/s	$2.1\cdot10^{-4}$ kg/s	$4.2\cdot10^{-4}$ kg/s	$6.3\cdot10^{-4}$ kg/s
Inlet	2.1	3.7	0.1	0.2	7.4	11.0	3.3	3.5	0.5
T-junction	1.2	3.3	1.4	2.5	4.4	7.8	4.0	7.7	5.2
Outlet	1.8	2.0	0.4	3.2	6.5	9.8	1.8	5.7	2.8

Closer inspection of table 7 revealed the following:

- on average, the closest agreement between model prediction and measurements was found for Newtonian fluid (glycerol/water), the highest deviation was 3.7%;

- the highest percentage deviation was demonstrated by PAA100, viscoelastic Boger fluid, increasing with growth of the mass flow rate;

- for higher concentration of polyacrylamide the percentage deviation fluctuated from 0.5% to 7.7% and did not show dependence on the mass flow rate;

- for all liquids tested under different mass flow rates the deviation did not exceed 10%, with one exception (11% for PAA100, inlet sensor), and did not demonstrate the impact of either mass flow rate or pressure sensor positioning.

Significantly, the higher percentage deviation of pressure field data for PAA100 liquid could not been explained by the fluctuation of conditions of the experiment because each flow

regime for each tested liquid was repeated at least 3 times, and then the average value of the registered pressure was calculated. However, accuracy of the numerical simulation depends on input parameters and stabilisation mechanisms built into the algorithm. Nevertheless, the higher percentage deviation for PAA100 in comparison with two other liquids is low enough to be sufficient for numerical prediction of pressure field with an acceptable degree of accuracy. Exhibited deviation of measured pressure from simulated values could be explained by an inadequacy of the model to the real physics processes in viscoelastic flows.

In conclusion, analysis of the percentage deviation demonstrates good agreement between predicted and measured pressure, thus the Oldroyd-B model is valid for the purposes of the research.

6.4. Velocity profile measurements

Experimental and analytical results for characterisation of the velocity field are compared in order to prove applicability of the capacitance method of the velocity measurements for the viscoelastic fluid flow under the stress applied, described in the section 2.7.1.

6.4.1. Experimental capacitance data analysis

A picture of the electrodes of the capacitors is presented in fig. 26. Pulsing laminar flows of two types were generated: short pulse and long pulse (fig. 33 (b, c)). Flow wave propagation was determined between each possible combination of couples of the sensors. The results were analyzed using a cross-correlation technique (5.6). The different types of pulsed flows formed the basis of the physical processes of mass and momentum transfer. The aim of the velocity study was to measure the time delay between the electrical signals detected between adjacent sensors. For each liquid from 5 to 15 pulses were applied and then the mean value and deviation were calculated. The results are presented in table 8.

Table 8. Time delay of the wave propagation, s

Glycerol/water		PAA100		PAA300	
Short pulse	Long pulse	Short pulse	Long pulse	Short pulse	Long pulse
0.3	2.4	6	n/a	n/a	n/a

The capacitance tests revealed significant difference in fluid behaviour under voltage and pulsing pressure applied. The Newtonian liquid (glycerol/water) exhibited a clear and distinguished response on the electrodes of the capacitance sensors corresponding to each pulse, either short or long. Adding of the polymer to the solution changes electrical properties of test fluids. For both Boger fluids only the very first pulses were observed (fig. 36). This could be explained by the microstructure of the liquids. Glycerol/water liquid contains dipoles of water molecules, which results in considerable conductivity of matter between the electrodes of the capacitors. Adding a small quantity of a long chain polymer to the solver changes dielectric properties of Boger liquids, decreasing elecrocondactivity of a fluid.

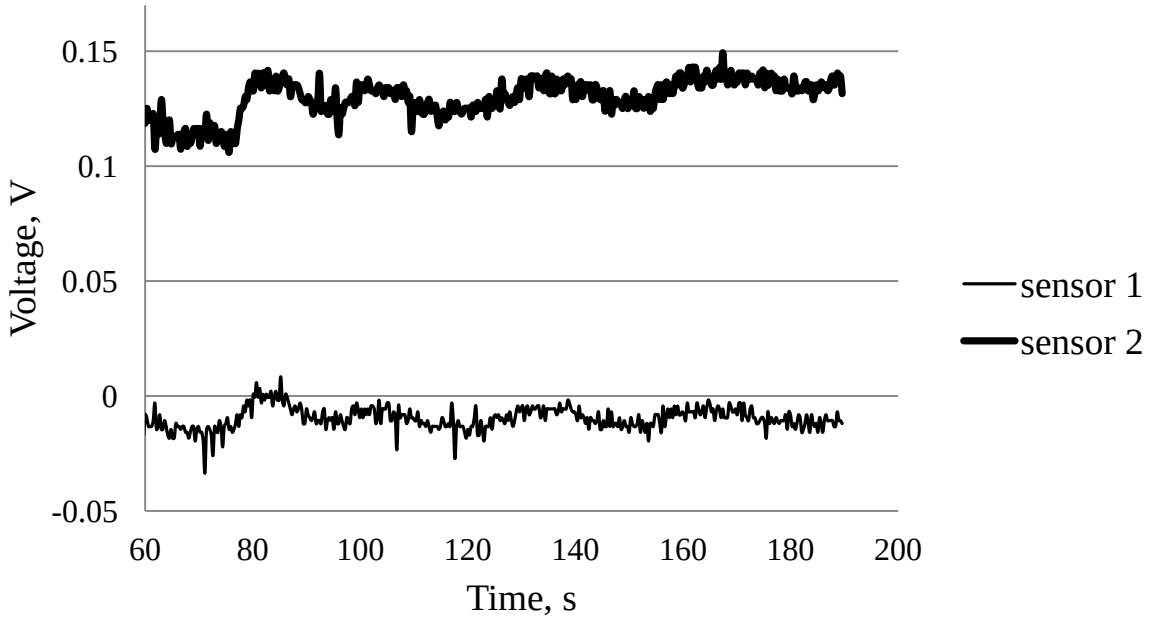

a

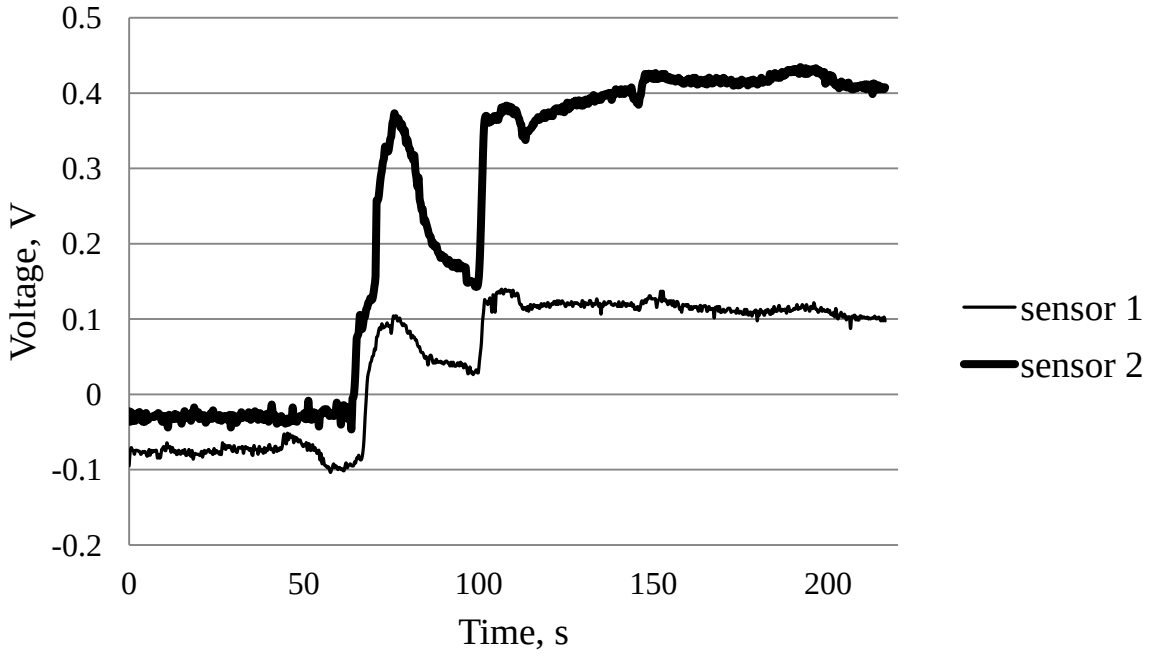

b

Figure 36. Voltage magnitude of pulsing flow for PAA100 (a) and PAA300 (b).

Velocity of the wave propagation could be calculated analytically:

$$v=\Delta L/\Delta t, \quad (6.1)$$

where ΔL - the distance between two neighbouring capacitance sensors, Δt - the time of wave propagation.

Knowing the distance between sensors, equal to 5×10^{-3} m, and based on the pulse propagation time delay, shown in the table 8, it was possible to calculate the velocity of the signal for glycerol/water and PAA100 liquids (6.1):

$v_{glycerol/water} = 1.7\times10^{-2}$ m·s^{-1},

$v_{PAA100} = 8.3\times10^{-4}$ m·s^{-1}.

The difference of the velocity magnitude could be explained by elastic effects arising from the nature of polymer solutions, which led to a retardation in wave propagation.

6.4.2. Numerical simulation of pulsating flow

Principles for simulation of transient flow were described in chapter 4.2.3. A Gaussian function for an input flow modification was implemented to model the flow pulse of Newtonian and PAA100 liquids. Pulsating fluid flow for PAA300 sample was not simulated because a capacitance measurements of the velocity field of the flow did not provide meaningful data to compare with numerical results.

Results of computer simulations for the two above mentioned liquids are presented in fig. 37. The velocity magnitude was evaluated at points corresponding to the configuration of the capacitance sensors, shown in fig. 33 (a).

No time delay was found for either liquid. This could be explained by the fluid properties, which were described by the Oldroyd-B model. In this model the pressure driven flow of incompressible liquid was simulated, assuming that dynamic processes do not affect density of the liquid. In fluids with constant density pulsating flow propagates with the speed of sound in the media, thus for the glycerol/water mixture of the same composition this value is equal to 1578 $m \cdot s^{-1}$ (http://www.rshydro.co.uk/sound-speeds/). Knowing the distance between the sensors, the analytically calculated time of wave propagation is equal to 3×10^{-6} s, less than a time step in a model and data acquisition rate, so the analytical solution and the model prediction results show a negligible time delay in signal transfer, whilst the time of a pulse propagation is readily measurable. Thus a discrepancy revealed between measurement and simulation results. To solve this problem, modification of the T-ometer construction should be carried out, with capacitance sensors spaced further apart.

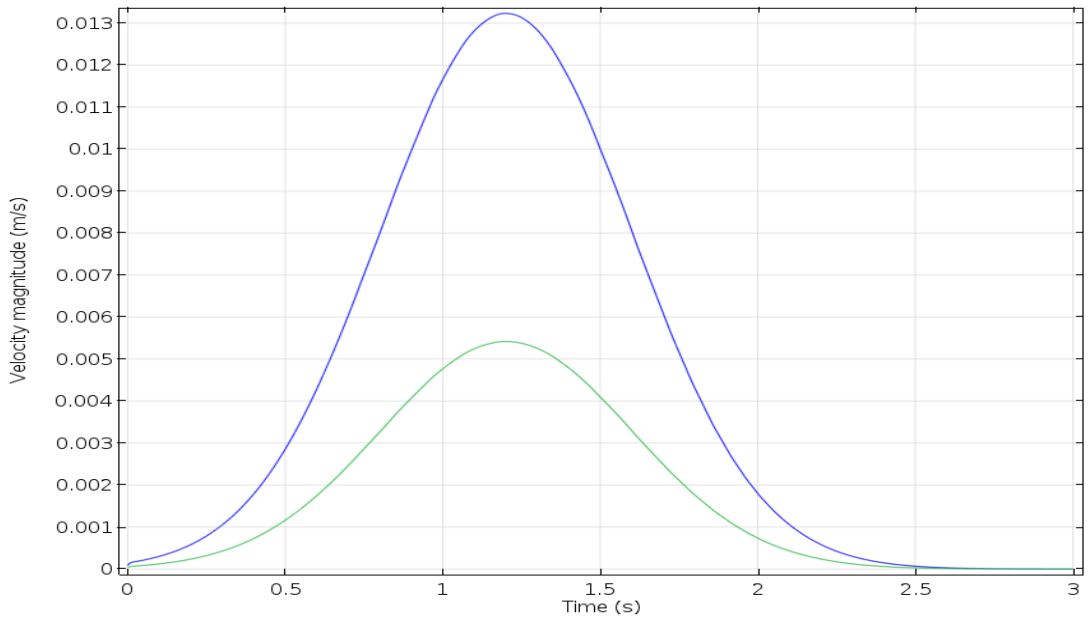

a

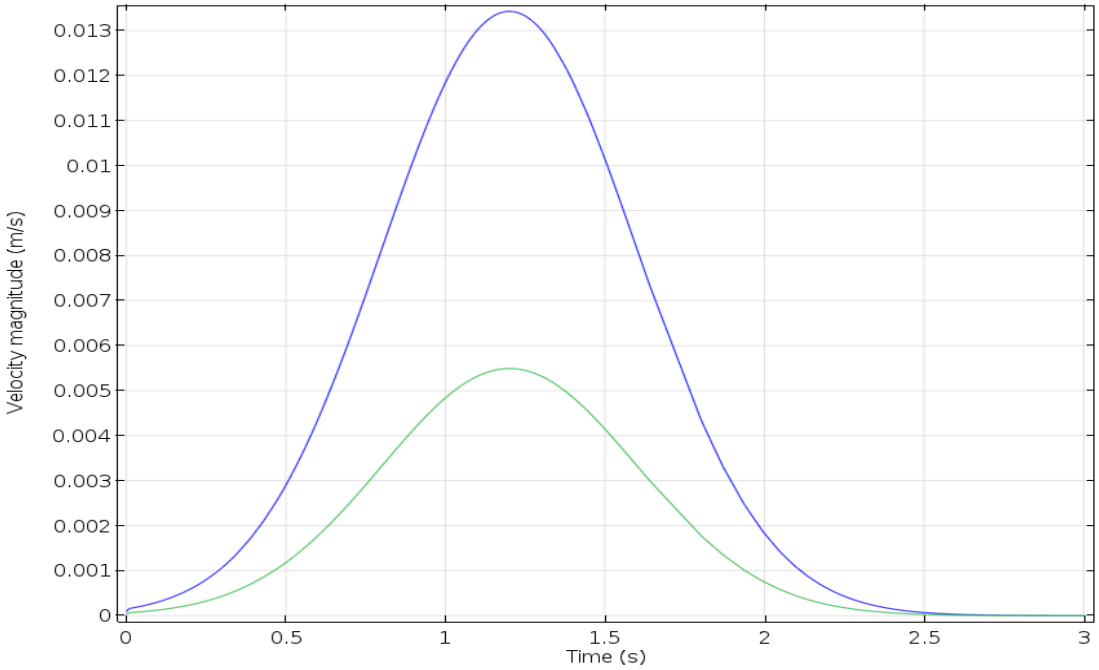

b

Figure 37. Velocity magnitude along the time range for two capacitance sensors, the green signal belongs to the sensor, situated downstream to the sensor with the blue signal. Glycerol/water - (a), PAA100 - (b).

Controversy of a model approach and experimental data is a widely discussed problem in rheology. It could be explained by the fact that physical processes in viscoelastic fluids are not so trivial. Suddenly accelerated flow response consists of two components: transfer of momentum and transfer of mass. Depending on conditions of the pulse, impact of either component could prevail over the other, and mass transfer could cause a time delay of voltage response due to a change of dielectric properties of media between electrodes of a capacitor.

In order to achieve better accuracy and predictability of the inverse procedure further development of the CFD simulation is needed that includes molecular and bulk phenomena in a single model.

6.5. Inverse problem discussion

An inverse method approach to the determination of constitutive parameters of viscoelastic fluids through the measurement of global statistics of a pressure driven flow was described in chapter 3. Stagnation point flows cause the change of flow velocity in the vicinity of the stagnation point, thus generating a range of extension rates along the channel. To construct the system, being able to define extensional properties, inferred from flow fields, it is essential that global parameters are sensitive to elastic parameters of Oldroyd-B model, taking into account that shear constitutive parameters are constant (viscosity). Another necessary condition for mapping of global physics to parameters of interest is the uniqueness of matching flow parameters to extensional parameters. Accuracy of the method is also dependent on error propagation arising from measurement error and deviation of model predictions from experimental data.

6.5.1. Uniqueness and sensitivity investigation

As was described in chapter 2, it is not possible to measure directly parameters of interest in complicated industrial, natural and scientific processes. It is often the case that it is possible to derive sought parameters from readily measured ones. This is possible only if two sets of parameters (measurable and of interest) are mathematically related to each other. The first step is to check sensitivity, in other words, to study whether change of one parameter causes statistically significant change in another.

Consider the cross-coupling "pressure-relaxation time" computer simulation with dimensionless Weissenberg number (*Wi*) as an input parameter was used for prediction of pressure as a shear response of the flow:

$$Wi=\lambda\dot{\gamma} \tag{6.2}$$

A range of *Wi* value was chosen to cover an appropriate range of a relaxation time and then discretised to build a foundation for one-to-one mapping between the parameters to infer. The previously validated Oldroyd-B model was implemented to find out corresponding values, so that $\delta Wi=f(\delta P)$. The Weissenberg number varied in the range

$$0<Wi<0.5.$$

The relaxation time, corresponding to the definition *Wi*, is different for different sensor positions, because *Wi* depends on shear rate, and the latter is dependent on the velocity and geometry of the channel. Thus the same relaxation time gives different *Wi* values according to the key parameters of the flow.

Numerical results of CFD are presented in fig. 38. A parametric sweep solver was used to investigate the dependence of pressure as a global parameter on the extensional constitutive parameter, the Weissenberg number. The Weissenberg number range applied in the model was transformed to give a relaxation time range. The average pressure at the location of each pressure sensor was predicted and then plotted against relaxation time.

First of all, the data obtained provides the necessary information for assessing the feasibility of the inverse procedure for pressure/relaxation time coupling. For all three sensors pressure exhibited sensitivity to the extension constitutive parameter. All three curves obtained demonstrated continuity, which is the one of necessary conditions of invertibility. At the same time, the condition of uniqueness is correct only for pressure gauges situated at the T-junction and the outlet of the channel. This finding could be explained by the conclusion made previously in research papers studying pressure driven flow in T-shaped channels (Craven, Rees and Zimmerman, 2010), (Bandulasena, William and Julia, 2011): the most information rich regions in a T-shaped channel are in the vicinity of the stagnation point and along the back wall of the channel, where extensional forces are presented in a wide range.

Considering only numerical predictions for two downstream sensors, it should be noted that whilst the range of relaxation times varies in order of magnitude, for pressure variability this

amounts to 1% and less than 1 Pa, which is under the sensitivity limit of the pressure sensors. Thus this aspect questions the possibility of using the rheometer investigated for the stated objections - determination of extensional constitutive parameter. Nevertheless, this problem could be overcomed with the fitting of the parameters of the channel and flow conditions.

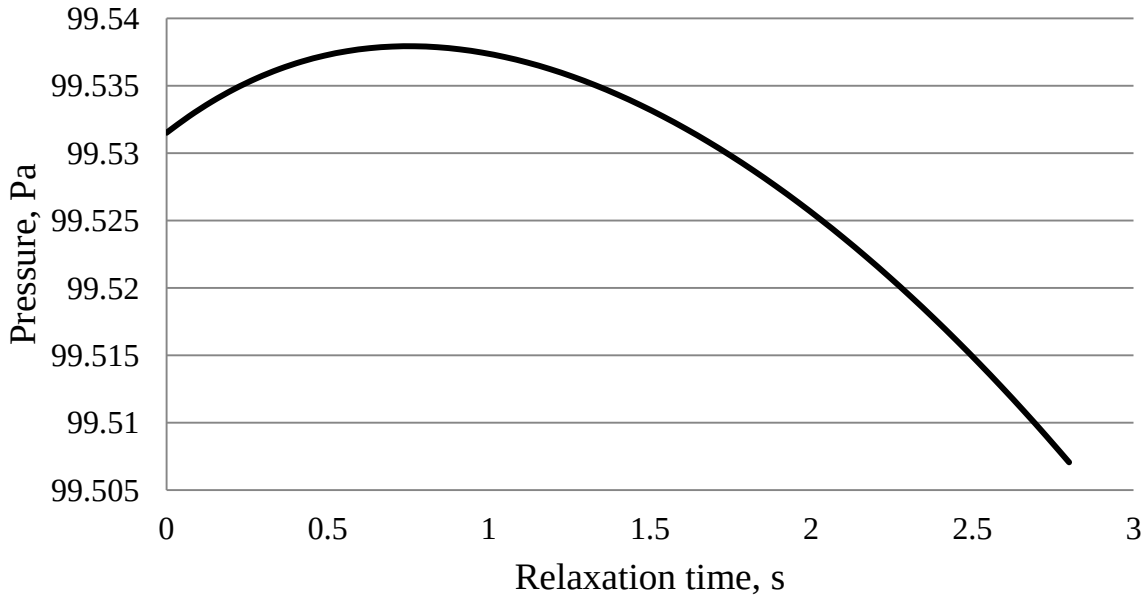

a

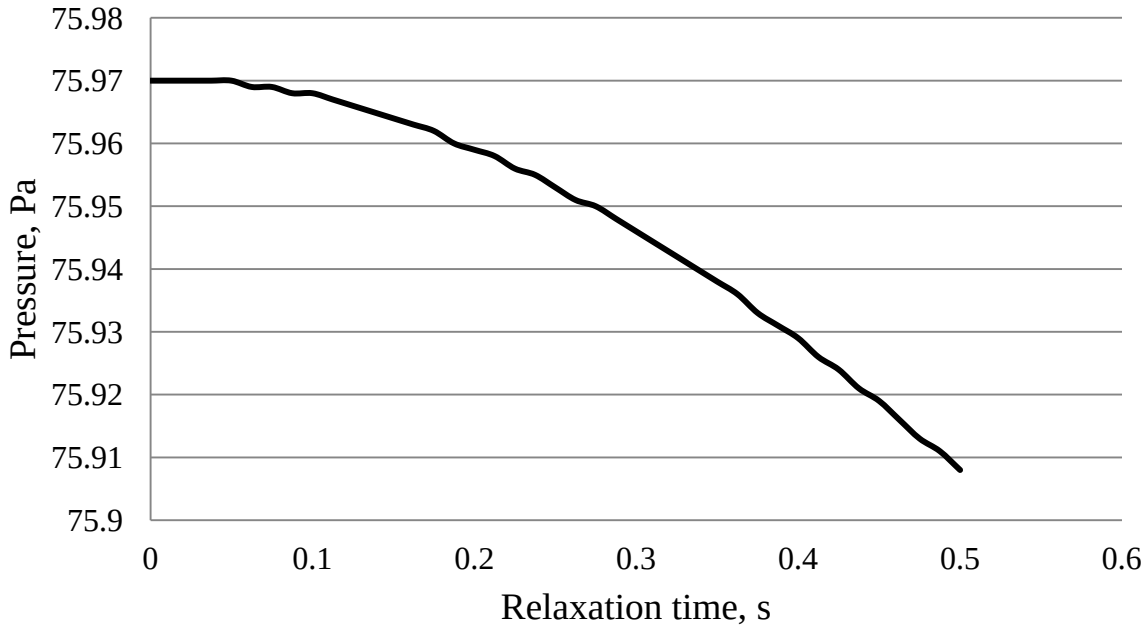

b

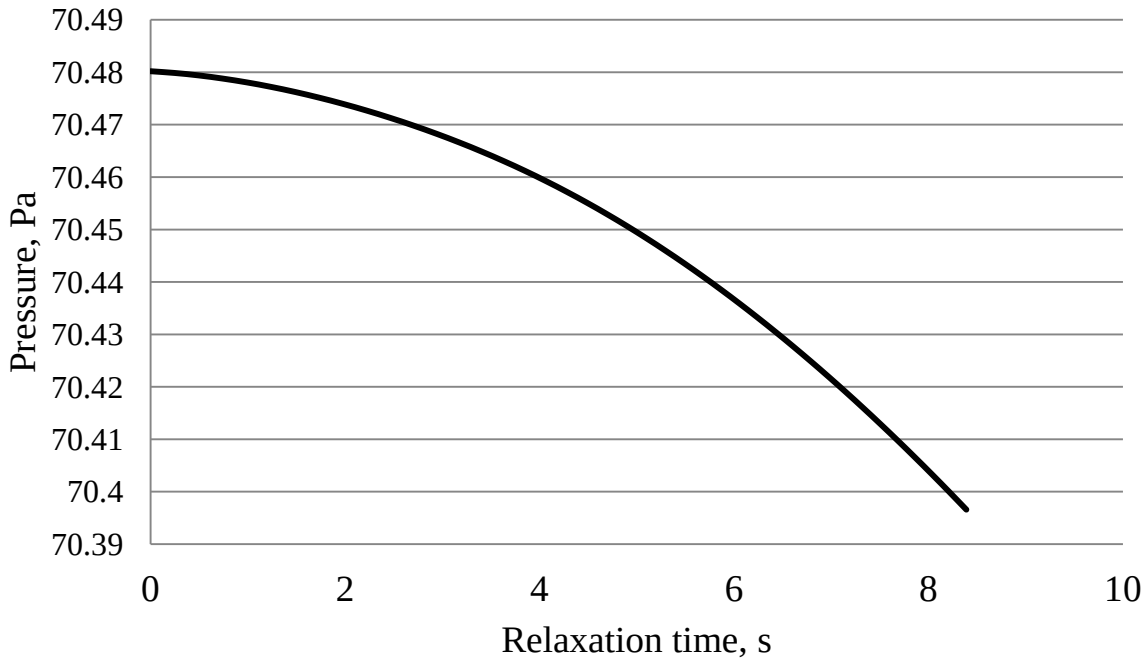

c

Figure 38. Simulated data of pressure at inlet (a), T-junction (b) and outlet (c) pressure sensors plotted against relaxation time.

All capacitance sensors for velocity measurements are situated in T-junction area (fig. 33 (a)), close to each other, so no discrepancy was observed between velocity patterns. The curve representing numerical prediction of velocity variation as a response to *Wi* parametrical sweep is shown in fig. 39.

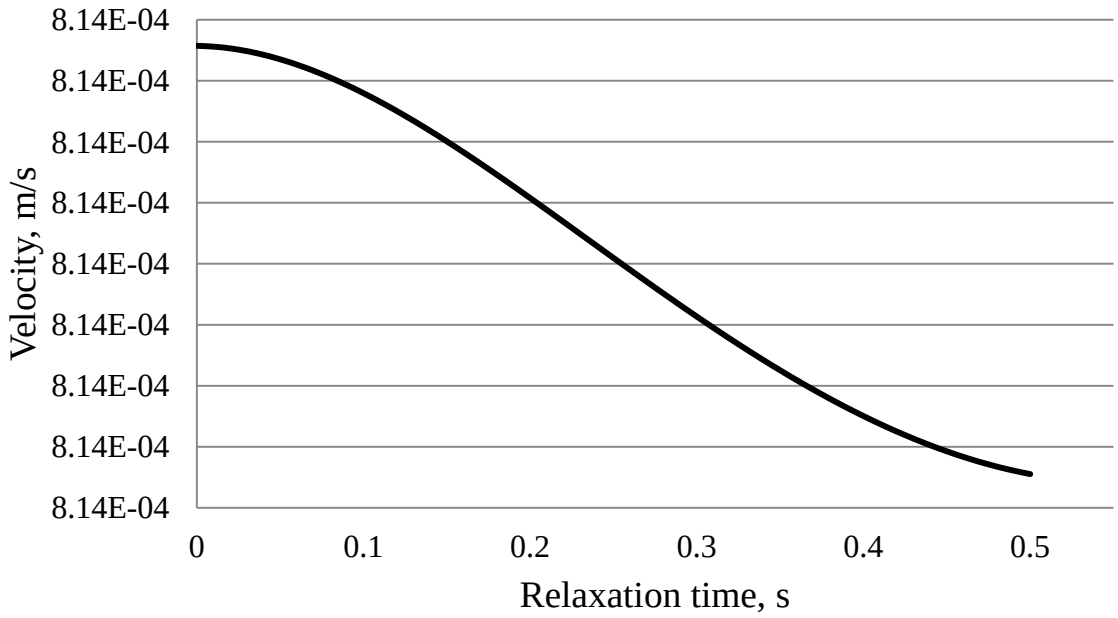

Figure 39. Velocity magnitude, predicted based on relaxation time variation.

The graph, which represents the dependence of the velocity on the relaxation time, demonstrates continuity and uniqueness. As in the case of pressure/relaxation time coupling, there is a clear mathematical relationship between velocity and relaxation time, but the $\delta v=2\times10^{-8}$ m/s, which is literally constant in real experiments and sensitivity of capacity sensors.

6.5.2. Graphical mapping of parameters to infer

It might be possible to modify the T-ometer to make global statistics more sensitive to the extensional constitutive parameter, relaxation time. To investigate the uniqueness and dependence of pressure and velocity profiles on the dimensionless Weissenberg number, a 3D plot was built using MATLAB. The relationship of pressure, velocity and Weissenberg number is presented in fig. 40 Wi varies from 0 to 0.5 with a constant step size $\delta Wi=0.0125$.

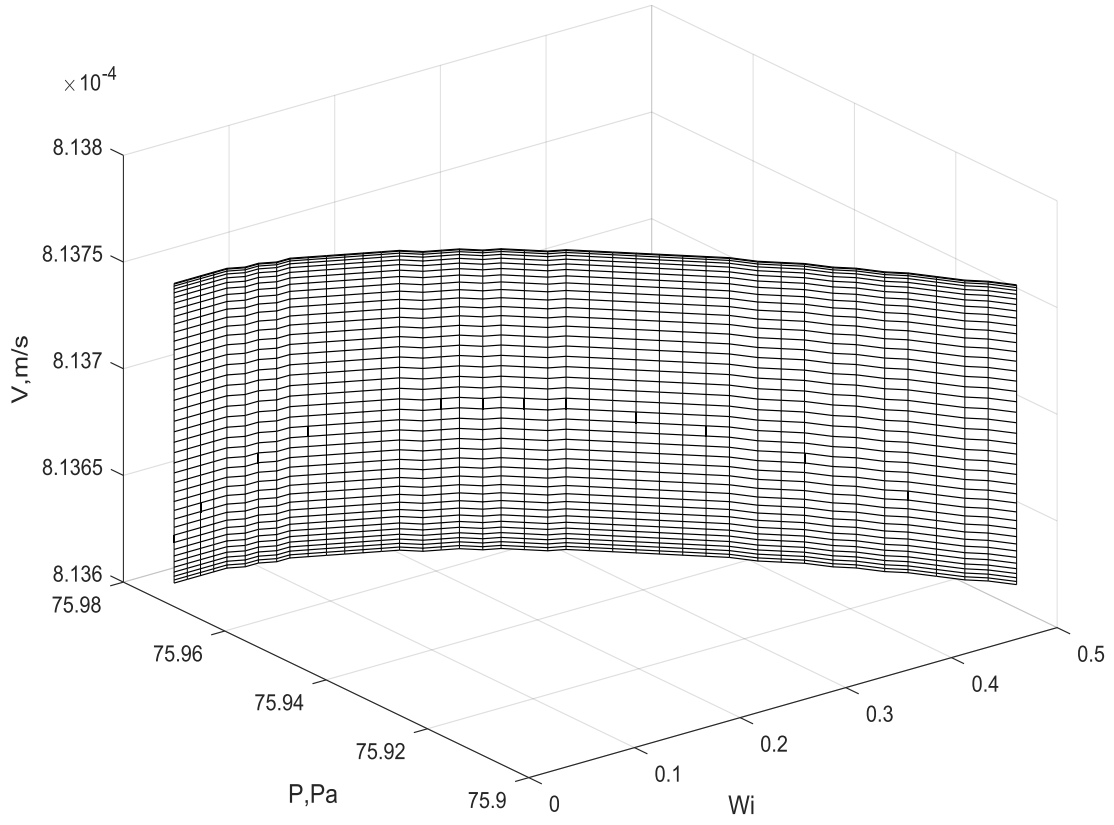

Figure 40. Graphical presentation of Weissenberg number as a dimensionless derivative of the relaxation time and pressure and velocity numerical prediction values.

The resulting surface does not intersect itself on the entire range of all three parameters, which means that the extensional constitutive parameter could be determined from measured global statistics. In addition, it could be seen that either pressure or velocity are less sensitive at the beginning and the end of the *Wi* range, nevertheless, dependent functions could be ascertained from computer simulation results.

6.5.3. Development of inverse procedure

The inverse function theorem described in chapter 3, states that to be inverted a function must match the criteria of det J≠0 (3.5). From fig. 39 - 40 it is clear that either

$\frac{\partial P}{\partial \lambda} \neq 0$ and $\frac{\partial V}{\partial \lambda} \neq 0$,

because the curves did not reveal zero gradient regions along the given range of the Weissenberg number.

Hence, in order to find inverse functions for constitutive parameters of Boger fluid, initially, curves

p=$p(Wi)$ and $v=v(Wi)$

should be fitted.

Consider the cross-coupling "pressure-relaxation time", computer simulation with dimensionless Weissenberg number (*Wi*) as an input parameter was used for prediction of pressure as a shear response of the flow.

Since *Wi* is dimensionless parameter, inversion is possible only if the dependent parameters have similar dimension, in that case dimensionless. Thus, the forward problem is the function relationship between *Wi* and ratio of pressure difference:

$$\frac{P_{inlet}-P_{T-junction}}{P_{T-junction}-P_{outlet}} = f(Wi) \qquad (6.3).$$

Let the ratio of the pressure difference be P_{dif}. The simulated relationship of the pressure difference ratio is presented in fig. 41.

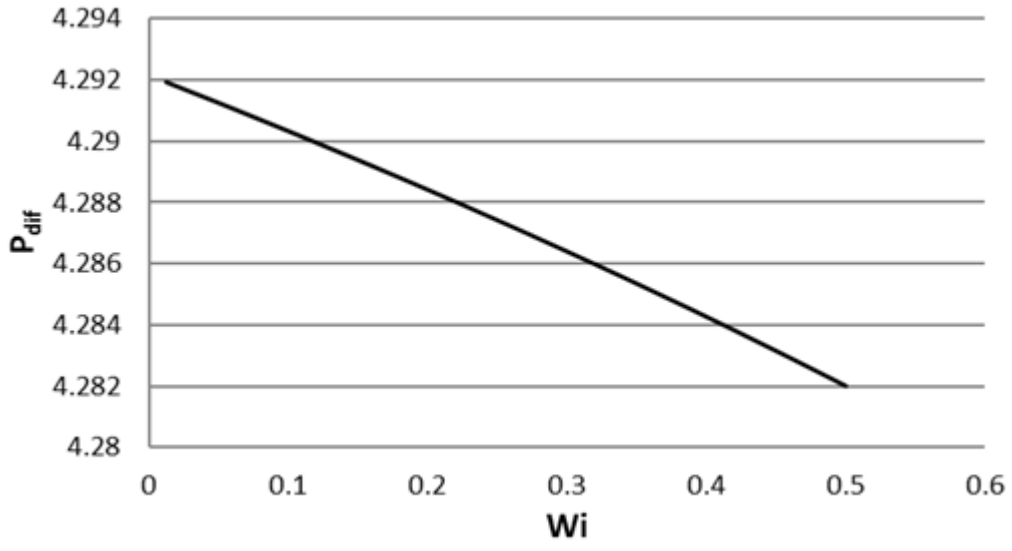

Figure 41. Dependence of the ratio of simulated pressure difference on *Wi*.

The inverse function theorem states that to be inverted a function must match the criteria of

det J≠0. From fig. 41 it is clear that

$\frac{\partial P_{dif}}{\partial Wi} \neq 0$,

because the curve did not reveal zero gradient regions across the given range of the Weissenberg number. Also the conditions of uniqueness and continuity have been fulfilled.

6.5.4. Invertibility investigation

Hence, as inversion functions were determined, the next step of the inverse procedure would be the investigation of an accuracy and feasibility of calculation of the constitutive parameter (relaxation time) by using global statistics of the rheological response of viscoelastic fluid under the stress applied.

Two curves were fitted to describe relationship between the pressure difference and Weissenberg number attributed to test liquids PAA100 and PAA300. For either function R squared was equal to 0.99, which indicated high level of accuracy. Inverse functions f^{-1} to find *Wi* from pressure filed for PAA100 and PAA300 were as follows:

$$Wi'_{PAA100} = \frac{2.6674 \pm \sqrt{-2.6674^2 - 4 \cdot 0.9728 \cdot (5.3543 - P_{dif})}}{2 \cdot 0.9728} \quad (6.4)$$

$$Wi'_{PAA300} = \frac{0.3787 \pm \sqrt{-0.3787^2 - 4 \cdot 0.0858 \cdot (4.6221 - P_{dif})}}{2 \cdot 0.0858} \quad (6.5)$$

Results obtained from the Oldroyd-B model inverse functions f^{-1} for PAA100 and PAA300 (6.4) and (6.5) were used to reconstruct the extensional constitutive parameters *Wi'* of a non-Newtonian liquids from the pressure flow field. The values obtained were compared with an initial *Wi* of corresponding to the test liquids. The relative deviation of the given *Wi* from *Wi*' obtained using the inverse function $Wi' = f^{-1}(P_{dif})$ was increasing whilst *Wi* decreased, nevertheless, the average *Wi* deviation is equal to 5.25%. The maximum value of deviation was 83%.

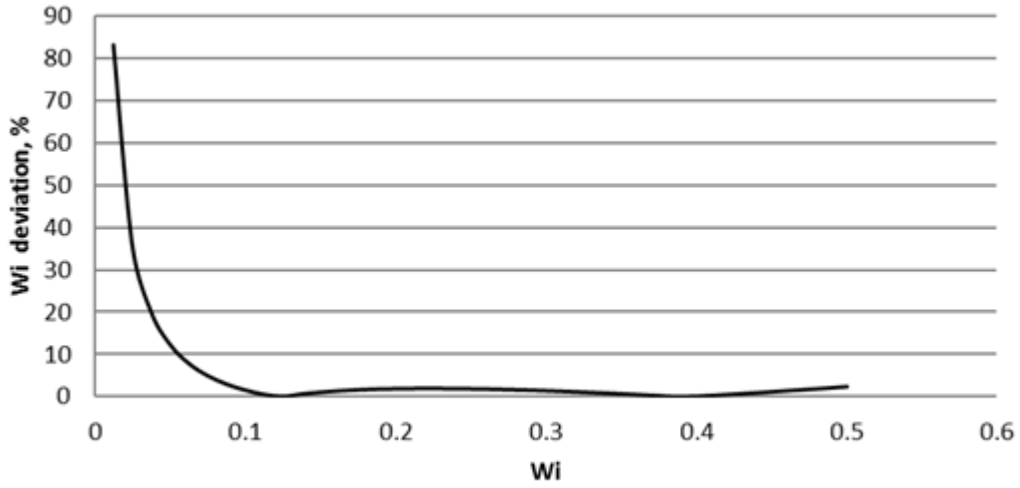

Figure 42. Relative deviation of initial *Wi* from inverted *Wi'* dependent on given *Wi* range.

The reconstructed relaxation time for PAA100 and PAA300 liquids was calculated from *Wi'* by dividing by the shear rate. The reconstructed relaxation time is shown in fig. 43. The graph for both PAA100 and PAA300 are not linear, this could be explain by the fact that inverse functions do not describe the dependence of relaxation time on pressure difference ratio with appropriate level of accuracy.

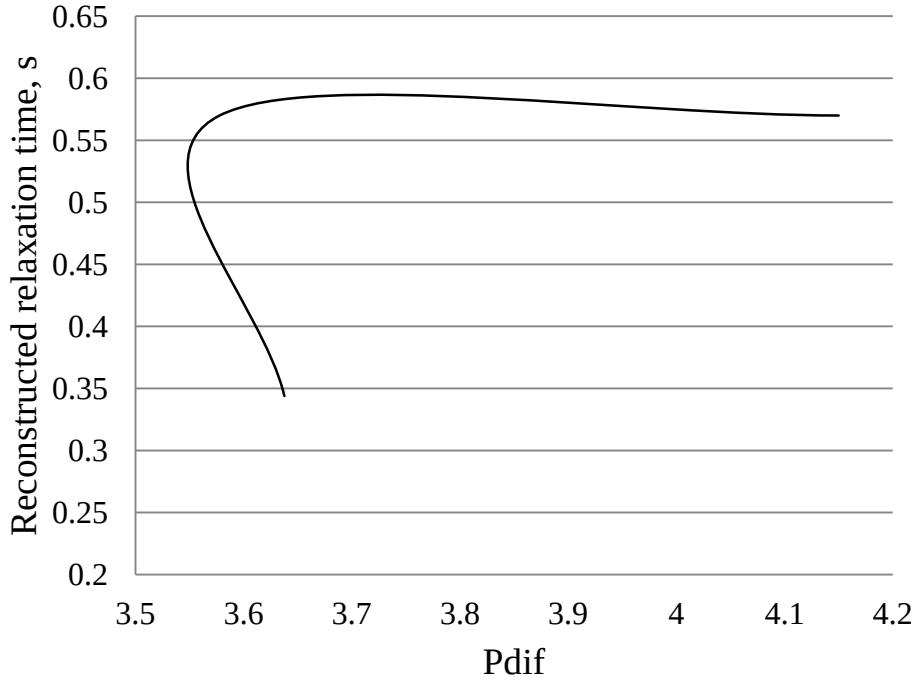

a

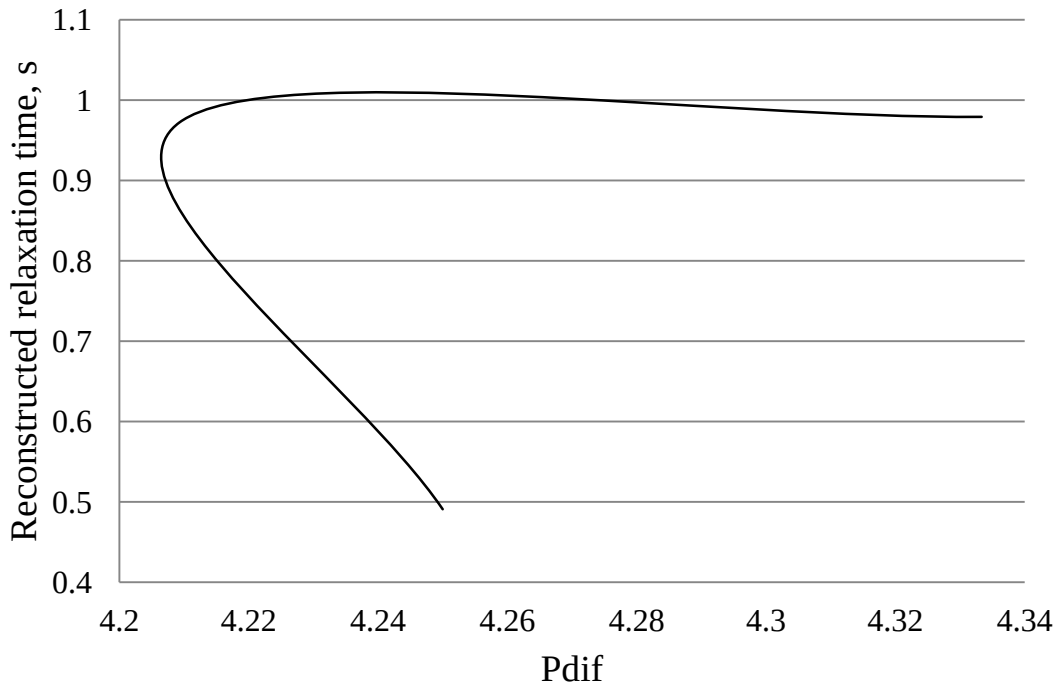

b

Figure 43. Dependence of the reconstructed relaxation time on the pressure difference ratio: PAA100 (a), PAA300 (b)

The relative deviation of the measured relaxation time from the reconstructed relaxation time is presented in the table 9.

Table 9. Relative deviation of the measured relaxation time from the reconstructed relaxation time.

Q, kg·s^{-1}	Relative deviation, %	
	PAA100	PAA300
2.1e-4	0.006	0.081
4.2e-4	0.012	0.79
6.3e-4	39.65	49.91

For both viscoelastic liquids, the reconstructed and measured relaxation times are in good agreement for low and moderate mass flow rates, whilst for the large mass flow rates the

deviation of the inverted value of the relaxation time demonstrates such a significant discrepancy that it makes it impossible to use the inverse approach to calculate extensional constitutive parameter of viscoelastic liquids from the global physics of the stagnation point flow. This problem can arise from two sources: shortcomings of the configuration of the T-shaped rheometer and accuracy of the Oldroyd-B model at relatively high mass flow rates.

The velocity field may possibly be used for the definition of the relaxation time if the problem of adequate computer simulation is resolved. Also selection of viscoelstic liquids with more expressed electro-kinetic properties would be of great help. Another possible way to improve the velocity field determination can be reached through the development of capacitance sensors configuration, making them more sensitive and increasing the distance between them.

Chapter 7: Conclusions and future work

7.1. Conclusions

The aim of this project was to develop a T-shaped stagnation point rheometer with an incorporated system of imbedded sensors, which enables measurement of the velocity and the pressure fields of a pressure driven viscoelastic flow. The research was carried out as follows: firstly the system was modeled using a CFD simulation and then various experiments were carried out to evaluate the feasibility of the use an inverse method for mapping the constitutive parameters of viscoelastic fluids from global statistics in a single experiment. In the present study the stagnation point flow of fluids with constant shear viscosity and high elastic component, known as a Boger fluid, was investigated.

The inverse method allows finding the parameters of interest, which typically are not easily measured due to either not using an appropriate experimental procedure or due to complexity of the processes involved. In the case of non-Newtonian fluids, the definition of the eminent characteristics of the viscoelastic fluids, such as constitutive parameters describing the dynamic and the extensional viscosities, consists of finding a master curve for the liquid of interest. It involves off-line testing at different flow conditions and could be time consuming. Whereas, in contrast, a stagnation point flow simultaneously generates a range of shear rate values from a single experiment, where the contributions of global physical parameters are evaluated. This could be used to define the constitutive parameters of the test liquids from the on-line and in-line measurement approaches.

A numerical finite element scheme for the thermodynamic processes was implemented to develop heat transfer within the T-junction device to provide the control over temperature during the experiments. Due to the high sensitivity of the physical parameters of the viscoelastic fluids to the temperature it is crucial to evaluate the low temperature gradient along the channel. A 3D numerical model simulating the temperature distribution in the prototype rheometer was developed using the COMSOL 4.3b software, implementing "Heat transfer in solids" module. A finite element scheme was used to predict the temperature field for a copper plate, which had multiple embedded aluminium cylindrical electrodes arranged in several different combinations. An external heating plate with the channels for heating elements was chosen as an optimal method for temperature control along the channel.

When designing the rheometer computational model proved to be beneficial as it helped to understand the underlying physical processes thus making it possible to perform temperature and parametric control of an experiment.

The inverse methodology used to define the elastic constitutive parameters of complex fluids was tested on one Newtonian fluid (glycerol/water mixture) and two polyacrylamide Boger fluids with the same shear viscosity and concentrations of the polymer of 100 ppm and 300 ppm. All three test fluids were tested using conventional rheometers, and parameters obtained were used for the Oldroyd-B model validation. The model was developed in COMSOL 5.2a software, using the "Laminar flow" module for the Newtonian fluid and "General form of PDE" module for the Boger fluids. The discrepancy between the measured data and the simulation results did not exceed 5%, thus it was accepted that the model was validated.

The pressure sensor system was used to define the pressure field across the channel. Several flow regimes were created under the controlled flow rate condition, whereas the computer simulation was implemented across the wide range of the relaxation time corresponding to the *Wi,* ranging from 0 to 0.5. The percentage deviation analysis of the measured and simulated pressure demonstrated that the two values were in good agreement with each other. The Boger fluid with the polymer concentration of 100 ppm exhibited the higher percentage deviation than the two other tested fluids, though the deviation was low enough to be sufficient for the numerical prediction of the pressure field to an acceptable degree of accuracy.

The velocity field investigation showed that it was possible to obtain the explicit results of measurements of the pulsing flow only for the Newtonian fluid, whilst for the Boger fluids the results were non-conclusive and therefore could not be used for the purpose of this research. The cross-correlation analysis of the response on the electrodes of the capacitance sensors revealed that the time delay of the electric signal propagation varied from 0.3 to 2.4 s, which was not predicted by either the analytical or the numerical results. The computer simulation of the pulsing flow conditions demonstrated zero time delay in the wave propagation from one capacitance sensor to another. Thus the use of the velocity field for the prediction of the relaxation time of viscoelastic fluids needs further investigation.

Inversion of readily measured pressure statistics into the relaxation time for both Boger fluids was in a good agreement with the measured relaxation time for low and moderate mass flow rates. For the large mass flow rates the deviation of the inverted value of the relaxation time

demonstrated such a significant discrepancy that it made it impossible to use the inverse approach to calculate the extensional constitutive parameter of the viscoelastic liquids from the global physics of the stagnation point flow.

This research demonstrated how the inverse approach was combined with the stagnation point channel to develop a system which could allow to reconstruct the extensional constitutive parameters of Boger fluids in the single experiment. For this purpose a new device was developed, which had the pressure and capacitance sensors to measure the pressure and the global velocity statistics of the pressure driven viscoelastic flow. The optimisation of the T-shaped rheometer was carried out using a model of thermo-dynamic conductivity to define the heat distribution along the channel. The forward problem was solved by using the Oldroyd-B model for steady state and pulsing flows. The results of the simulation were in a good agreement with the measured data. Numerous detailed investigations demonstrated promising results for the reconstruction of the relaxation time of the viscoelastic fluids from the pressure flow field for a wide range of *Wi*. The pulsing flow experiments for the velocity field determination and the experiments with the high flow rate revealed several shortcoming of the new T-shaped rheometer when used in combination with the inverse method. These flaws should be addressed in the future work.

7.2. Future work

Further investigations should be focused on two directions: the improvement of the construction of the T-shaped rheometer and the development of an appropriate pulsing flow model, which would correctly describe the mass and momentum transfer. A more precise development of the modelling of the viscoelastic stagnation point flow could improve the outcome of the inverse method for the rheometric system for the characterisation of non-Newtonian liquids.

The prototype development should include adjustment of the measurement system. Firstly, the usage of more precise miniature pressure transducers with a small footprints could increase the accuracy of the measurements of the pressure drop along the T-shaped channel.

The capacitance measuring system could benefit from a different capacitance sensors configuration: two parallel electrodes provide higher density of electromagnetic field and, as a consequence, a higher sensitivity of the sensors. In addition, increasing the distance between sensors will increase the wave propagation time and will permit to obtain more

meaningful measurements, highlighting the contrast in the propagation times. Although the most information rich region in T-shaped channel is situated in the vicinity of the stagnation point, placing the sensors at the input and both outputs of the channel is of potential interest, what will increase the distance between the capacitance sensors.

These further improvements would permit to overcome the revealed shortcomings of the measurement system for the characterisation of the viscoelastic fluids based on the usage T-shaped channel rheometer and the inverse approach.

References

Aboubacar, M., Matallah, H. and Webster, M. F. (2002) 'Highly elastic solutions for Oldroyd-B and Phan-Thien/Tanner fluids with a finite volume/element method: Planar contraction flows', *Journal of Non-Newtonian Fluid Mechanics*. Elsevier, 103(1), pp. 65–103. doi: 10.1016/S0377-0257(01)00164-1.

Adachi, T. *et al.* (2009) 'Pressure drop characteristics of flow in a symmetric channel with periodically expanded grooves', *Chemical Engineering Science*. Pergamon, 64(3), pp. 593–597. doi: 10.1016/j.ces.2008.10.041.

Alves, M. A., Oliveira, P. J. and Pinho, F. T. (2004) 'On the effect of contraction ratio in viscoelastic flow through abrupt contractions', *Journal of Non-Newtonian Fluid Mechanics*. Elsevier, 122(1–3), pp. 117–130. doi: 10.1016/j.jnnfm.2004.01.022.

Anagnostopoulos, J. S. and Mathioulakis, D. S. (2004) 'Unsteady flow field in a square tube T-junction', *Physics of Fluids*. AIP, 16(11), pp. 3900–3910. Available at: http://link.aip.org/link/?PHF/16/3900/1.

Andrade, R., Skurtys, O. and Osorio, F. (2013) 'Drop impact behavior on food using spray coating: Fundamentals and applications', *Food Research International*. Elsevier, 54(1), pp. 397–405. doi: 10.1016/j.foodres.2013.07.042.

Anna, S. L., Rogers, C. and McKinley, G. H. (1999) 'On controlling the kinematics of a filament stretching rheometer using a real-time active control mechanism', *Journal of Non-Newtonian Fluid Mechanics*. Elsevier, 87(2–3), pp. 307–335. doi: 10.1016/S0377-0257(99)00072-5.

Anne-Archard, D. *et al.* (2013) 'Aggregation of silica nanoparticles in concentrated suspensions under turbulent, shear and extensional flows', *Chemical Engineering Science*. Pergamon, 95, pp. 184–193. doi: 10.1016/j.ces.2013.03.005.

Arabo, E. Y. M. (2011) 'Shear and extensional viscosities of hard wheat flour dough using a capillary rheometer', *Journal of Food Engineering*. Elsevier, 103(3), pp. 294–298. doi: 10.1016/j.jfoodeng.2010.10.027.

Ardakani, H. A., Mitsoulis, E. and Hatzikiriakos, S. G. (2011) 'Thixotropic flow of toothpaste through extrusion dies', *Journal of Non-Newtonian Fluid Mechanics*, 166(21–22), pp. 1262–1271. doi: http://dx.doi.org/10.1016/j.jnnfm.2011.08.004.

Arola, D. F. *et al.* (1997) 'Use of nuclear magnetic resonance imaging as a viscometer for process monitoring', *Chemical Engineering Science*. Pergamon, 52(13), pp. 2049–2057. doi: 10.1016/S0009-2509(97)00033-X.

BAER, T. A. and FINLAYSON, B. A. (1992) ‘COMPARISON OF NUMERICAL SIMULATIONS OF POLYMER FLOW WITH EXPERIMENTAL DATA’, in *Theoretical and Applied Rheology*. Elsevier, pp. 247–249. doi: 10.1016/B978-0-444-89007-8.50097-6.

Bandalusena, H. C. H., Zimmerman, W. B. and Rees, J. M. (2010) ‘Creeping flow analysis of an integrated microfluidic device for rheometry’, *Journal of Non-Newtonian Fluid Mechanics*, 165(19–20), pp. 1302–1308. doi: http://dx.doi.org/10.1016/j.jnnfm.2010.06.013.

Bandulasena, H. C. H., William, B. Z. and Julia, M. R. (2011) ‘An inverse method for rheometry of power-law fluids’, *Measurement Science and Technology*, 22(12), p. 125402. Available at: http://stacks.iop.org/0957-0233/22/i=12/a=125402.

Bandulasena, H. C. H., Zimmerman, W. B. and Rees, J. M. (2008) ‘An inverse methodology for the rheology of a power-law non-Newtonian fluid’, *Journal of Mechanical Engineering Science* , 222(5).

Barnes, H. A. and Roberts, G. P. (1992) ‘A simple empirical model describing the steady-state shear and extensional viscosities of polymer melts’, *Journal of Non-Newtonian Fluid Mechanics*, 44(0), pp. 113–126. doi: http://dx.doi.org/10.1016/0377-0257(92)80047-2.

Barthel, F. *et al.* (2015) ‘Velocity measurement for two-phase flows based on ultrafast X-ray tomography’, *Flow Measurement and Instrumentation*. Elsevier, 46, pp. 196–203. doi: 10.1016/j.flowmeasinst.2015.06.006.

Berg, S., Kröger, R. and Rath, H. J. (1994) ‘Measurement of extensional viscosity by stretching large liquid bridges in microgravity’, *Journal of Non-Newtonian Fluid Mechanics*, 55(3), pp. 307–319. doi: http://dx.doi.org/10.1016/0377-0257(94)80075-8.

Berta, M. *et al.* (2016) ‘Correlation between in-line measurements of tomato ketchup shear viscosity and extensional viscosity’, *Journal of Food Engineering*. Elsevier, 173, pp. 8–14. doi: 10.1016/j.jfoodeng.2015.10.028.

Bieberle, M. and Barthel, F. (2016) ‘Combined phase distribution and particle velocity measurement in spout fluidized beds by ultrafast X-ray computed tomography’, *Chemical Engineering Journal*. Elsevier, 285, pp. 218–227. doi: 10.1016/j.cej.2015.10.003.

Binding, D. M. and Walters, K. (1988) ‘On the use of flow through a contraction in estimating the extensional viscosity of mobile polymer solutions’, *Journal of Non-Newtonian Fluid Mechanics*, 30(2–3), pp. 233–250. doi: http://dx.doi.org/10.1016/0377-0257(88)85026-2.

Bird, R. B. *et al.* (1989) ‘Nonlinear viscoelastic behavior’, *Comprehensive Polymer Science and Supplements*. Elsevier, pp. 236–269. doi: 10.1016/B978-0-08-096701-1.00045-8.

Birkhofer, B. H. *et al.* (2008) ‘Monitoring of fat crystallization process using UVP-PD

technique', *Flow Measurement and Instrumentation*. Elsevier, 19(3–4), pp. 163–169. doi: 10.1016/j.flowmeasinst.2007.08.008.

Boger, D. V (1996) 'Viscoelastic fluid mechanics: Interaction between prediction and experiment', *Experimental Thermal and Fluid Science*, 12(2), pp. 234–243. doi: http://dx.doi.org/10.1016/0894-1777(95)00088-7.

Boger, D. V. (1977) 'A highly elastic constant-viscosity fluid', *Journal of Non-Newtonian Fluid Mechanics*. Elsevier, 3(1), pp. 87–91. doi: 10.1016/0377-0257(77)80014-1.

Brydson (1981) *Flow properties of polymer melts*. London: Godwin.

Campo-Deaño, L. *et al.* (2011) 'Flow of low viscosity Boger fluids through a microfluidic hyperbolic contraction', *Journal of Non-Newtonian Fluid Mechanics*, 166(21–22), pp. 1286–1296. doi: http://dx.doi.org/10.1016/j.jnnfm.2011.08.006.

Cartalos, U. and Piau, J. M. (1992) 'Pressure drop scaling laws and structural stress contributions for complex flows of flexible polymer solutions in thick solvents', *Journal of Non-Newtonian Fluid Mechanics*. Elsevier, 44(C), pp. 55–83. doi: 10.1016/0377-0257(92)80045-Y.

Casanellas, L. and Ortín, J. (2011) 'Laminar oscillatory flow of Maxwell and Oldroyd-B fluids: Theoretical analysis', *Journal of Non-Newtonian Fluid Mechanics*. Elsevier, 166(23–24), pp. 1315–1326. doi: 10.1016/j.jnnfm.2011.08.010.

Chan, P. S.-K. *et al.* (2007) 'Study of the shear and extensional rheology of casein, waxy maize starch and their mixtures', *Food Hydrocolloids*, 21(5–6), pp. 716–725. doi: http://dx.doi.org/10.1016/j.foodhyd.2007.02.001.

Chhabra, R. P. and Richardson, J. F. (2008) *Non-Newtonian Flow and Applied Rheology*. Second edi. Elsevier Ltd.

Coussot, P. (2014) 'Yield stress fluid flows: A review of experimental data', *Journal of Non-Newtonian Fluid Mechanics*. Elsevier, pp. 31–49. doi: 10.1016/j.jnnfm.2014.05.006.

Craven, T. J., Rees, J. M. and Zimmerman, W. B. (2010) 'Pressure sensor positioning in an electrokinetic microrheometer device: simulations of shear-thinning liquid flows', *Microfluidics and Nanofluidics*. Springer-Verlag, 9(2–3), pp. 559–571. doi: 10.1007/s10404-010-0573-8.

Cullen, P. J. *et al.* (2001) 'Process viscometry for the food industry', *Trends in Food Science and Technology*. Elsevier, pp. 451–457. doi: 10.1016/S0924-2244(01)00034-6.

Davies, A. R. and Devlin, J. (1993) 'On corner flows of Oldroyd-B fluids', *Journal of Non-Newtonian Fluid Mechanics*. Elsevier, 50(2–3), pp. 173–191. doi: 10.1016/0377-0257(93)80030-F.

Dealy, J. M. (1984) ‘Official Nomenclature for Material Functions Describing the Response of a Viscoelastic Fluid to Various Shearing and Extensional Deformations’, *Journal of Rheology*, 28(3), p. 181. doi: 10.1122/1.549739.

Demori, M. *et al.* (2011) ‘A microfluidic capacitance sensor for fluid discrimination and characterization’, *Sensors and Actuators A: Physical*, 172(1), pp. 212–219. doi: http://dx.doi.org/10.1016/j.sna.2011.07.013.

Dong, X. *et al.* (2015) ‘Oil-water two-phase flow velocity measurement with continuous wave ultrasound Doppler’, *Chemical Engineering Science*. Pergamon, 135, pp. 155–165. doi: 10.1016/j.ces.2015.05.011.

Eastman, J. R., Goodwin, J. W. and Howe, A. M. (2000) ‘Extensional viscosity of aqueous solutions of SDS and PVP measured on the rheometrics RFX’, *Colloids and Surfaces A: Physicochemical and Engineering Aspects*. Elsevier, 161(2), pp. 329–338. doi: 10.1016/S0927-7757(99)00380-5.

Evensen, G. (1994) ‘Inverse methods and data assimilation in nonlinear ocean models’, *Physica D: Nonlinear Phenomena*, 77(1–3), pp. 108–129. doi: http://dx.doi.org/10.1016/0167-2789(94)90130-9.

Fischer, P. and Windhab, E. J. (2011) ‘Rheology of food materials’, *Current Opinion in Colloid and Interface Science*. Elsevier, pp. 36–40. doi: 10.1016/j.cocis.2010.07.003.

Fu, J., Caers, J. and Tchelepi, H. A. (2011) ‘A multiscale method for subsurface inverse modeling: Single-phase transient flow’, *Advances in Water Resources*, 34(8), pp. 967–979. doi: http://dx.doi.org/10.1016/j.advwatres.2011.05.001.

Fuchs, A. *et al.* (2009) ‘CAPACITIVE SENSING IN PROCESS INSTRUMENTATION’, *Metrol. Meas. Syst.*, XVI(4), pp. 557–568.

Gavrus, A., Massoni, E. and Chenot, J. L. (1996) ‘An inverse analysis using a finite element model for identification of rheological parameters’, *Journal of Materials Processing Technology*, 60(1–4), pp. 447–454. doi: http://dx.doi.org/10.1016/0924-0136(96)02369-2.

de Gennes, P. G. (1974) ‘General features of lipid organization’, *Physics Letters A*. North-Holland, 47(2), pp. 123–124. doi: 10.1016/0375-9601(74)90376-4.

Glibowski, P. and Kowalska, A. (2012) ‘Rheological, texture and sensory properties of kefir with high performance and native inulin’, *Journal of Food Engineering*. Elsevier, 111(2), pp. 299–304. doi: 10.1016/j.jfoodeng.2012.02.019.

Guillot, P. *et al.* (2006) ‘Viscosimeter on a microfluidic chip’, *Langmuir*, 22, p. 8.

Gulati, S., Muller, S. J. and Liepmann, D. (2008) ‘Direct measurements of viscoelastic flows of DNA in a 2:1 abrupt planar micro-contraction’, *Journal of Non-Newtonian Fluid*

Mechanics, 155(1–2), pp. 51–66. doi: http://dx.doi.org/10.1016/j.jnnfm.2008.05.005.

Gupta, R. K., Puszynski, J. and Sridhar, T. (1986) 'Steady spinning of the oldroyd fluid B. I: Theory', *Journal of Non-Newtonian Fluid Mechanics*. Elsevier, 21(1), pp. 99–113. doi: 10.1016/0377-0257(86)80065-9.

Hadamard, J. (1923) *Lectures on the Cauchy problem in linear partial differential equations.* New Haven: Yale University Press.

Hall, S. *et al.* (2011) 'Droplet break-up by in-line Silverson rotor-stator mixer', *Chemical Engineering Science*. Pergamon, 66(10), pp. 2068–2079. doi: 10.1016/j.ces.2011.01.054.

Hammer, E. A., Tollefsen, J. and Olsvik, K. (1989) 'Capacitance transducers for non-intrusive measurement of water in crude oil', *Flow Measurement and Instrumentation*. Elsevier, 1(1), pp. 51–58. doi: 10.1016/0955-5986(89)90010-1.

Han, J. and Kim, C. (2013) 'Spreading of Boger fluid on horizontal surface', *Journal of Non-Newtonian Fluid Mechanics*. Elsevier, 202, pp. 120–130. doi: 10.1016/j.jnnfm.2013.10.002.

Harjo, B., Wibowo, C. and Ng, K. M. (2004) 'Development of natural product manufacturing processes: phytochemicals', *Chemical Engineering Research and Design*. Elsevier, 82(8), pp. 1010–1028. doi: 10.1205/0263876041580695.

Haward, S. J. *et al.* (2010) 'Flow of dilute to semi-dilute polystyrene solutions through a benchmark 8:1 planar abrupt micro-contraction', *Journal of Non-Newtonian Fluid Mechanics*. Elsevier, 165(23–24), pp. 1654–1669. doi: 10.1016/j.jnnfm.2010.09.002.

Haward S. J. Alves M. A., McKinley G. H., O. M. S. N. (2012) 'An Optimized Cross-Slot Flow Geometry for Microfluidic Extensional Rheometry', *Physical Review Letters*, 109(12), p. 5.

Hernández-Estrada, Z. J. *et al.* (2014) 'Creep recovery tests to measure the effects of wheat glutenins on doughs and the relationships to rheological and breadmaking properties', *Journal of Food Engineering*. Elsevier, 143, pp. 62–68. doi: 10.1016/j.jfoodeng.2014.06.034.

Hsu, L. C. *et al.* (2015) 'Two-phase pressure drops and flow pattern observations in 90° bends subject to upward, downward and horizontal arrangements', *Experimental Thermal and Fluid Science*. Elsevier, 68, pp. 484–492. doi: 10.1016/j.expthermflusci.2015.06.012.

Jackson, K. P., Walters, K. and Williams, R. W. (1984) 'A rheometrical study of boger fluids', *Journal of Non-Newtonian Fluid Mechanics*. Elsevier, 14(C), pp. 173–188. doi: 10.1016/0377-0257(84)80043-9.

James, D. F., Chandler, G. M. and Armour, S. J. (1990) 'A converging channel rheometer for the measurement of extensional viscosity', *Journal of Non-Newtonian Fluid Mechanics*, 35(2–3), pp. 421–443. doi: http://dx.doi.org/10.1016/0377-0257(90)85063-5.

Jing, J. *et al.* (2016) 'Investigation on flow patterns and pressure drops of highly viscous crude oil-water flows in a horizontal pipe', *Experimental Thermal and Fluid Science*. Elsevier, 72, pp. 88–96. doi: 10.1016/j.expthermflusci.2015.10.022.

Joyce, G. and Soliman, H. M. (2016) 'Pressure drop for two-phase mixtures combining in a tee junction with wavy flow in the combined side', *Experimental Thermal and Fluid Science*. Elsevier, 70, pp. 307–315. doi: 10.1016/j.expthermflusci.2015.09.024.

Kawatra, S. K. and Bakshi, A. K. (1996) 'On-line measurement of viscosity and determination of flow types for mineral suspensions', *International Journal of Mineral Processing*. Elsevier, 47(3–4), pp. 275–283. doi: 10.1016/0301-7516(96)00009-9.

Keiller, R. A. (1993) 'Entry-flow calculations for the Oldroyd-B and FENE equations', *Journal of Non-Newtonian Fluid Mechanics*. Elsevier, 46(2–3), pp. 143–178. doi: 10.1016/0377-0257(93)85045-C.

De Kerpel, K. *et al.* (2013) 'Flow regime based calibration of a capacitive void fraction sensor for small diameter tubes', *International Journal of Refrigeration-Revue Internationale Du Froid*, 36(2), pp. 390–401. doi: 10.1016/j.ijrefrig.2012.10.010.

Keska, J. K., Smith, M. D. and Williams, B. E. (1999) 'Comparison study of a cluster of four dynamic flow pattern discrimination techniques for multi-phase flow', *Flow Measurement and Instrumentation*, 10(2), pp. 65–77. doi: http://dx.doi.org/10.1016/S0955-5986(98)00048-X.

Keska, J. K. and Williams, B. E. (1999) 'Experimental comparison of flow pattern detection techniques for air-water mixture flow', *Experimental Thermal and Fluid Science*. Elsevier, 19(1), pp. 1–12. doi: 10.1016/S0894-1777(98)10046-8.

Keska, J. K. and Williams, B. E. (1999) 'Experimental comparison of flow pattern detection techniques for air–water mixture flow', *Experimental Thermal and Fluid Science*, 19(1), pp. 1–12. doi: http://dx.doi.org/10.1016/S0894-1777(98)10046-8.

Lanzaro, A. and Yuan, X. F. (2011) 'Effects of contraction ratio on non-linear dynamics of semi-dilute, highly polydisperse PAAm solutions in microfluidics', *Journal of Non-Newtonian Fluid Mechanics*. Elsevier, 166(17–18), pp. 1064–1075. doi: 10.1016/j.jnnfm.2011.06.004.

Li, D. *et al.* (2013) 'Large-scale particle tracking velocimetry with multi-channel CCD cameras', *International Journal of Sediment Research*, 28(1), pp. 103–110. doi: http://dx.doi.org/10.1016/S1001-6279(13)60022-0.

Li, J.-M. *et al.* (2000) 'Birefringence and computational studies of a polystyrene Boger fluid in axisymmetric stagnation flow', *Journal of Non-Newtonian Fluid Mechanics*, 91(2–3), pp.

189–220. doi: http://dx.doi.org/10.1016/S0377-0257(99)00094-4.

Li, J., Xu, C. and Wang, S. (2012) 'Local particle mean velocity measurement using electrostatic sensor matrix in gas-solid two-phase pipe flow', *Flow Measurement and Instrumentation*. Elsevier, 27, pp. 104–112. doi: 10.1016/j.flowmeasinst.2012.05.005.

Li, X.-B. *et al.* (2012) 'Very-low-Re chaotic motions of viscoelastic fluid and its unique applications in microfluidic devices: A review', *Experimental Thermal and Fluid Science*, 39(0), pp. 1–16. doi: http://dx.doi.org/10.1016/j.expthermflusci.2011.12.014.

Liao, S. H., Chen, W. J. and Lu, M. S. C. (2013) 'A CMOS MEMS Capacitive Flow Sensor for Respiratory Monitoring', *Ieee Sensors Journal*, 13(5), pp. 1401–1402. doi: 10.1109/jsen.2013.2245320.

Longo, S. *et al.* (2013) 'On the axisymmetric spreading of non-Newtonian power-law gravity currents of time-dependent volume: An experimental and theoretical investigation focused on the inference of rheological parameters', *Journal of Non-Newtonian Fluid Mechanics*. Elsevier, 201, pp. 69–79. doi: 10.1016/j.jnnfm.2013.07.008.

Ma, J. and Yan, Y. (2000) 'Design and evaluation of electrostatic sensors for the measurement of velocity of pneumatically conveyed solids', *Flow Measurement and Instrumentation*. Elsevier, 11(3), pp. 195–204. doi: 10.1016/S0955-5986(00)00019-4.

Ma, Q. *et al.* (2015) 'Theoretical studies of hydrolysis and stability of polyacrylamide polymers', *Polymer Degradation and Stability*. Elsevier Ltd, 121, pp. 69–77. doi: 10.1016/j.polymdegradstab.2015.08.012.

Mackay, M. E. and Boger, D. V (1993) 'Flow Visualisation in Rheometry', in Collyer, A. A. and Clegg, D. W. (eds) *Rheological Measurement*. Dordrecht: Springer Netherlands, pp. 433–477. doi: 10.1007/978-94-017-2898-0_14.

Macosko, C. W. (1993) 'Rheology: principles, measurements, and applications. ', p. 550.

Macosko, C. W., Ocansey, M. A. and Winter, H. H. (1982) 'Steady planer extension with lubricated dies', *Journal of Non-Newtonian Fluid Mechanics*. Elsevier, 11(3–4), pp. 301–316. doi: 10.1016/0377-0257(82)80037-2.

Magda, J. J. *et al.* (1991) 'Second normal stress difference of a Boger fluid', *Polymer*. Elsevier, 32(11), pp. 2000–2009. doi: 10.1016/0032-3861(91)90165-F.

Maia, J. M. *et al.* (1999) 'Measuring uniaxial extensional viscosity using a modified rotational rheometer', *Journal of Non-Newtonian Fluid Mechanics*, 80(2–3), pp. 183–197. doi: http://dx.doi.org/10.1016/S0377-0257(98)00086-X.

Mainçon, P. and Barnardo-Viljoen, C. (2013) 'An inverse finite element method for the analysis of VIV data', *Marine Structures*, 33(0), pp. 143–159. doi:

http://dx.doi.org/10.1016/j.marstruc.2013.04.005.

Martin, O., Averous, L. and Della Valle, G. (2003) 'In-line determination of plasticized wheat starch viscoelastic behavior: Impact of processing', *Carbohydrate Polymers*. Elsevier, 53(2), pp. 169–182. doi: 10.1016/S0144-8617(03)00040-7.

McKinley, G. *et al.* (2007) 'Extensional flows of polymer solutions in microfluidic converging/diverging geometries', *Journal of Central South University of Technology*. Central South University of Technology, 14(1), pp. 6–9. doi: 10.1007/s11771-007-0202-1.

Miyawaki, O. *et al.* (1996) 'Application of shielded hot-wire viscosity sensor to monitoring cultivations of Xanthomonas campestris and Nicotiana tabacum BY-2', *Journal of Fermentation and Bioengineering*, 82(1), pp. 68–72. doi: http://dx.doi.org/10.1016/0922-338X(96)89457-8.

Mohamad, E. J. *et al.* (2016) 'Measurement and analysis of water/oil multiphase flow using Electrical Capacitance Tomography sensor', *Flow Measurement and Instrumentation*. Elsevier, 47, pp. 62–70. doi: 10.1016/j.flowmeasinst.2015.12.004.

Mompean, G. and Deville, M. (1997) 'Unsteady finite volume simulation of Oldroyd-B fluid through a three-dimensional planar contraction', *Journal of Non-Newtonian Fluid Mechanics*. Elsevier, 72(2–3), pp. 253–279. doi: 10.1016/S0377-0257(97)00033-5.

Morrison, F. a (2001) 'Understanding Rheology', *Oxford University Press*, pp. 387–394. doi: 10.3933/ApplRheol-12-233.

Muke, S. *et al.* (2001) 'Extensional rheology of polypropylene melts from the Rheotens test', *Journal of Non-Newtonian Fluid Mechanics*, 101(1–3), pp. 77–93. doi: http://dx.doi.org/10.1016/S0377-0257(01)00142-2.

van Nieuwkoop, J. and Muller von Czernicki, M. M. O. (1996) 'Elongation and subsequent relaxation measurements on dilute polyisobutylene solutions', *Journal of Non-Newtonian Fluid Mechanics*, 67(0), pp. 105–123. doi: http://dx.doi.org/10.1016/S0377-0257(96)01441-3.

Van Nieuwkoop, J. and Muller Von Czernicki, M. M. O. (1996) 'Elongation and subsequent relaxation measurements on dilute polyisobutylene solutions', *Journal of Non-Newtonian Fluid Mechanics*. Elsevier, 67(1–3), pp. 105–123. doi: 10.1016/S0377-0257(96)01441-3.

Núñez, M., Della Valle, G. and Sandoval, A. J. (2010) 'Shear and elongational viscosities of a complex starchy formulation for extrusion cooking', *Food Research International*, 43(8), pp. 2093–2100. doi: http://dx.doi.org/10.1016/j.foodres.2010.07.006.

Odell, J. A. and Carrington, S. P. (2006) 'Extensional flow oscillatory rheometry', *Journal of Non-Newtonian Fluid Mechanics*, 137(1–3), pp. 110–120. doi:

http://dx.doi.org/10.1016/j.jnnfm.2006.03.010.

Owens, R. G. and Phillips, T. N. (2005) *Computational Rheology*. London: Imperial College Press.

Padmanabhan, M. (1995) 'Measurement of extensional viscosity of viscoelastic liquid foods', *Journal of Food Engineering*, 25(3), pp. 311–327. doi: http://dx.doi.org/10.1016/0260-8774(94)00016-3.

Padmanabhan, M. and Bhattacharya, M. (1993) 'Planar extensional viscosity of corn meal dough', *Journal of Food Engineering*. Elsevier, 18(4), pp. 389–411. doi: 10.1016/0260-8774(93)90054-N.

Pathak, J. A. and Hudson, S. D. (2006) 'Rheo-optics of Equilibrium Polymer Solutions: Wormlike Micelles in Elongational Flow in a Microfluidic Cross-Slot', *Macromolecules*. American Chemical Society, 39(25), pp. 8782–8792. doi: 10.1021/ma061355r.

Pérez-Camacho, M. *et al.* (2015) 'Pressure-drop and kinematics of viscoelastic flow through an axisymmetric contraction-expansion geometry with various contraction-ratios', *Journal of Non-Newtonian Fluid Mechanics*. Elsevier, 222, pp. 260–271. doi: 10.1016/j.jnnfm.2015.01.013.

Petrie, C. J. S. (2006) 'One hundred years of extensional flow', *Journal of Non-Newtonian Fluid Mechanics*, 137(1–3), pp. 1–14. doi: http://dx.doi.org/10.1016/j.jnnfm.2006.01.010.

Phillips, T. N. and Williams, A. J. (2002) 'Comparison of creeping and inertial flow of an Oldroyd B fluid through planar and axisymmetric contractions', *Journal of Non-Newtonian Fluid Mechanics*. Elsevier, 108(1–3), pp. 25–47. doi: 10.1016/S0377-0257(02)00123-4.

Pipe, C. J. and McKinley, G. H. (2009) 'Microfluidic rheometry', *Mechanics Research Communications*, 36(1), pp. 110–120. doi: http://dx.doi.org/10.1016/j.mechrescom.2008.08.009.

Prilutski, G. *et al.* (1983) 'Model viscoelastic liquids', *Journal of Non-Newtonian Fluid Mechanics*. Elsevier, 12(2), pp. 233–241. doi: 10.1016/0377-0257(83)80040-8.

Rees, J. M. (2014) 'Towards online, continuous monitoring for rheometry of complex fluids', *Advances in Colloid and Interface Science*. Elsevier, 206, pp. 294–302. doi: 10.1016/j.cis.2013.05.006.

dos Reis, E. and Goldstein, L. (2013) 'Fluid dynamics of horizontal air-water slug flows through a dividing T-junction', *International Journal of Multiphase Flow*, 50, pp. 58–70. doi: 10.1016/j.ijmultiphaseflow.2012.10.008.

Rocha, G. N. *et al.* (2009) 'On extensibility effects in the cross-slot flow bifurcation', *Journal of Non-Newtonian Fluid Mechanics*, 156(1–2), pp. 58–69. doi:

http://dx.doi.org/10.1016/j.jnnfm.2008.06.008.

Rodd, L. E. *et al.* (2005) 'The inertio-elastic planar entry flow of low-viscosity elastic fluids in micro-fabricated geometries', *Journal of Non-Newtonian Fluid Mechanics*, 129(1), pp. 1–22. doi: http://dx.doi.org/10.1016/j.jnnfm.2005.04.006.

Rondon, J., Barrufet, M. A. and Falcone, G. (2012) 'A novel downhole sensor to determine fluid viscosity', *Flow Measurement and Instrumentation*. Elsevier, 23(1), pp. 9–18. doi: 10.1016/j.flowmeasinst.2011.12.001.

Rothstein, J. P. and McKinley, G. H. (1999) 'Extensional flow of a polystyrene Boger fluid through a 4:1:4 axisymmetric contraction/expansion', *Journal of Non-Newtonian Fluid Mechanics*. Elsevier, 86(1–2), pp. 61–88. doi: 10.1016/S0377-0257(98)00202-X.

Rothstein, J. P. and McKinley, G. H. (2001) 'The axisymmetric contraction-expansion: The role of extensional rheology on vortex growth dynamics and the enhanced pressure drop', *Journal of Non-Newtonian Fluid Mechanics*. Elsevier, 98(1), pp. 33–63. doi: 10.1016/S0377-0257(01)00094-5.

Różańska, S. *et al.* (2013) 'Extensional viscosity of o/w emulsion stabilized by polysaccharides measured on the opposed-nozzle device', *Food Hydrocolloids*, 32(1), pp. 130–142. doi: http://dx.doi.org/10.1016/j.foodhyd.2012.12.018.

S. Smith, J., M. N. H. Irving, H. and B. Simpson, R. (1970) *An automatic capillary viscometer*, *Analyst*. doi: 10.1039/an9709500743.

Sadat, A. and Khan, I. A. (2007) 'A novel technique for the measurement of liquid viscosity', *Journal of Food Engineering*. Elsevier, 80(4), pp. 1194–1198. doi: 10.1016/j.jfoodeng.2006.09.009.

Sánchez, M. C. *et al.* (1998) 'Evolution of the microstructure and rheology of O/W emulsions during the emulsification process', *The Canadian Journal of Chemical Engineering*. Wiley Subscription Services, Inc., A Wiley Company, 76(3), pp. 479–485. doi: 10.1002/cjce.5450760318.

Sankaran, A. K. *et al.* (2013) 'Increasing the stability of high contraction ratio flow of Boger fluids by pre-deformation', *Journal of Non-Newtonian Fluid Mechanics*. Elsevier, 196, pp. 27–35. doi: 10.1016/j.jnnfm.2012.12.015.

Schoonen, J. F. M. *et al.* (1998) 'A 3D numerical/experimental study on a stagnation flow of a polyisobutylene solution', *Journal of Non-Newtonian Fluid Mechanics*, 79(2–3), pp. 529–561. doi: http://dx.doi.org/10.1016/S0377-0257(98)00118-9.

Schweizer, T. *et al.* (1990) 'Mechanical and optical responses of the M1 fluid subject to stagnation point flow', *Journal of Non-Newtonian Fluid Mechanics*. Elsevier, 35(2–3), pp.

277–286. doi: 10.1016/0377-0257(90)85054-3.

Seraj, H., Rahmat, M. F. and Khalid, M. (2013) ‘Measurement of velocity of solid/air two phase fluid using electrostatic sensors and cross correlation technique’, *Scientia Iranica*. No longer published by Elsevier, 20(3), pp. 786–792. doi: 10.1016/j.scient.2012.12.019.

Silva, J., Santos, A. C. and Canevarolo, S. V. (2015) ‘In-line monitoring flow in an extruder die by rheo-optics’, *Polymer Testing*. Elsevier, 41, pp. 63–72. doi: 10.1016/j.polymertesting.2014.10.007.

Solomon, M. J. and Muller, S. J. (1996) ‘Flow past a sphere in polystyrene-based Boger fluids: The effect on the drag coefficient of finite extensibility, solvent quality and polymer molecular weight’, *Journal of Non-Newtonian Fluid Mechanics*. Elsevier, 62(1), pp. 81–94. doi: 10.1016/0377-0257(95)01398-9.

Soulages, J. *et al.* (2008) ‘Lubricated optical rheometer for the study of two-dimensional complex flows of polymer melts’, *Journal of Non-Newtonian Fluid Mechanics*, 150(1), pp. 43–55. doi: http://dx.doi.org/10.1016/j.jnnfm.2007.10.006.

Soulages, J. *et al.* (2009) ‘Investigating the stability of viscoelastic stagnation flows in T-shaped microchannels’, *Journal of Non-Newtonian Fluid Mechanics*, 163(1–3), pp. 9–24. doi: http://dx.doi.org/10.1016/j.jnnfm.2009.06.002.

Strazza, D. *et al.* (2011) ‘Capacitance sensor for hold-up measurement in high-viscous-oil/conductive-water core-annular flows’, *Flow Measurement and Instrumentation*, 22(5), pp. 360–369. doi: http://dx.doi.org/10.1016/j.flowmeasinst.2011.04.008.

Syed Mustapha, S. M. F. D. *et al.* (1999) ‘Viscometric flow interpretation using qualitative and quantitative techniques’, *Engineering Applications of Artificial Intelligence*, 12(3), pp. 255–272. doi: http://dx.doi.org/10.1016/S0952-1976(99)00002-0.

Szeliga, D., Gawad, J. and Pietrzyk, M. (2006) ‘Inverse analysis for identification of rheological and friction models in metal forming’, *Computer Methods in Applied Mechanics and Engineering*, 195(48–49), pp. 6778–6798. doi: http://dx.doi.org/10.1016/j.cma.2005.03.015.

Tabilo-Munizaga, G. and Barbosa-Cánovas, G. V (2005) ‘Rheology for the food industry’, *Journal of Food Engineering*, 67(1–2), pp. 147–156. doi: http://dx.doi.org/10.1016/j.jfoodeng.2004.05.062.

Taklifi, A. *et al.* (2016) ‘Experimental investigation on heat transfer and pressure drop of supercritical water flows in an inclined rifled tube’, *The Journal of Supercritical Fluids*. Elsevier, 107, pp. 209–218. doi: 10.1016/j.supflu.2015.09.011.

Tan, C. *et al.* (2015) ‘Characterization of oil-water two-phase pipe flow with a combined

conductivity/capacitance sensor and wavelet analysis', *Chemical Engineering Science*. Pergamon, 134, pp. 153–168. doi: 10.1016/j.ces.2015.04.046.

Tanner, R. I. (2009) 'The changing face of rheology', *Journal of Non-Newtonian Fluid Mechanics*, 157(3), pp. 141–144. doi: http://dx.doi.org/10.1016/j.jnnfm.2008.11.007.

Thais, L., Helin, L. and Mompean, G. (2006) 'Numerical simulation of viscoelastic flows with Oldroyd-B constitutive equations and novel algebraic stress models', *Journal of Non-Newtonian Fluid Mechanics*. Elsevier, 140(1–3), pp. 145–158. doi: 10.1016/j.jnnfm.2006.01.016.

Tomé, M. F. *et al.* (2008) 'Numerical simulation of viscoelastic flows using integral constitutive equations: A finite difference approach', *Journal of Computational Physics*. Academic Press, 227(8), pp. 4207–4243. doi: 10.1016/j.jcp.2007.12.023.

Torres-Moreno, M. *et al.* (2015) 'Nutritional composition and fatty acids profile in cocoa beans and chocolates with different geographical origin and processing conditions', *Food Chemistry*. Elsevier, 166, pp. 125–132. doi: 10.1016/j.foodchem.2014.05.141.

Tretheway, D. C. and Leal, L. G. (2001) 'Deformation and relaxation of Newtonian drops in planar extensional flows of a Boger fluid', *Journal of Non-Newtonian Fluid Mechanics*, 99(2–3), pp. 81–108. doi: http://dx.doi.org/10.1016/S0377-0257(01)00123-9.

Verhoef, M. R. J., Van Den Brule, B. H. A. A. and Hulsen, M. A. (1999) 'On the modelling of a PIB/PB Boger fluid in extensional flow', *Journal of Non-Newtonian Fluid Mechanics*. Elsevier, 80(2–3), pp. 155–182. doi: 10.1016/S0377-0257(98)00080-9.

Wang, Q. J. and Huang, H. X. (2013) 'Detecting extensional viscosity of polypropylene melt using the Rheotens test: A comparison between standard and steady state test modes', *Polymer Testing*. Elsevier, 32(8), pp. 1400–1407. doi: 10.1016/j.polymertesting.2013.09.001.

Wang, Z. *et al.* (2012) 'Dynamic visualization approach of the multiphase flow using electrical capacitance tomography', *Chinese Journal of Chemical Engineering*. Elsevier, 20(2), pp. 380–388. doi: 10.1016/S1004-9541(12)60401-7.

Wei, Y. *et al.* (2007) 'Dynamic wetting of Boger fluids', *Journal of Colloid and Interface Science*. Academic Press, 313(1), pp. 274–280. doi: 10.1016/j.jcis.2007.04.020.

Williams, P. R. and Williams, R. W. (1985) 'On the planar extensional viscosity of mobile liquids', *Journal of Non-Newtonian Fluid Mechanics*, 19(1), pp. 53–80. doi: http://dx.doi.org/10.1016/0377-0257(85)87012-9.

Wu, H. *et al.* (2015) 'Design of a Conductance and Capacitance Combination Sensor for water holdup measurement in oil-water two-phase flow', *Flow Measurement and Instrumentation*. Elsevier, 46, pp. 218–229. doi: 10.1016/j.flowmeasinst.2015.06.026.

Xie, F., Halley, P. J. and Avérous, L. (2012) 'Rheology to understand and optimize processibility, structures and properties of starch polymeric materials', *Progress in Polymer Science (Oxford)*. Pergamon, pp. 595–623. doi: 10.1016/j.progpolymsci.2011.07.002.

Yang, C. B., Sakai, M. and Jones, S. B. (2013) 'Inverse method for simultaneous determination of soil water flux density and thermal properties with a penta-needle heat pulse probe', *Water Resources Research*, 49(9), pp. 5851–5864. doi: 10.1002/wrcr.20459.

Yang, Y. and Kang, B. S. (2015) 'Development and validation of digital holographic particle velocity measurement system for rotational flows', *Optik*. Urban & Fischer, 126(19), pp. 2223–2227. doi: 10.1016/j.ijleo.2015.05.103.

Yue, J., Chen, G. and Yuan, Q. (2004) 'Pressure drops of single and two-phase flows through T-type microchannel mixers', *Chemical Engineering Journal*, 102(1), pp. 11–24. doi: http://dx.doi.org/10.1016/j.cej.2004.02.001.

Zatloukal, M. *et al.* (2002) 'Improvement in techniques for the determination of extensional rheological data from entrance flows: computational and experimental analysis', *Journal of Non-Newtonian Fluid Mechanics*, 107(1–3), pp. 13–37. doi: http://dx.doi.org/10.1016/S0377-0257(02)00111-8.

Zatloukal, M. and Musil, J. (2009) 'Analysis of entrance pressure drop techniques for extensional viscosity determination', *Polymer Testing*, 28(8), pp. 843–853. doi: http://dx.doi.org/10.1016/j.polymertesting.2009.07.007.

Zhai, L. *et al.* (2015) 'Liquid holdup measurement with double helix capacitance sensor in horizontal oil-water two-phase flow pipes', *Chinese Journal of Chemical Engineering*. Elsevier, 23(1), pp. 268–275. doi: 10.1016/j.cjche.2014.10.010.

Zhai, L. S. *et al.* (2014) 'Cross-correlation velocity measurement of horizontal oil-water two-phase flow by using parallel-wire capacitance probe', *Experimental Thermal and Fluid Science*. Elsevier, 53, pp. 277–289. doi: 10.1016/j.expthermflusci.2013.12.021.

Zhou, J., Qi, L. and Chen, G. (2006) 'New inverse method for identification of constitutive parameters', *Transactions of Nonferrous Metals Society of China*, 16(1), pp. 148–152. doi: http://dx.doi.org/10.1016/S1003-6326(06)60026-5.

Zimmerman, W. B. and Rees, J. M. (2009) 'Optimal modelling and experimentation for the improved sustainability of microfluidic chemical technology design', *Chemical Engineering Research and Design*, 87(6), pp. 798–808. doi: http://dx.doi.org/10.1016/j.cherd.2008.11.010.

Zimmerman, W. B., Rees, J. M. and Craven, T. J. (2006) 'Rheometry of non-Newtonian electrokinetic flow in a microchannel T-junction', *Microfluidics and Nanofluidics*, 2(6).